NPS69-88-012PR

NAVAL POSTGRADUATE SCHOOL

Monterey, California

PROGRESS REPORT

HEAT PIPE COOLING OF
LARGE ELECTRIC MOTORS

P.J. Marto
A.S. Wanniarachchi

December 1988

Project Report for the period
1 October 1987 - 30 September 1988

Prepared for: David Taylor Research Center
Annapolis, Maryland 21402

NAVAL POSTGRADUATE SCHOOL
Monterey, California

RADM R. C. Austin
Superintendent

H. Shull
Provost

This report was prepared in conjunction with research conducted for the David Taylor Research Center and funded by the Naval Postgraduate School.

This report was prepared by:

INTRODUCTION

The U.S. Navy has a continued interest in using components having greater performance-to-weight ratios than those in current use. Such efficient components would provide more space for other components that have a direct bearing on the mission capabilities of naval vessels. This is especially the case for submarines as there are severe restrictions on the size and weight of any components on board these vessels.

The navy is interested in using electric propulsion for future vessels. Such vessels will require large electric motors and generators. If conventional motors (cooled by forced-air convection) are used, their size and weight may be too excessive. Therefore, to achieve the navy's goal, more efficient motors and generators, which are cooled by more advanced means, should be used. Such electric machinery may be cooled by liquids (such as water or oil), or by two-phase heat pipes. Liquid cooling of rotors is a very challenging problem as the liquid must be forced into and out of the rotating shaft, from the stationary frame of reference. Such a scheme, of course, requires the use of rotating seals. On the other hand, such rotors may be cooled by air-cooled, heat pipes fitted near the periphery of the rotor.

The theoretical treatment of the above two cooling techniques is very complex owing to the three-dimensional flow patterns, further complicated by rotation. Therefore, experimental modelling on prototypes has become very important in assessing the feasibility and the advantages of these advanced cooling

techniques. The David Taylor Research Center (DTRC) has designed and built an apparatus for testing the performance of both liquid cooling and heat-pipe cooling of electric motors and generators. Data have been collected for the past three years for liquid cooling using water and oil as the working fluids.

In support of this effort at DTRC, the Naval Postgraduate School has been providing technical guidance pertaining to basic heat-transfer mechanisms that occur with rotation, heat pipe technology and experimental techniques. During the past year, two specific efforts were carried out. One pertained to the design and fabrication of rotating, off-axis heat pipes for use in the DTRC apparatus. The other involved an assessment of rotating heat pipe technology in Europe.

HEAT-PIPE DESIGN

In July 1988, Professor Wanniarachchi terminated his employment with the U.S. Government to accept a position at the University of California, Santa Barbara. Prior to his departure, he was intimately involved with the design of the off-axis heat pipes.

Design conditions

Water was selected as the working fluid, and the design conditions are listed below:

Rotational speed	=	1000 rpm
Heat duty per bar	=	100 watts
Saturation temperature	=	80°C

Ambient temperature = 22°C

Radius of rotation = 389 mm

Three feasible inside diameters were selected (see Table 1) for the cavity in each conductor bar. To match this geometry, three different copper finned tubes were selected and purchased (see Table 1 and Figure 1).

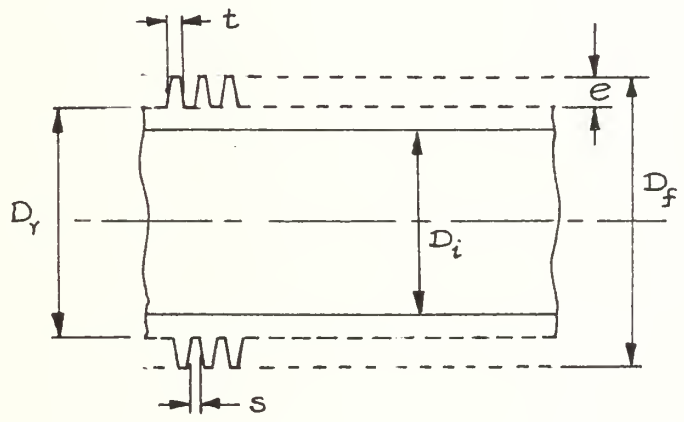

Figure 1. Finned Tube Geometry

Table 1

Dimensions of Finned Tubes

Tube #1	Fin Density (fins/inch)	Fin Dia, D_f (mm)	Root Dia, D_r (mm)	Inside Dia, D_i (mm)	Fin Spacing, s (mm)	Fin Thickness, t (mm)
1	19	11.8	8.6	4.83	0.89	0.38
2	26	12.7	9.5	6.58	0.60	0.38
3	26	12.7	9.5	7.90	0.60	0.38

Thermal Analysis Procedure

As shown in Figure 2, it was assumed that each conductor bar will be fitted with two condenser sections; thus, the heat duty on each condenser would be 50 watts.

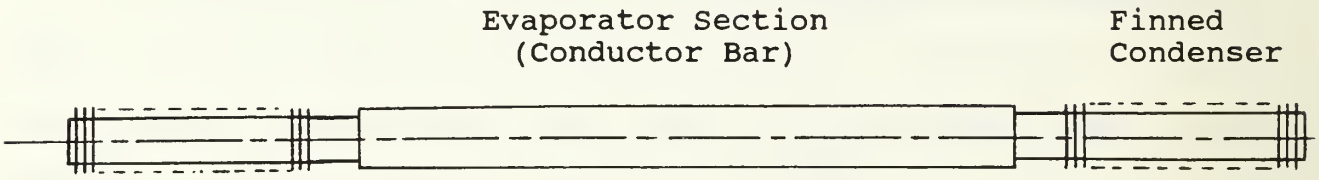

Figure 2. Schematic of Heat-Pipe Assembly.

A. Inside Condensing Heat-Transfer Coefficient

The problem of film condensation inside a horizontal tube has been treated by Jaster and Kosky [1]. In this situation, the condensate collects at the bottom of the tube due to the acceleration of gravity as shown in Figure 3. Jaster and Kosky

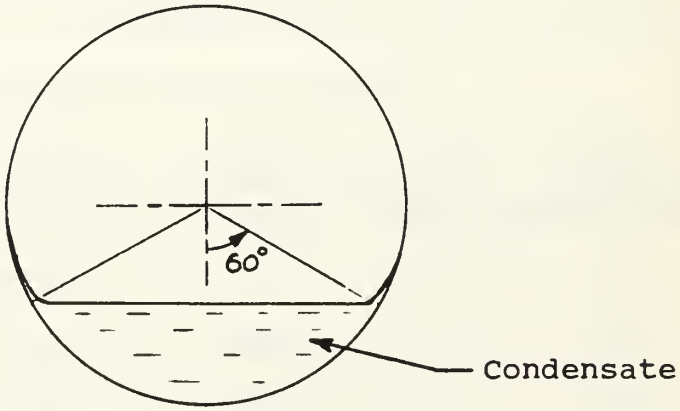

Figure 3. Condensate Stratification in Heat Pipes.

arrived at the following expression for the average heat-transfer coefficient around the tube circumference:

$$h_i = \Omega \left(\frac{k_l^3 \rho_l}{\mu_e} \frac{g\, h_{fg}}{D_i \Delta T} \right)^{1/4} \qquad (1)$$

where

$$\Omega = 0.728\, \epsilon_g^{3/4}$$

$$\epsilon_g = \left(1 + \left(\frac{1-x}{x}\right) \left(\frac{\rho_v}{\rho_l}\right)^{2/3} \right)^{-1}$$

h_{fg} = Specific enthalpy of condensation

k_l = Thermal conductivity of condensation

x = Vapor quality

ρ_l = Density of condensate

ρ_v = Density of vapor

μ_l = Viscosity of condensate

Notice that, for the case of rotation, the "g" term in equation (1) must be replaced by $\omega^2 R$, where ω is the angular velocity and R is the radius of rotation. For the above calculation, a fill angle of 120° was used as shown in Figure 3.

B. Air-side Heat-Transfer Coefficient

To compute the air-side heat-transfer coefficient, the correlation developed by Briggs and Young [2] was used:

$$h_a = 0.1507 \frac{k_a}{D_r} Re^{2/3} Pr^{1/3} \left(\frac{s}{e}\right)^{0.164} \left(\frac{s}{t}\right)^{0.075} \qquad (2)$$

where

k_a = Thermal conductivity of air

Pr = Prandtl number of air

Re = Air-side Reynolds number

e = Fin height

The use of rotor peripheral velocity (ωR) in computing the air-side Reynolds number raises two important questions. First, in the actual case, each condenser lies in the wake of another one. Thus, the entire condenser would not experience high air velocities. Second, the Briggs and Young correlation has not been tested at as high Reynolds numbers as would be present for this situation. For these reasons, the air-side coefficient computed by the above equation was degraded, somewhat arbitrarily, by 50 percent.

Computer Program

A computer program was developed to compute the size of the condenser necessary for the design conditions stated earlier using all three condenser sections. As condenser #1 has the smallest inside diameter, this determined the minimum length necessary. Also, the maximum condenser length allowable was limited to 12 inches by the test facility at DTRC.

The results obtained for the three condensers (1, 2 and 3), are listed in Tables 2, 3 and 4, respectively.

Structural Considerations

All critical stress calculations were incorporated into the computer program to ensure safe operation of the heat pipes on the rotating apparatus. While, as noted earlier, the heat-transfer

TABLE 2

TUBE CODE = 1
Di = 4.8 (MM)

OPERATING CONDITIONS:

Required heat duty	=	50.0	(W)
Rotational speed	=	1000.0	(RPM)
Saturation temperature	=	80.0	(Deg C)
Ambient temperature	=	22.0	(Deg C)
Omega ^2*R/g	=	434.8	
Fill angle	=	120.0	(Degrees)

COMPUTED HEAT-TRANSFER PERFORMANCE:
NOTE: Air-Side Coefficient Has Been Degraded by
50.0 Percent

Air-side coefficient	=	147.2	(W/m^2.K)
Inside coefficient	=	4211.0	(W/m^2.K)
Vapor-side temp drop	=	8.3	(K)

COMPUTED DESIGN PARAMETERS:

Number of intermediate supports	=	5	
Required water fill volume	=	8.5	(cc)
Maximum steam velocity	=	1.1	(m/s)
Length of portion between supports	=	23.6	(mm)
Overall condenser length	=	209.3	(mm)

COMPUTED STRUCTURAL STRENGTH FOR COPPER
FINNED TUBE (AT 3000 RPM):

Yield stress of condenser material	=	2.620E+01	(MPa)
Computed maximum bending stress	=	2.204E+01	(MPa)
Computed shear stress	=	1.042E+00	(MPa)
Available safety factor for bending	=	2.816E+00	

STRENGTH CALCULATIONS FOR STEEL SUPPORT STRUCTURE:

Yield stress	=	2.620E+02	(MPa)
Maximum bending stress	=	5.779E+01	(MPa)
Available safety factor for bending	=	4.534E+00	
Maximum deflection	=	6.343E-02	(mm)
Normal stress of copper supports	=	6.860E-01	(MPa)

STRUCTURAL STRENGTH OF HEAT PIPE UNDER CIRCUMFERENTIAL
LOADING OWING TO AIR DRAG:

Maximum bending stress	=	1.958E-01	(MPa)
Available safety factor	=	3.170E+02	

ESTIMATED UPPER LIMIT FOR AIR DRAG (AT 3000 RPM)

Power consumption due to air drag	=	1.179E+00	(kW)

TABLE 3

TUBE CODE = 2
Di = 6.6 (mm)

OPERATING CONDITIONS:

Required heat duty	=	50.0	(W)
Rotational speed	=	1000.0	(RPM)
Saturation temperature	=	80.0	(Deg C)
Ambient temperature	=	22.0	(Deg C)
Omega ^2*R/g	=	434.8	
Fill angle	=	120.0	(Degrees)

COMPUTED HEAT-TRANSFER PERFORMANCE:
NOTE: Air-Side Coefficient Has Been Degraded by 50.0 Percent

Air-side coefficient	=	133.3	(W/m^2.K)
Inside coefficient	=	3884.5	(W/m^2.K)
Vapor-side temp drop	=	8.4	(K)

COMPUTED DESIGN PARAMETERS:

Number of intermediate supports	=	4	
Required water fill volume	=	14.8	(cc)
Maximum steam velocity	=	0.6	(m/s)
Length of portion between supports	=	22.2	(mm)
Overall condenser length	=	171.3	(mm)

COMPUTED STRUCTURAL STRENGTH FOR COPPER FINNED TUBE (AT 3000 RPM):

Yield stress of condenser material	=	6.206E+01	(MPa)
Computed maximum bending stress	=	1.640E+01	(MPa)
Computed shear stress	=	1.211E+00	(MPa)
Available safety factor for bending	=	3.785E+00	

STRENGTH CALCULATIONS FOR STEEL SUPPORT STRUCTURE:

Yield stress	=	2.620E+02	(MPa)
Maximum bending stress	=	4.770E+01	(MPa)
Available safety factor for bending	=	5.493E+00	
Maximum deflection	=	4.303E-02	(mm)
Normal stress of copper supports	=	7.390E-01	(MPa)

STRUCTURAL STRENGTH OF HEAT PIPE UNDER CIRCUMFERENTIAL LOADING OWING TO AIR DRAG:

Maximum bending stress	=	1.587E-01	(MPa)
Available safety factor	=	3.911E+02	

ESTIMATED UPPER LIMIT FOR AIR DRAG (AT 3000 RPM)

Power consumption due to air drag	=	9.881E-01	(kW)

TABLE 4

TUBE CODE = 3
Di = 7.9 (mm)

OPERATING CONDITIONS:

Required heat duty	=	50.0	(W)
Rotational speed	=	1000.0	(RPM)
Saturation temperature	=	80.0	(Deg C)
Ambient temperature	=	22.0	(Deg C)
Omega ^2*R/g	=	434.8	
Fill angle	=	120.0	(Degrees)

COMPUTED HEAT-TRANSFER PERFORMANCE:
NOTE: Air-Side Coefficient Has Been Degraded by
50.0 Percent

Air-side coefficient	=	133.4	(W/m^2.K)
Inside coefficient	=	3660.8	(W/m^2.K)
Vapor-side temp drop	=	8.9	(K)

COMPUTED DESIGN PARAMETERS:

Number of intermediate supports	=	3	
Required water fill volume	=	20.6	(cc)
Maximum steam velocity	=	0.4	(m/s)
Length of portion between supports	=	23.3	(mm)
Overall condenser length	=	148.3	(mm)

COMPUTED STRUCTURAL STRENGTH FOR COPPER
FINNED TUBE (AT 3000 RPM):

Yield stress of condenser material	=	6.206E+01	(MPa)
Computed maximum bending stress	=	1.608E+01	(MPa)
Computed shear stress	=	1.633E+00	(MPa)
Available safety factor for bending	=	3.859E+00	

STRENGTH CALCULATIONS FOR STEEL SUPPORT STRUCTURE:

Yield stress	=	2.620E+02	(MPa)
Maximum bending stress	=	4.156E+01	(MPa)
Available safety factor for bending	=	6.304E+00	
Maximum deflection	=	3.254E-02	(mm)
Normal stress of copper supports	=	5.912E-01	(MPa)

STRUCTURAL STRENGTH OF HEAT PIPE UNDER CIRCUMFERENTIAL
LOADING OWING TO AIR DRAG:

Maximum bending stress	=	2.526E-01	(MPa)
Available safety factor	=	2.457E+02	

ESTIMATED UPPER LIMIT FOR AIR DRAG (AT 3000 RPM)

Power consumption due to air drag	=	8.554E-01	(kW)

calculations were performed for 1000 rpm, structural calculations were performed for 3000 rpm. Owing to the quite low yield stress of copper, each finned condenser had to be supported at each 1-inch interval. No details of the structural calculational procedures used will be provided in this report. However, all critical safety factors available were found to be greater than 2.4.

To support the condensers at each 1-inch interval, clamps (see Figure 4) were manufactured using high-strength aluminum alloy (Al 6061T6, σ_{yield} = 40,000 psi). These clamps were, in turn, supported by an angular plate (see Figure 4) made of high-strength aluminum alloy (Al 7075, $\sigma_{yield} \approx$ 73,000 psi).

Notice that, as the support structures will be shared by all three types of condensers, the length of each condenser was fixed at 10 inches, based on a value of 209.3 mm computed for the limiting case determined by condenser #1.

Fabrication of Heat Pipes

Two 1/2" x 1/2" x 38" copper conductor bars (provided by DTRC) were machined so that they could be fitted with electric heaters and condenser sections. To accommodate four electric heaters, 1/16" x 1/16" axial grooves were machined at the four corners of each bar. Also, the two ends of the bars were countersunk to enable proper installation of the condenser sections (see Figure 5). Aluminum sleeves were made with dimensions of 3/8" ID x 1/2" OD x 1/4", and were split axially. Two of these half sleeves would be placed in each location of the condenser to be supported (area

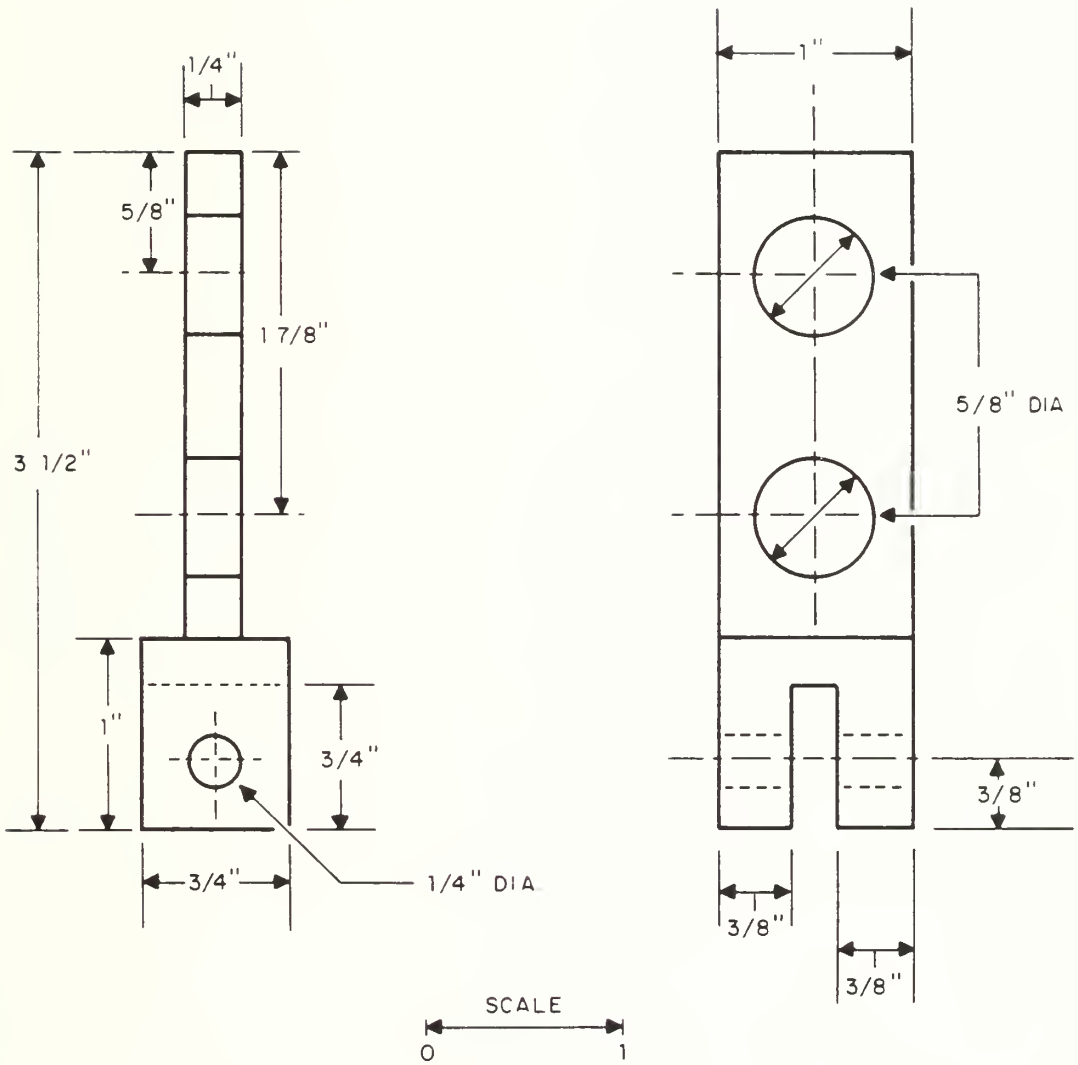

Figure 4. Details of Condenser Support Clamps

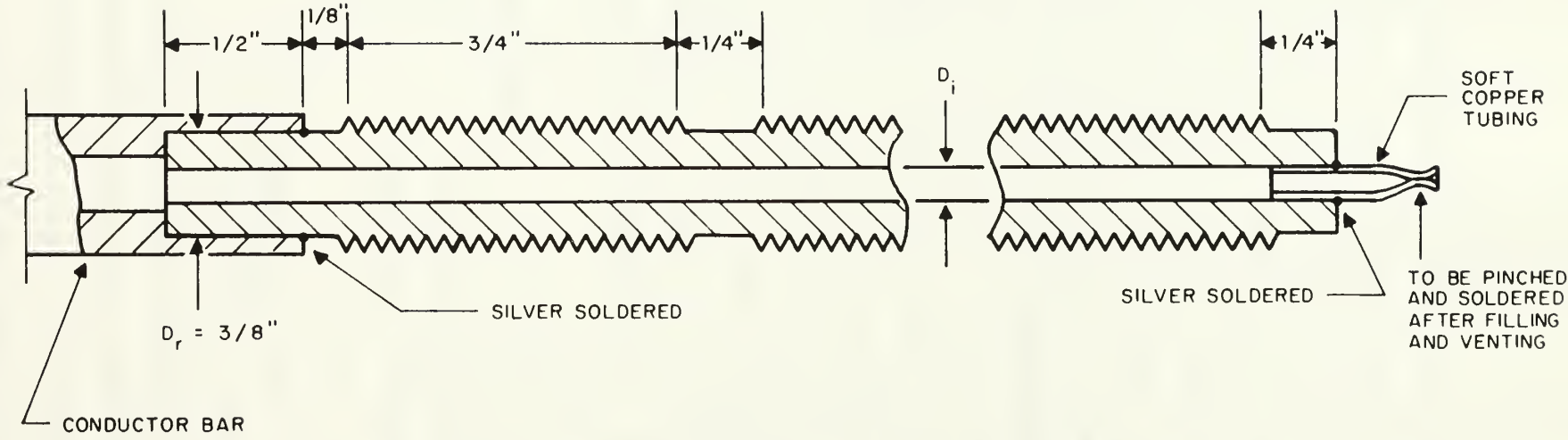

Figure 5. Design Specifications for Heat Pipe Condensers

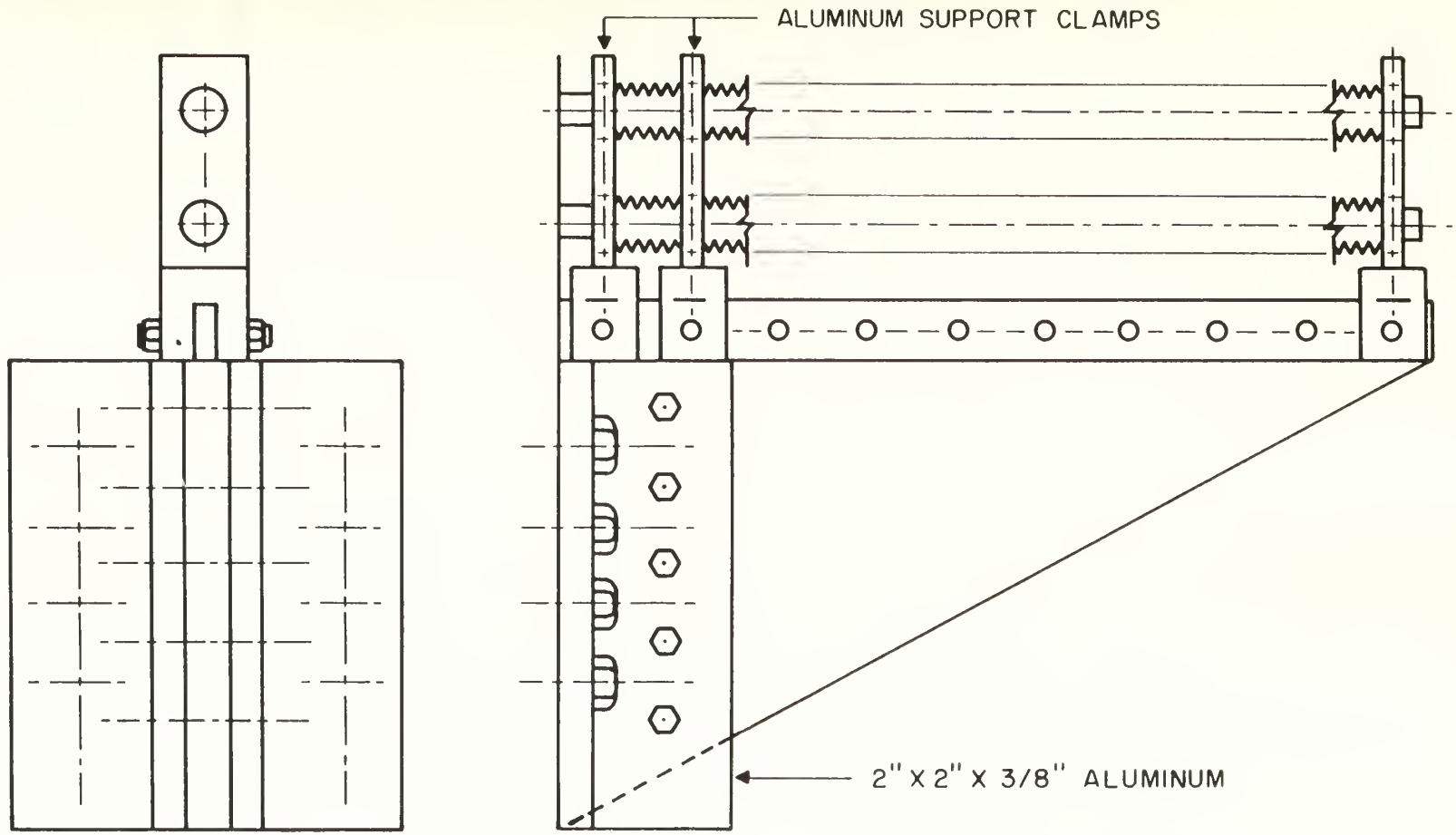

Figure 6. Heat Pipe Assembly Including Support Structures

with fins machined off) and the clamp would be slid over these half sleeves.

Assembly

All the manufactured items were delivered unassembled to DTRC. The actual assembly of these components should be achieved as follows:

1. Silver solder the condenser sections to the conductor bar. Silver solder a soft-copper tubing at the far end of each condenser. Attach a graduated glass vial (through a metal-to-glass adapter) to one copper tubing. This vial should contain sufficient amount of distilled water so that just the correct amount of water would be left after purging. This should be determined by trials on a piece of copper tubing having inside dimensions identical to the heat-pipe assembly. Place the assembly upright with the glass vial on the bottom. Attach the upper copper tubing to a vacuum pump. Provide heat to the glass vial to expell any dissolved gases and to boil off excess water. While the vacuum pump is running, crimp off the upper copper tubing, and turn off heat to the glass vial. Turn the assembly over and make sure all the water flows to the bottom. Crimp off the other copper tubing and disconnect the glass vial.
2. Attach heaters to each evaporator section. Thermocouples should be installed at various axial and circumferential locations on the heat pipe assembly to enable testing of its

performance.

3. Mount the heat-pipe assembly on the rotating apparatus.
4. Mount the support structures to the vertical plates of the rotor (see Figure 6).
5. Place a pair of half sleeves on each area of condenser section to be supported and slide a clamp over them. Attach the clamp to the angular support structure.

After proper tightening of all fittings, the assembly should be ready for low-speed testing. During this testing, increase the rotational speed gradually and operate at about 300 RPM for about 5 minutes. Stop the rotation and check all fittings and joints to see if they have performed well. Follow this procedure by increasing the rotational speed in increments of 200-300 RPM until safe operation is demonstrated at 1000 RPM. The apparatus should then be ready for operation under a thermal load.

ROTATING HEAT PIPE TECHNOLOGY IN EUROPE

During this report period, Professor Marto spent four months of his Sabbatical Leave at the Centre D'Etudes Nucleaires de Grenoble in Grenoble, France, which was the site of the 6th International Heat Pipe Conference in May 1987. As a result, Professor Marto was able to examine the proceedings of that conference to investigate world-wide activities pertaining to rotating heat pipe technology. In addition, while in Grenoble, Professor Marto visited the Institute for Electrical Machines at the Technical University in Aachen, West Germany. This laboratory has conducted the most intensive research on heat-pipe-cooled electric motors. A summary of Professor Marto's findings are provided below.

6th International Heat Pipe Conference

There were more than 150 oral presentations at the conference including three invited Regional Survey Reports:

1. Polasek, F. (Czechoslovakia) "Heat Pipe Research and Development in East European Countries"
2. Groll, M. (Federal Republic of Germany) "Heat Pipe Research and Development in Western Europe"
3. Dobran, F. (U.S.A.) "Heat Pipe Research and Development in the Americas"

The conference presentations were organized into the following sessions:

- Fundamental and Basic Research
- Theoretical and Experimental Studies
- Technological Studies
- The Heat Pipe as an Aerospace Component
- Heat Exchangers
- Thermosyphons
- Scientific and Industrial Applications

The following papers (copies enclosed in Appendix A) included specific information on rotating heat pipe technology:

1. Chen, J., Tu, C. and Zhou, Z., "Condenser Heat Transfer in Inclined Rotating Heat Pipes"
2. Katsuta, M., Wanniarachchi, A.S. and Marto, P.J., "Condensation Heat Transfer Measurements in Co-axial Rotating Heat Pipes"
3. Shimizu, A. and Yamazachi, S., "Helical Guide-Type Rotating Heat Pipes"
4. Reddy, R.S., Venkateswarlu, P. and Sastri, V.M.K., "Experimental Heat Transfer Characteristics of a Rotating Heat Pipe with an Air-Cooled Condenser"
5. Giessler, F., Sattler, P.K. and Thorem, F., "Heat Pipe Cooling of Electric Machines"

Paper No. 1 provides experimental and theoretical data for off-axis heat pipes that are inclined with respect to the axis of rotation. This helps to pump the condensate from the condenser back to the evaporator. Paper No. 2 provides new experimental information on condensation heat transfer within stepped-condenser, co-axial rotating heat pipes. Paper No. 3 describes the performance of co-

axial rotating heat pipes that contain helical inserts. Paper No. 4 studies co-axial rotating heat pipe performance with an air-cooled finned condenser. Paper No. 5 presents results of four heat-pipe-cooled induction motors of 75 kW and 150 kW. This paper reviews how heat pipes can be used in both the stator and rotor of electric motors. Two open 150 kW motors were tested having longitudinally-grooved capillary heat pipes in the stator slots and yoke and off-axis rotating heat pipes in the rotor. The second motor was designed with smaller heat pipes to save on weight. They found that it was possible to reduce the active stator material weight (compared to a motor with only a 90 kW rating) by 16-22 percent for this 150 kW motor. The third examined motor was a totally-enclosed 75 kW motor with a water-cooled, co-axial heat pipe in the shaft. They found that the heat pipe action reduced the rotor bar temperature from 185°C to 102°C and the shaft temperature from 180°C to 82°C. The temperature rise of the stator was also significantly decreased. The fourth motor tested was a totally-enclosed 150 kW machine with heat pipe cooling in the stator and rotor. They reported that this totally enclosed induction machine will perform the same electrically (and with the same volume/weight) as an open type 150 kW machine whereas conventional enclosed induction motors are much heavier than open machines. They point out that the use of a heat pipe in the motor shaft seems to be very promising.

Visit to Technical University, Aachen, Germany

On 8 June 1988, Professor Marto visited the Institute for Electrical Machines at the Technical University of Aachen in West Germany. This Institute has been the most active group in the world in conducting research on heat-pipe-cooled motors. The Institute is directed by Professor P.K. Sattler who is assisted by Dr. F. Giessler. During my visit, Professor Sattler was on travel, so the visit was conducted with Dr. Giessler, who provided a tour of their laboratory facilities, discussed various research papers and their future plans.

The Germans have been interested in rotating heat pipe technology since 1970 when Siemens Co. incorporated a hollow shaft to cool a motor. Since then, most of the research has been conducted at the University of Stuttgart and the Technical University of Aachen. The University of Stuttgart has developed a technique to deposit copper on the inside of a hollow steel shaft. This copper lining permits water to be used as the heat pipe fluid, otherwise the water would attack the steel and generate non-condensible gases that deteriorate the heat pipe effectiveness. The work at Aachen has been largely the result of a Ph.D. thesis by Dr. F. Thoren who graduated in 1985. His thesis, titled "Various Heat Pipe Systems for Cooling Synchronous Machines," contains a good Bibliography on rotating heat pipe technology. This Bibliography is listed in Appendix B of this report. Certain references that deal specifically with the cooling of electric motors are marked with an asterisk.

The results at Aachen have shown that heat-pipe cooling can provide about a 20 percent improvement in power density of electric machines (whether open or enclosed). They have been most interested in machines in the size range of 75-150 kW. They have also studied forced convection cooling of electric machines. Figure 7 shows a schematic of their experimental apparatus.

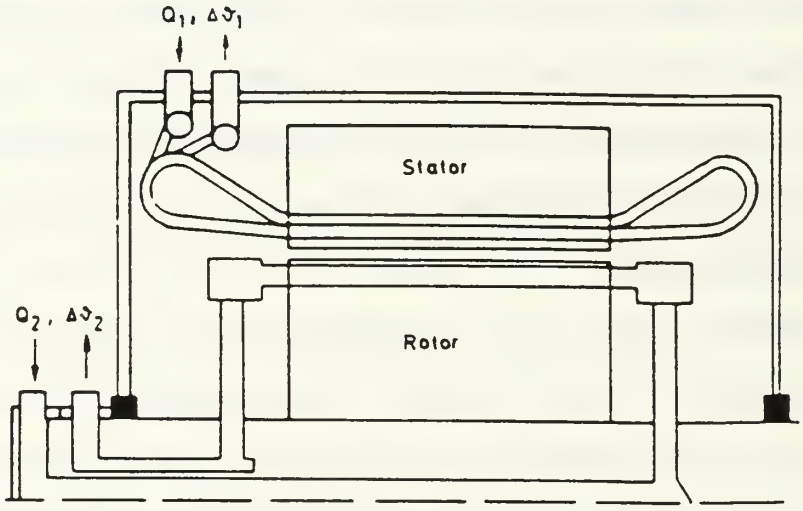

Figure 7. Schematic of Convective Cooled Machine

However, they discovered serious problems in the following area:

- seals
- expense (pumps, coolers, purifiers)
- water purity

As a result, this research was not active during the visit.

Apparently, heat pipes have been shown to be most effective in cooling motors. However, their introduction has increased the cost of the motor and this has created an uneconomical atmosphere for their commercial use. For example, FANUC in Japan has

manufactured a heat-pipe-cooled motor (See Appendix C for their brochure), but is phasing this motor out due to a lack of customers. Potential customers are concerned with the long-term reliability of these devices and a long-term bench test is needed to verify continued good performance. Dr. Giessler mentioned that the research program at Aachen on heat pipe cooling will be completed in 1988 and there are no plans to continue the work. He pointed out that efforts must continue to be made to reduce cost and weight. Perhaps composite shafts could be examined? In addition, the merits and relative costs of using air cooling, water cooling and refrigerant cooling of the heat pipe condenser deserve attention as well.

Although heat-pipe-cooled motors may not be economically attractive for commercial use, they can provide a significant weight reduction for shipboard use, which may be an ideal application of their capabilities. The Navy should therefore continue to pursue the use of rotating heat pipes in electrical machines.

REFERENCES

1. Jaster, H. and Kosky, P.G., "Condensation Heat Transfer in a Mixed Flow Regime," Int. J. Heat Mass Transfer, Vol. 19, pp. 95-99, 1976.

2. Briggs, D.E. and Young, E.H., "Convective Heat Transfer and Pressure Drop of Air Flowing Across Triangular Pitch Banks of Finned Tubes," Chemical Engineering Progress Symposium Series, No. 41, Vol. 59, pp. 1-10, 1963.

APPENDIX A

Copies of Rotating Heat Pipe Papers

CONDENSER HEAT TRANSFER IN INCLINED ROTATING HEAT PIPE

Chen Jian, Tu Chuanjing , Zhejiang University,China

Zhou Zhongyan, Hangzhou Waste Heat Boiler Research Institute, China

ABSTRACT

The condenser heat transfer of the inclined rotating heat pipe which was less analyzed are investigated. A physical model is creatively proposed consisting of a laminar filmwise condensation region and a bottom condensation flow region. The theoretical formulas of the average Nusselt number and the local Nusselt number are obtained by solving the flow differential equations. The effect of centrifugal acceleration on condenser heat transfer characteristics is also investigated. The relations between the rotational speed and average condenser heat transfer coef. and local condenser heat transfer coef. are shown. There are good agreement between theoretical and experimental results, especially in high rotational speed range.

NOMENCLATURE

- a --- centrifugal acceleration at tube axis
- A --- cross sectional area of bottom flow
- Cp--- specific heat of condensate
- d --- tube diameter
- f --- fanning's friction factor
- F --- force on an element of bottom flow
- h --- heat transfer coefficient
- l --- condenser section length
- L --- latent heat of condensation
- Q --- volumetric flow rate of bottom flow
- r_o --- tube radius
- R --- radius of rotation
- Ts--- temperature of saturated vapor
- Tw--- condenser wall temperature
- u --- local circumferential velocity component of condensate film
- U --- mean velocity of bottom flow
- v --- local axial velocity component of condensate film
- x --- distance along tube axis
- z --- distance normal to tube interior surface
- α --- angle between heat pipe axis and rotation axis
- β --- momentum correction factor
- δ --- thickness of condensate film
- λ --- heat conductivity of condensate
- ρ --- density of condensate
- ν --- kinematic viscosity of condensate
- θ --- angle of bottom flow level
- ϕ --- co-ordinate in circumferential direction
- G = $\mathrm{ctg}\alpha$
- Ga = $a\sin\alpha d^3/\nu^2$
- H = $Cp(Ts-Tw)/L$
- Nu--- local nusselt number = hd/λ = $= (2GaPrG/(3HZ))^{1/4}$
- Pr--- prandtl number = $\rho\nu Cp/\lambda$
- Re--- Relnolds number = $(Ga/2)^{1/2}(\Gamma/\theta)$
- X --- dimensionless axial distance = Gx/r_o
- Z --- dimensionless condensate film thickness = $(2GaPrG/(3H))(\delta/d)^{1/4}$

INTRODUCTION

For promoting the energy conservation by utilizing the waste heat from factories, the study and development of efficient heat recovery systems which make use of heat pipe have been promoted. It is well known that heat pipe heat exchanger has a great deal of advantages for gas to gas heat exchange.such as its excellent heat transfer performance and simple structure, so its practical applications have been made most progressively till now. However, in highly fouling environment such as heavy oil flue gas, it becomes an important subject of study that the dust accumulation make heat transfer performance degeneration, one of the best way to solve this problem is to use rotating heat pipe heat exchanger which has a rotating heat pipe bundle. According to the relative position between the heat pipe axis and the axis of rotation, rotating heat pipes can be devided into three basic groups, such as, co-axial, parallel, and inclined. Performance characteristics of a co-axial or parallel rotating heat pipe has been described in previous literatures, but only little is known about the performance of a inclined rotating heat pipe. The longitudinal axis of the inclined rotating heat pipe is inclined to the axis of rotation(Fig.1.), which depends on the component of centrifugal force to pump the condensate from the condenser to evaporator to complete the cycle. The purpose of this study was to investigate theoretically the condenser heat transfer characteristics of a inclined rotating heat pipe, with a new physical model, discuss the condenser heat transfer mechanism according to the flow patterns of working liquid which was shown in physical model.

EXPERIMENTAL EQUIPMENTS

The apparatus used for this study was similar to the one used in earlier study[1], Fig.1. shows a schematic diagram of the overall experimental equipment.

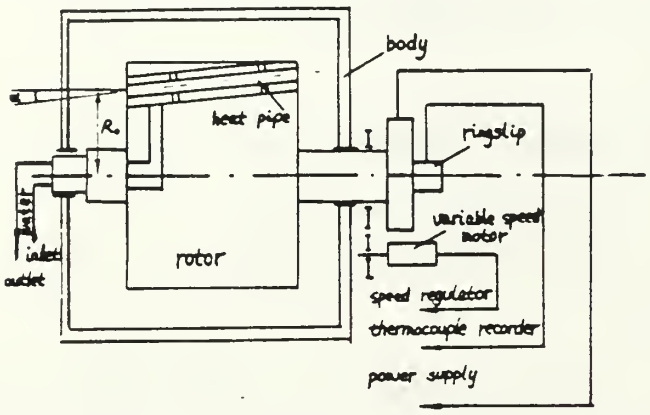

Fig.1 Schematic diagram of experimental equipment

The heat pipe was rotated using a variable speed motor, and heated electrically, and cooled by water. Further details of the experimental equipment are provide in reference[1].

OPERATION PARAMETERS

heat pipe length	1500	mm
internal diameter	19	mm
external diameter	22	mm
condenser length	410	mm
evaporator length	820	mm
min. eccentricity(R_o)	500	mm
working fluid	water	
heat pipe wall	copper	
max. power transmitted by each pipe	3	kw

THEORETICAL PROGRAM

For condensation within a non-capillary, cylindrical, inclined rotating heat pipe, forces acting on the condensation film formed over the tube surface are the gravitational force, the centrifugal force and, when the steam flow velocity is large, shear force along the vapor-liquid interface. In the operation cases, the flow patterns as shown by Fig.2.

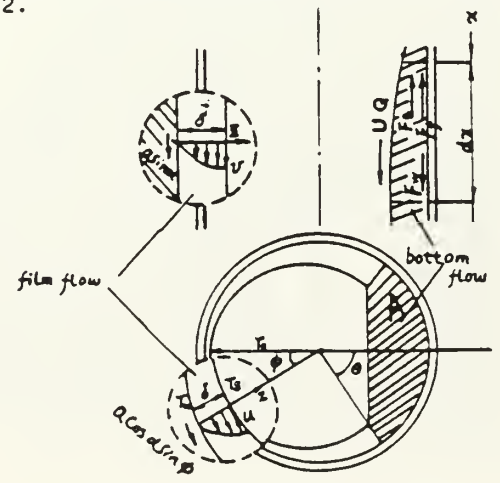

Fig.2 Analytical model and geometry

To discuss more detail, the patterns will be defined as follows: a) condensate with the film flows along the tube interior surface as shown by the broken line in Fig.2; b) a bottom flow represented by the hatch area in Fig.2, this bottom flow region, in general, blocks most of heat flow across itself and the tube surface covered by it becomes ineffective as a condensation heat transfer surface. Therefore, when calculating the overall condenser heat transfer coef. for the whole condenser section, it is not necessary to take into accout the bottom flow over the tube surface. Here we only analyzed the behavior of the bottom flow.

Condensate film flow

Analysis was made under assumptions similar to those of Nusselt's well-known basic condensation theory. Otherwise, we assume the effects of vapor shear and gravity are small enough to be negligible.

From Fig.2 we see, on the condensate act the circumferential component of centrifugal acceleration, $a\cos\alpha\sin\phi$, in the ϕ-direction ($a\cos\alpha\sin\phi$ can be found from geometrical consideration), and the longitudinal component of centrifugal acceleration, $a\sin\alpha$, in x-direction.

The momentum equations in the x-direction and ϕ-direction become:

$$x: \nu\frac{\partial^2 v}{\partial z^2}+a\sin\alpha = 0 \qquad (1)$$

$$\phi: \nu\frac{\partial^2 u}{\partial z^2}+a\cos\alpha\sin\phi = 0 \qquad (2)$$

where $a = \omega^2(R_o+x\sin\alpha)$

ω = angular velocity of heat pipe

boundary conditions:

$$u = v = 0, \text{ at the tube wall, } z = 0$$

$$\frac{\partial u}{\partial z} = \frac{\partial v}{\partial z} = 0, \text{ at vapor-liquid interface, } z = \delta$$

An energy balance on the differential element of volume $\delta r_o\, dx d\phi$ may be written as:

$$\frac{\partial}{r\partial\phi}\left(\int_o^\delta u\,dz\right) + \frac{\partial}{\partial x}\left(\int_o^\delta v\,dz\right) = \frac{\lambda(Ts-Tw)}{\rho\delta L} \qquad (3)$$

Substituting solutions u,v of equation (1) and (2) into equation (3), (3) may be expressed as:

$$\frac{\partial}{r\partial\phi}\left(\frac{a\cos\alpha\sin\phi}{\nu}\frac{\delta^3}{3}\right) + \frac{\partial}{\partial x}\left(\frac{a\sin\alpha}{\nu}\frac{\delta^3}{3}\right) = \frac{\lambda(Ts-Tw)}{\rho\delta L} \qquad (4)$$

Now introducing the following nondimensional variables:

$$X = Gx/r_o \ , \ (G = ctg\alpha)$$

$$Z = \frac{\rho a\cos\alpha L\delta^4}{3r_o\nu\lambda(Ts-Tw)} = \left(\frac{2GaPrG}{3H}\right)\left(\frac{\delta}{d}\right)^4$$

We obtain an equation for nondimensional film thickness,

$$\frac{\partial Z}{\partial X} + \sin\phi\frac{\partial Z}{\partial\phi} = \frac{4}{3}(1-Z\cos\phi) \qquad (5)$$

The boundary condition can be found from the fact that the film flow is smooth and continuous for $\phi=0$, as follows:

$$\text{for } \phi = 0, \ \frac{\partial Z}{\partial\phi} = 0, \text{ for } X = 0, \ Z = 0$$

In equation (5), $\partial Z/\partial X = 0$ as $X \to \infty$, and according to Hasan and Jakob's study[2], it is reasonable to let $\partial Z/\partial X = 0$ for $X > 3.2$. In this case, Z can easily be obtained as a function of ϕ alone as follows:

$$Z = \frac{4}{3(\sin\phi)^{1/3}} \int_0^{\phi} (\sin\phi)^{1/3} d\phi \qquad (6)$$

The length x_{x*}, such that $X = 3.2$ is extremely small for large G (e.g. $x_{x*} = 0.168d$ for $G = 9.5$), and is negligible compared to the whole length of condenser. Hence, in subsequent calculations, equation (6) will be adopted as a good approximate solution of equation (5).

Bottom flow

Now we discuss the momentum equation for an element of bottom flow over an differential length, dx, as shown in Fig.2. The forces in x-direction acting on this element are the viscous friction force at wall, Ff, the component of centrifugal acceleration, Fw, and the force due to difference in liquid level of bottom flow under centrifugal acceleration , Fa, the equation of momentum for the element of bottom flow in x-direction may be written as follows:

$$\beta \frac{d}{dx}(\rho QU)dx = Ff + Fw + Fa \qquad (7)$$

where β is momentum correction factor to accout for the non-uniform flow velocity distribution in bottom:

$$\beta = \frac{4}{3} \text{ , for } Re \leq 2300$$

$$\beta = 1.05, \text{ for } Re \geq 3000$$

An interpolated value of β is used, for $2300 < Re < 3000$.

Each term on equation (7) may be expressed as follows:

$$\beta \frac{d}{dx}(\rho QU)dx = \beta\rho\left\{2Q(dQ/dx)/A - Q^2\left(\frac{dA}{d\theta}\right)\left(\frac{d\theta}{dx}\right)/A^2\right\}dx \qquad (8)$$

$$Ff = -\tau w \theta dx d \qquad (9)$$

where $\tau w = \frac{\rho f}{8} U^2$, f is fanning's friction factor will be discussed later.

$$Fw = \rho a \sin\alpha A dx \qquad (10)$$

$$Fa = -\rho a \cos\alpha A d \sin\theta \left(\frac{d\theta}{dx}\right)\frac{dx}{2} \qquad (11)$$

We introduce the following nondimensional variables:

$$\Psi = \frac{A}{\pi r_*^2} = (2\theta - \sin 2\theta)/2\pi$$

$$\Gamma = Q/(g r_*^5)^{1/2}$$

We may obtain the differential equation for level angle, θ , of bottom flow:

$$\frac{d\theta}{dX} = \frac{8\beta\pi\Gamma G\Psi d\Gamma/dX - 4\varepsilon \sin\alpha \Psi^2 \pi^2 + f\Gamma^2\theta}{8\beta\Gamma^2 G \sin^2\theta - 4\varepsilon G \pi^2 \Psi \cos\alpha \sin\theta} \qquad (12)$$

where $\varepsilon = a/g$, Γ is the flow rate of the bottom flow. It is a result of condensate inflow from filmwise condensation region, we have

$$\Gamma = \frac{4}{3}\sin\theta(\varepsilon\sin\alpha)^{1/4}(2Ga)^{1/2}\left(\frac{3H}{2GaPrG}\right)^{3/4}\int_0^X Z_\theta^{3/4} dX \qquad (13)$$

where subscript θ denotes values at $\phi = \pi - \theta$ and Z is a quantity from equation (6).

The shear stress may be expressed in terms of the friction factor:

$$\tau w = \frac{f}{8}\rho U^2 \qquad (14)$$

The friction factor can be approximated in terms of Reynolds number [3].

$$f = a(Re)^b \qquad (15)$$

$a = 18, b = -1$, for $Re < 3000$

$a = 0.0085, b = 0$, for $Re \geq 3000$

where $Re = \frac{4Q}{\theta d U}$

Overall Nusselt number

As it can be assumed that tube surface covered by bottom flow loses its effectiveness as heat transfer surface, the mean Nusselt number, Num, over the circumference and the overall Nusselt number, Nu_M, for the whole condenser can be expressed respectively:

$$Num = \frac{1}{\pi}\int_0^{\pi-\theta} Nu\, d\phi = \frac{1}{\pi}\int_0^{\pi-\theta}\left(\frac{2GaPrG}{3HZ}\right)^{1/4} d\phi \qquad (16)$$

$$Nu_M = \frac{1}{l}\int_0^{l} Num\, dx \qquad (17)$$

Initial value for equation(12) and procedure of numerical calculation

Because the equation(12) can't be evaluated at starting point, X=0, of condensation, the following method has adopted as a recommended method for obtaining the initial value.

At first assuming initial value, $\theta = \theta_*$, then calculating Γ_* from equation(13) in terms of initial value, θ_*, a suitable tube length increment, Δx, is selected and equation(13) is used to calculate the change, $\Delta\Gamma$, in Γ. Then, selecting a suitable value of a and b for f depending on Re, equation(12) is solved to obtain the change, $\Delta\theta$, in θ in the increment Δx by finite difference method. The calculation with equation(12) and (13) are repeated for every increment until the length of condenser is reached. Lastly comparing the value of Q with $\bar{Q}$, volumetric flow rate of condensate which is evaluated in terms of the heat transfer quantity measured. If the difference between them is not small enough, assuming another initial value of θ_*, repeating the procedure of numerical calculation mentioned above until the difference is satisfactory.

COMPARISIONS BETWEEN EXPERIMENTAL AND THEORETICAL RESULTS

Before comparing experimental with theoretical results, it must be mentioned here that, in obtaining the overall coefficient of heat transfer by experiment, it is customary to use the mean of the measured tube wall tempersture as the representive temperature of the heat transfer surface when the wall temperature is not uniform. However, in this experiment as centrifugal acceleration becomes large, a bottom flow which is a large heat resistance range forms. The portion of the tube wall covered by bottom flow loses its role as the surface of heat transfer and its temperature drops significantly. Therefore, it seems more reasonable to evaluate the representative temperature of the heat transfer surface by excluding the temperature of this region covered by bottom flow when comparing the results with theoretical values obtained for a uniform wall tem-

perature.

Based on the above consideration, the experiment results are presented in Fig.3.

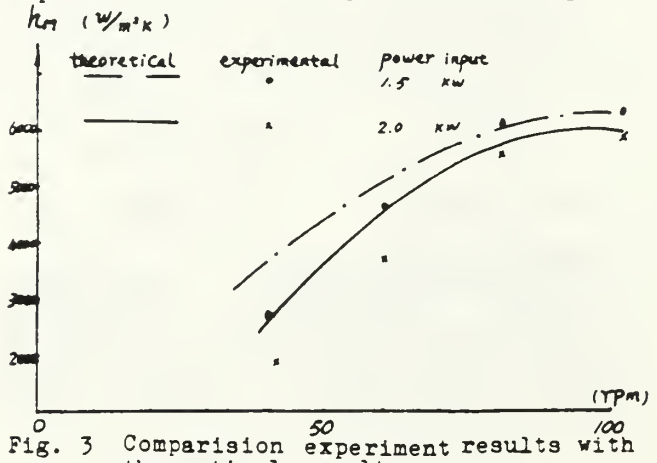

Fig. 3 Comparision experiment results with theoretical results

The experiment and theoretical values shows a good agreement,which indicate the appropriateness of the treatment of wall temperature described above. From this figure it can be seen that the overall condenser heat transfer coefficient increases definitely as the rotational speed increases, but the increasing magnitude of condenser heat transfer coef. at low rotational speed region is larger than that at high rotational speed region. The larger the rotational speed, the better the agreement between experimental and theoretical results. This is because in large rotational speed the operation conditions are better agreement to assumption—the effect of centrifugal acceleration is dominant.

CONCLUSIONS

1. In a inclined rotating heat pipe, working fluid is localized by centrifugal force, which yield circumferential temperature distribution.
2. The condenser heat transfer coefficient of the inclined rotating heat pipe affected by rotational speed, increases with the increasing of rotational speed.
3. The increasing magnitude of condenser heat transfer coefficient at low rotational speed region is larger than that at high rotational speed region.

REFERENCES

[1]CHEN JIAN and TU CHUANJING,"Theoretical and experiment research of condensation heat transfer in parallel rotating heat pipe", Preprints of Int. heat pipe symposium,Osaka,Japan,1986,pp155-165.

[2]K.E.HASSAN and M.JAKOB," Laminar film condensation of pure saturated vapors on inclined circular cylinders", Transaction of the ASME,Journal of heat transfer,Aug., 1958,pp 887-894.

[3]J.C.CHATO," Laminar condensation inside horizontal and inclined tube", ASHRAE J., Feb.,1962,pp 52-60.

[4]S.MOCHIZUKI and T.SHIRATORI,"Condensation heat transfer within a circular tube under centrifugal acceleration field",Transaction of the ASME,Journal of heat transfer, Vol.102,Feb.,1980,pp158-162.

CONDENSATION HEAT-TRANSFER MEASUREMENTS IN CO-AXIAL ROTATING HEAT PIPES

M. Katsuta*, A. S. Wanniarachchi and P. J. Marto

Department of Mechanical Engineering
Naval Postgraduate School
Monterey, California 93943, U.S.A.

*Department of Mechanical Engineering
Waseda University
Shinjuku-ku, Tokyo 160, Japan

ABSTRACT

A cylindrical, co-axial rotating heat pipe with a stepped condenser section was operated at rotational speeds of 700, 1400 and 2800 rpm, using distilled water as the test fluid. Film condensation heat-transfer data were obtained for three smooth-bore copper condenser sections having internal diameters of 23 mm, 29 mm and 37 mm. Data were also obtained for the medium-diameter tube with a smaller-diameter copper tube inserted into its vapor space to create co-current flow of liquid and vapor. Each condenser section was spray-cooled with tap water over an active length of 250 mm.

The condenser performance increased with increasing rotational speed and with increasing tube diameter. The data showed a strong influence of vapor shear, with indications of both laminar and turbulent conditions occurring, depending upon rotational speed and tube diameter. The use of a vapor-space insert increased the thermal performance by as much as 50 percent.

NOMENCLATURE

A_i	Inside heat-transfer area of condenser section
c_p	Specific heat of cooling water
h_{fg}	Specific enthalpy of vaporization
h_i	Average inside heat-transfer coefficient
k	Thermal conductivity of condensate
k_w	Thermal conductivity of tube wall material
L	Effective length of condenser section
$\dot{m}$	Mass flow rate of cooling water
Nu	Average Nusselt number on condensing side
Q	Heat-transfer rate
r_i	Inside diameter of condenser section
r_o	Outside diameter of condenser section
Re_f	Film Reynolds number
T_{ci}	Cooling water inlet temperature
T_{co}	Cooling water outlet temperature
T_s	Measured steam temperature
T_{wo}	Average outer wall temperature
μ	Viscosity of condensate
ν	Kinematic viscosity of condensate
ρ	Density of condensate
ω	Angular velocity

INTRODUCTION

During the last decade, co-axial rotating heat pipes have been used successfully in rotating components. Since the inception of the rotating-heat-pipe concept in 1969 [1], many theoretical and experimental investigations [2-7] have been conducted to better understand how it works. In 1982, Marto [8] described the concept of these devices and reviewed their heat-transfer characteristics.

The co-axial rotating heat pipe is an evacuated hollow shaft rotating about its axis. A series of studies have been conducted by Nakayama [9] to examine the effect of rotational speed and fill charge of the working fluid on the thermal performance of this device. More recently, Katsuta et al. [10] performed a similar experimental study and they suggested that the heat-transfer characteristics for the condenser and evaporator were closely related to the flow behavior, which was sensitive to the charge of the working fluid and the speed of rotation. They also suggested that the hysteresis phenomenon with rotational speed should be taken into account when designing this device.

Various investigations have been conducted to study the heat-transfer process in the condenser section of stepped-wall co-axial heat pipes rotating at high speeds. In this situation, since most of the working fluid exists in the evaporator section and only a thin liquid film covers the condenser wall, the thermal behavior is completely independent of the fill charge of liquid. In addition to this advantage, the presence of a stepped wall and high rotational speed improve upon thermal performance. Marto and Wagenseil [3] showed that the thermal performance of a smooth, cylindrical condenser section could be dramatically improved upon by tapering the condenser wall or using internal, helical fins along the cylindrical condenser surface. Marto and Weigel [4] studied several economical ways to improve upon the condenser performance by using off-the-shelf, internally finned tubing for the condenser sections. Vasiliev and Khrolenok [11] demonstrated that straight, longitudinal grooves in the condenser wall can also significantly improve thermal performance.

Marto and Wanniarachchi [12] discussed the condensation heat-transfer mechanisms for a smooth-walled cylinder and they obtained a new type of expression, which correlated the data successfully at three different rotational speeds (700, 1400, 2800 rpm), based on the presence of turbulence in the condensate film. They also suggested that the presence of axial fins enhanced heat transfer since a strong centrifugal force field generated very thin films on the flanks of the fins.

The purpose of this study is to report on some additional experimental work on stepped, co-axial heat pipes where the influence of condenser diameter and rotational speed on condensation heat-transfer mechanisms for a smooth-walled cylinder are examined. In addition, the effect of interfacial shear stress on the heat-transfer mechanism is discussed in detail

to provide more insight into the condensation heat-transfer chsracteristics of this device.

EXPERIMENTAL EQUIPMENT AND PROCEDURES

Figure 1 shows a schematic of the heat pipe apparatus which was identical to that used earlier [12]. Five copper condensers having different diameters and construction techniques were tested in this investigation. Each condenser was 295mm long with an effective length of 250 mm. Specifications of esch tube sre shown in Table 1. To check data repeatability, tube A', which was used recently by Msrto and Wanniarachchi [12], was used again in this experiment. Tube A differed from tube A' in that it was manufactured with a more precise concentricity than tube A'. Tube B* was identical to tube B except that, to eliminate the effect of interfacial shear stress, sn inner copper tube 20 mm in diameter with an effective length of 250 mm was inserted in it.

Cooling of the condenser section took place by spraying tap water along the length of the condenser using numerous jets issuing from distribution tubes placed 90 degrees apart around the condenser. This spray mechanism was located within an insulated cooling chamber so that accurate heat-transfer measurements could be obtained.

All temperstures were measured using 30-gage, type-E (chromel-constantan) thermocouples encased in Teflon and plastic insulation. Two vapor-space thermocouples were mounted inside a 3-mm-diameter, copper tuhe, which was inserted into a bracket located at the center of the glass window to ensure concentricity during rotation. One of these thermocouples projected approximstely 50 mm from the main bearing into the evaporator vapor space and the other one was located about the ssme distsnce away from the condenser end. Eight thermocouples were used to measure the condenser wall temperature distribution. They were placed at various axial and circumferential positions around the wall and were flush-mounted in the wall to measure the average wall temperature during condensation. Table 2 shows the axial and circumferential positions of these thermocouples. Care was taken to ensure that accurate temperature measurements were obtained [12].

Since the condenser heat-transfer rate wss determined using the cooling water flow rate and temperature rise through the cooling chamber, the temperature measurement of the cooling water was most critical to obtsining accurate data. To ensure the highest accuracy, a 10-junction, series-connected copper-constantan thermopile with a resolution of ± 0.003 K was used. When compared against two quartz thermometer probes, this thermopile agreed to within ± 0.02 K. The therompile probes were mounted downstream of the inlet and outlet insulated mixing boxes. In sddition to the temperature-rise

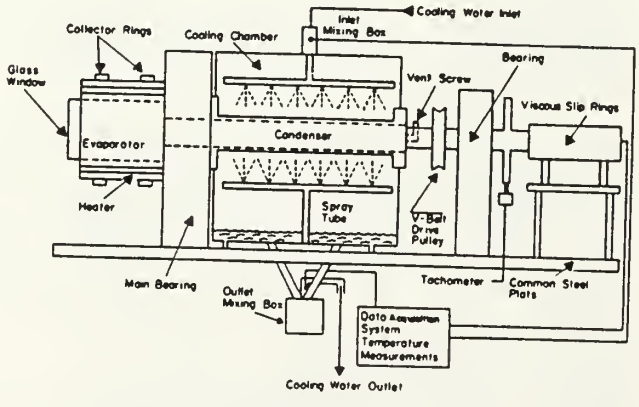

Figure 1 Schematic of Test Apparatus.

Table 1
Specifications of Experimental Condenser Tubes

Tube	Inside Dia. (mm)	Outside Dia. (mm)
A	22.9	25.0
A'	22.9	26.0
B	29.2	32.0
C	37.0	42.0
B*	29.2	32.0

NOTE: Tube B* is tube B fitted with the insert.

measurement, the cooling water inlet temperature was measured using a single thermocouple. Cooling flow rate through the cooling chamber was measured with a rotameter which had been calibrated using a weigh tank and stop watch.

An HP-9826A computer was used to control an HP-3497A data acquisition system to monitor all of the thermocouple readings. The revolving thermocouples were wired to the data-acquisition system through mercury slip rings.

Since it is well known that noncondensable gases can significantly reduce condensation heat-transfer rates in rotating heat pipes [13], care wss taken to eliminate system leaks. Repeated pressure and vacuum tests were made to ensure s tight system.

In order to improve the wettability of each copper condenser surface, the inner tube surface had to be treated to make sure that film condensation was occurring. A mixture of equal parts of sodium-hydroxide and ethyl alcohol was heated to about 80 °C and applied uniformly around the tube. The tube was then rinsed with distilled water. After this surface treatment, filling and venting were carried out following a procedure similar to the one used successfully by Marto and Weigel [4].

Operstion took place with the heat pipe in a horizontal orientation. Data were taken at three different rotational speeds and with different input power settings. Throughout this experiment, the input power to the heater was incrementally increased up to a required level while keeping the rotational speed constant. When a steady state was reached, all thermocouple readings were recorded slong with the cooling water flow rate.

The condenser heat-transfer rate was determined using the measured values of the cooling water flow rate and temperature increase:

$$Q = \dot{m} c_p (T_{co} - T_{ci}) \quad . \qquad (1)$$

A correction was made to this result to take into account frictional heating effects of the bearing and seals, and viscous dissipation effects

Table 2
Locations of Tube Wall Thermocouples

Thermocouple Number	Distance from Evaporator End (mm)	Relative Angular Position (degrees)
1	6	0
2	13	45
3	25	90
4	51	135
5	80	180
6	131	225
7	178	270
8	229	315

within the cooling water during rotation. The average inside heat-transfer coefficient of the condenser section h_i was calculated using the heat-transfer rate Q and measured values of vapor temperature T_s and the average outer wall temperature T_{wo}. From the one-dimensional radial conduction equation, the inside heat-transfer coefficent may be expressed as:

$$h_i = \left\{ A_i \left(\frac{T_s - T_{wo}}{Q} - \frac{\ln (r_o/r_i)}{2 \pi L k_w} \right) \right\}^{-1}, \quad (2)$$

where A_i is the inside surface area, r_i and r_o represent the inner and outer radii, respectively, k_w is the wall thermal conductivity and L is the effective length of the condenser.

RESULTS AND DISCUSSION

Each test condenser was operated at rotational speeds of 700, 1400 and 2800 rpm. Figure 2 shows the overall heat-transfer results for tubes A and A'. The dot-dashed lines in this figure represent the data of Nefesoglu [14] who used tube A' as a smooth-walled condenser.

From these data, it is clear that the thermal performance increases with increasing rotational speed. However, the divergence in the experimental results is very large. Tube A, which is a new one manufactured for this study, shows a markedly lower performance than the existing tube A'.

The discrepancy between the data of Nefesoglu [14] and the present data may be caused mainly by the difference of cooling water temperature measuring method. As mentioned earlier during this study, the condenser heat-transfer rate was determined using the temperature rise through the cooling chamber. Therefore, this temperature rise of cooling water is the most crucial measurement. A very accurate thermopile was adopted in this study to improve the experimental accuracy, whereas Nefesoglu [14] used five thermocouples wired in parallel only for outlet cooling water temperature measurement. In addition, the change of vapor-temperature measurement may have also affected this discrepancy. While Nefesoglu [14] measured the temperature only of the evaporator space, in this study both evaporator and condenser space vapor temperatures at the center-line were measured. Both measurement methods used in this study seem to be superior to those used in Nefesoglu's [14] study.

Next, to study the data discrepancy of tube A and A', the eccentricity of tube A' was checked. Careful measurement of the inside and outside

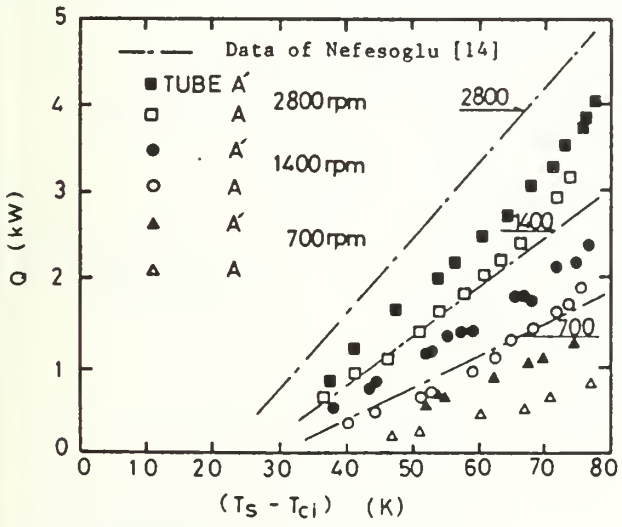

Figure 2 Comparison of Present Data with that of Nefesoglu [14].

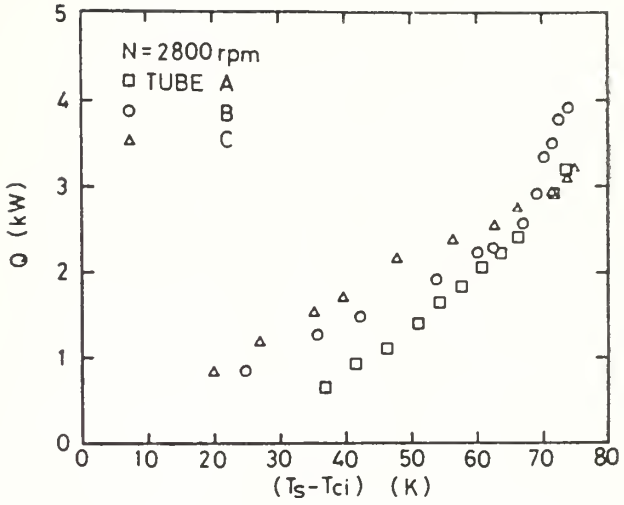

Figure 3 Effect of Tube Diameter on Overall Heat-Transfer Performance.

diameters of this tube were made with respect to the axis of rotation. From these measurements, the eccentricity of the inside diameter was determined to be about 0.1 mm, which is the same order of magnitude as the condensate film thickness during rotation. Thus, with this information, a possible explanation of this discrepancy is that the condensate film was experiencing turbulence due to inherent vibrations in the previous rotating heat pipe (tube A'), and this tube consistently gave superior performance.

In this experiment, care was taken to ensure that the new tube (tube A) had an eccentricity within 0.01 mm. In addition, a honing process was carried out on tubes A and B, after most of the lathe work was over. Only tube C didn't experience the honing process, but it was verified that its eccentricity was within the accepted accuracy.

Figure 3 shows the influence of tube diameter upon thermal performance while the rotational speed was kept constant at 2800 rpm. Notice that at low temperature differences, there is a clear trend that the performance improves as the diameter increases. On the other hand, at high temperature differences, the data show a cross-over trend that has not been recognized in a previous study [4]. These different and complicated trends will be discussed in a later part of this paper.

Figure 4 represents a comparison of the condenser wall axial temperature distribution at a

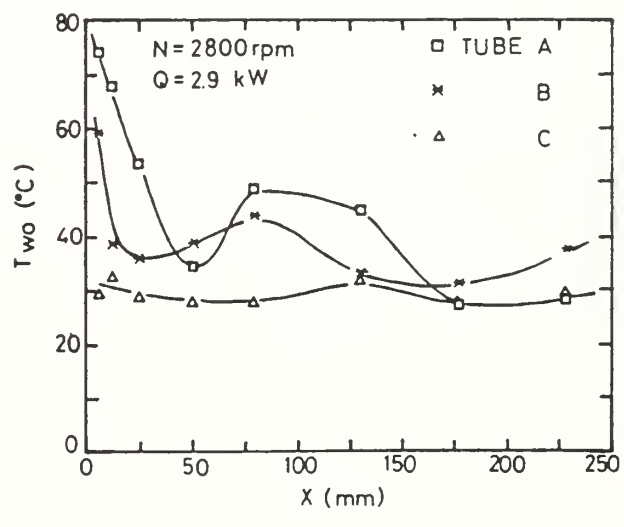

Figure 4 Variation of Local Condenser Tube Wall Temperature.

constant rotational speed of 2800 rpm and input power of 2.9 kW. Tube C has an almost flat temperature distribution along the axial direction. In contrast to this trend, the temperature distribution is irregular for the smaller diameter tubes A and B. This characteristic is very evident close to the evaporator section. This suggests that the variation of the local condensation heat-transfer coefficient may be very complicated.

It is well known that the film condensation process inside a co-axial rotating heat pipe, whose condenser section is a smooth-walled cylinder, should be similar to film condensation inside a rotating drum or to film condensation on a finite horizontal plate, and related studies and analyses were already published by Nimmo and Leppert [15-17], and later by Marto [21] and by Roetzel and Newman [19]. In each of these cases, it is assumed that the condensate that builds up on the condenser surface will flow over the edge of the condenser under the action of the hydrostatic forces on the condensate film created by either centrifugal force or the earth's gravitational force (in the case of the horizontal plate).

Nimmo and Leppert [17] originally analyzed film condensation on a finite horizontal surface, assuming laminar flow conditions in the condensate film and negligible liquid-vapor shear. They arrived at an expression for Nusselt number ($h_i L/k$) given by:

$$\overline{Nu} = 0.82 \left\{ \frac{g \rho^2 h_{fg} L^3}{k \mu (T_s - T_{wo})} \right\}^{1/4} , \qquad (3)$$

where the dimensionless grouping in the parenthesis is known as the Sherwood number. However, their experimental data gave approximately 20% lower values than their analytical expression. The recommended coefficient in the above equation was then modified from 0.82 to 0.64. This semi-empirical correlation has been generally used for designing rotational heat pipes. Of course, in order to he applicable for a rotating heat pipe, the models developed for the non-rotating, horizontal plate case should be modified by replacing the g-term by centrifugal acceleration $\omega^2 r_i$.

In this study, an attempt was performed to correlate the present data using the Nimmo and Leppert equation, and these data were plotted as average Nusselt number versus Sherwood number. However, only the data of tube C showed agreement with the correlation (with a slightly lower coefficient than 0.64). The data of the other tubes appeared to follow the Sherwood number trend in a very coarse way, but each data plot at a given rotational speed had considerable spread and an opposite sharp slope (as shown schematically in Figure 5), indicating that this correlation was not suitable for this study.

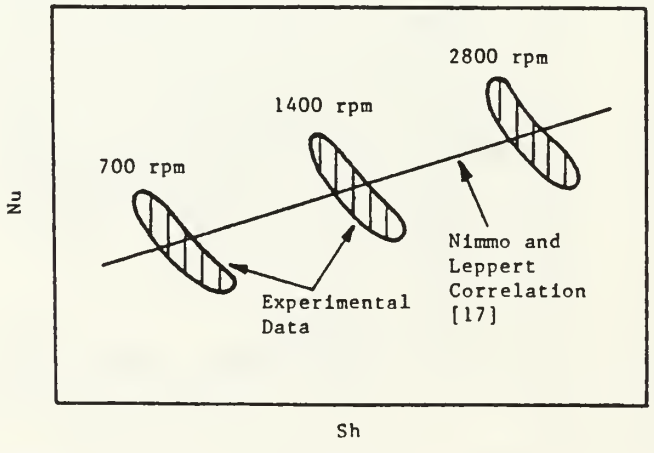

Figure 5 Schematic Representation of Data in Comparison with Laminar Theory.

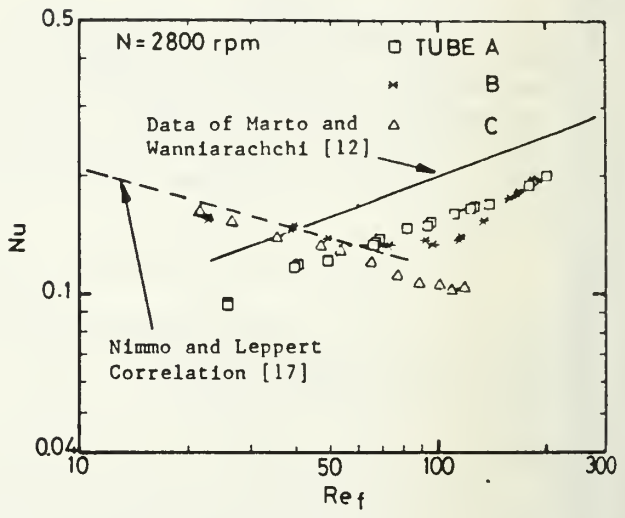

Figure 6 Effect of Tube Diameter on Condensing-Side Thermal Performance.

A possible explanation of this discrepancy is that the condensate film was not laminar. For condensation on a vertical surface, when the condensate accumulates and the film gets thicker, i.e., the film Reynolds number increases, it is possible for turbulence to occur within the film. Usually, a film Reynolds number of 1600 to 1800 (referred to as the critical Reynolds number) is required for the change to occur. Based on this information, Marto and Wanniarachchi [12] rearranged the data of Nefesoglu [14] using tube A' and plotted Nusselt number based on ω versus film Reynolds number. They obtained a new type of expression as follows:

$$\frac{h_i}{k} \left(\frac{\nu}{\omega} \right)^{1/2} = 0.045 \, Re_f^{0.328} . \qquad (4)$$

Notice that the coefficient on the right-hand side of this equation was reported incorrectly as 0.027 in reference [12]; the correct value is 0.045. In spite of the critical Reynolds number usually being in the range of 1600-1800 as mentioned above, their data showed that turbulence was perhaps occurring with a film Reynolds number range of only 25 to 300. From these facts, they concluded that the presence of the counter-current, interfacial shear stress played an important role in the change of the condensation mechanism.

To clarify the condensation heat-transfer mechanisms more in detail, all of the present data

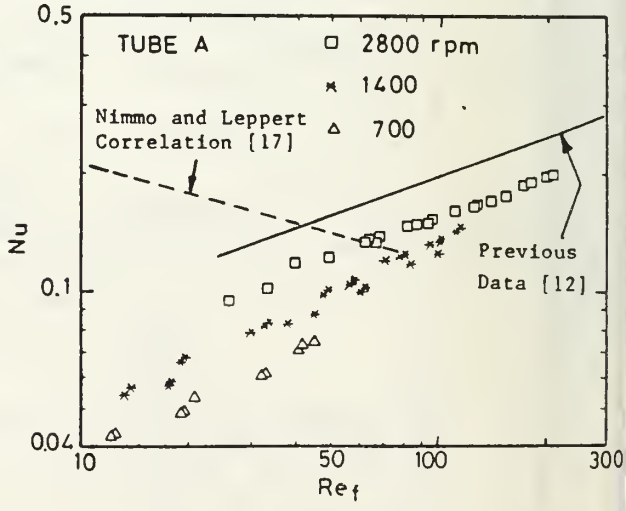

Figure 7 Effect of Rotational Speed on Condensing Side Performance of Tube A.

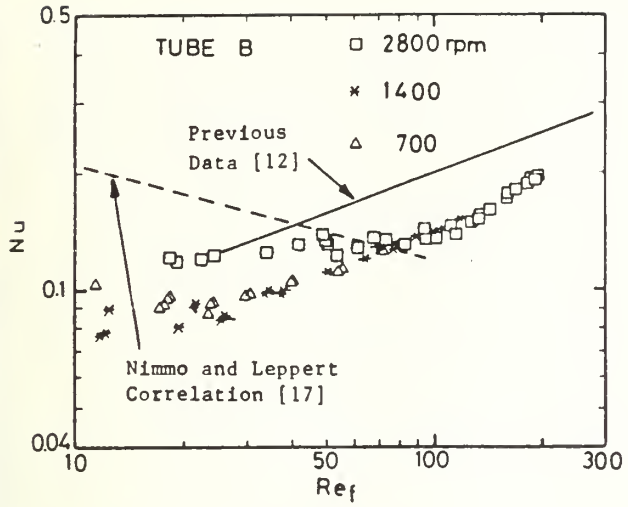

Figure 8 Effect of Rotational Speed on Condensing-Side Performance of Tube B.

are re-plotted as Nusselt number versus film Reynolds number, and these are shown in Figures 6 to 9. Figure 6 shows the variation of Nusselt number against film Reynolds number for tubes A, B and C at a constant rotational speed of 2800 rpm. Figures 7, 8 and 9 show Nusselt number versus film Reynolds number for each of the tubes as a function of rotational speed. In these figures, the solid line and dotted line represent the Marto and Wanniarachchi [12] expression for turbulent conditions (eqn. (4)) and the Nimmo and Leppert correlation [17] for laminar conditions (eqn. (3) with a coefficient of 0.64), respectively.

When the rotational speed is fixed (see Figure 6), the data of tube A, which has the minimum diameter, may be correlated by a turbulent type expression (although slightly shifted downward compared to the Marto and Wanniarachchi relationship) over the entire film Reynolds number range tested. On the other hand, different trends can be found for tubes B and C. For the medium tube B, the data follow the laminar condensation trend in the lower film Reynolds number range. However, beyond an intermediate film Reynolds number (for example, in Figure 6, the critical film Reynolds number seems to be at around 90), the data appear to be turbulent and the Nusselt number increases with increasing film Reynolds number. All the data of tube C (see Figure 9) coincide with a laminar type condensation trend. However, beyond a film Reynolds number of

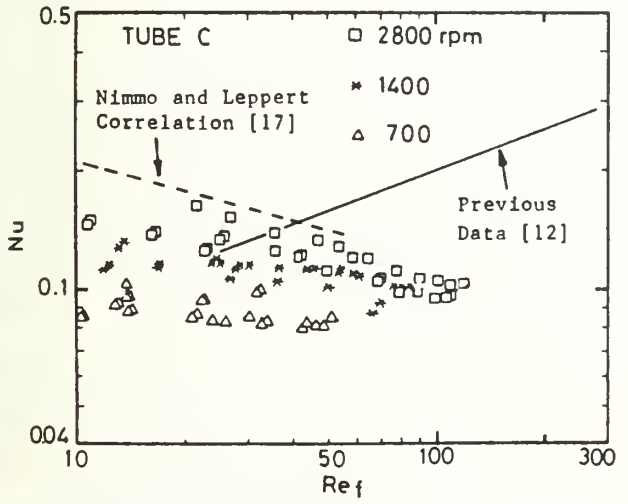

Figure 9 Effect of Rotational Speed on Condensing-Side Performance of Tube C.

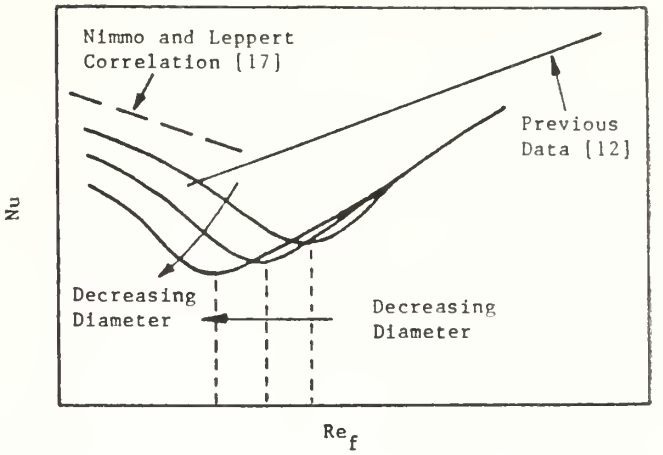

Figure 10 Schematic Representation of Tube-Diameter Effect on Condensing-Side Performance.

about 100-200, all the data appear to merge toward one expression, indicative of turbulent conditions.

Similar trends can be found from Figure 7 to 9. In the laminar condensation region, the Nusselt number increases with increasing rotational speed. When the rotational speed increases, the centrifugal force dominates the condensation mechanisms. In other words, as the rotational speed or the tube diameter or both increase, the centrifugal acceleration increases compared to gravitational acceleration. Since the tube is oriented horizontally, and the condensate must therefore flow horizontally, increased centrifugal acceleration is beneficial for effective drainage of condensate. Also, increased centrifugal acceleration makes the condensate film more and more stable, thus delaying the transition to turbulent conditions. Indeed, these effects can clearly be observed in Figures 6, 8, and 9.

These characteristics look very similar to those which occur during counter-current laminar and turbulent condensation with interfacial shear stress. Figure 10 depicts the characteristics schematically. In counter-current flow, as the vapor velocity increases, the condensate film thickens which leads to a decrease in thermal performance and to an earlier transition to turbulence. Thus, in a rotating heat pipe, for a given power input, the average Nusselt number will be smaller in a smaller-diameter tube. Also, smaller-diameter tubes will undergo transition to turbulence at a lower film Reynolds number.

Additional evidence of the strong influence of interfacial shear can be seen from the experimental results using a condenser with a tube insert. Because it was recognized that interfacial shear stress plays an adverse role in condensation heat transfer with rotation, tube B was modified to eliminate this effect. A smaller-diameter tube (20 mm OD) inserted into tube B (new tube is labelled as tube B* in Table 1) creating a 4.6-mm annular gap between them. Steam from the evaporator was constrained to enter the inner tube through a rounded entrance and travelled to the far end of the condenser. The steam then turned the corner and travelled back toward the evaporator end through the small annular gap. In this manner, the condensate and steam were in co-current flow in the vicinity of the condensing surface. As seen in Figure 11, the presence of the insert decreased significantly the temperature drop required to transfer a given heat load compared to the case without the insert (i.e., Tube B). This was especially true at high rotational speed. In fact, a comparison of Figure 12 with Figure 8 reveals that the insert increased the condensing heat-transfer performance (i.e., Nu) by a factor of 1.3 to 1.5 compared to the case without the

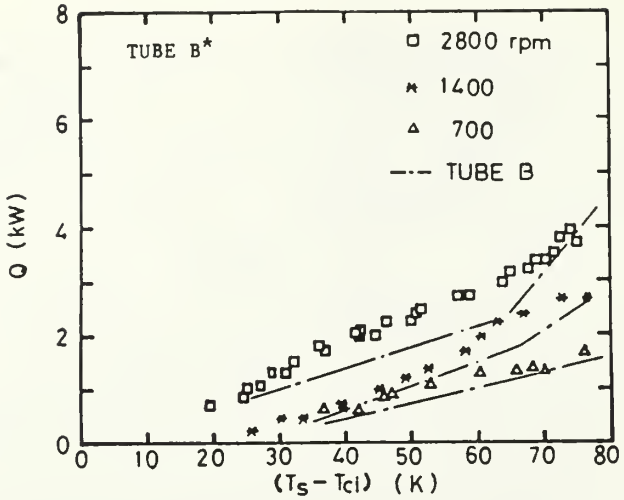

Figure 11 Effect of Co-Current and Counter-Current Flow of Vapor and Condensate on Overall Heat-Transfer Performance.

insert. It is clear that, when the vapor is in co-current flow with the condensate, there is an increase in the heat-transfer performance. Of course, further experimental information is needed in order to more fully understand the mechanisms involved.

CONCLUSIONS

From the above-described experimental results, several important conclusions were reached:

1. In a co-axial rotating heat pipe, the condenser performance increases with increasing rotational speed and with increasing inner diameter.
2. The presence of interfacial vapor shear appears to be very important, even in a high-centrifugal-force field.
3. The use of an insert within a heat pipe condenser space to change the liquid-vapor flow from counter-current to co-current improved the condensing heat-transfer performance significantly.
4. It would be very fruitful to model forced convection condensation in a high-centrifugal-force field, including the effects of interfacial shear stress.

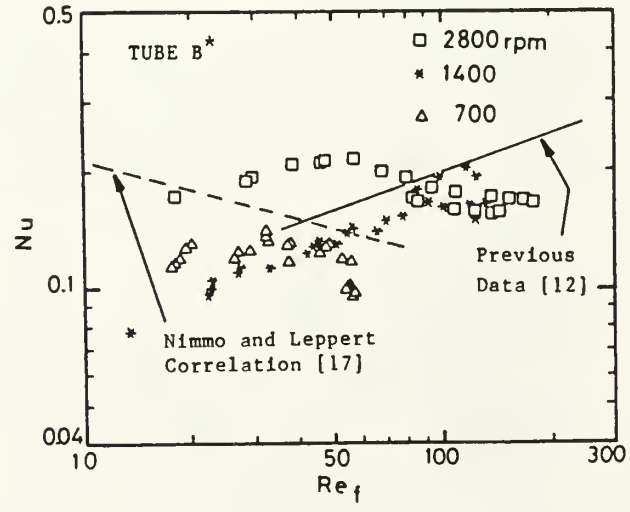

Figure 12 Condensing-Side Performance of Tube B* (with Co-Current Flow).

REFERENCES

1. Gray, V. H., "The Rotational Heat Pipe - A Wickless Hollow Shaft of Transferring High Heat Flux," ASME Paper, No. 69-HT-19, 1969.
2. Chan, S. G. and Yang, W. T., "Theory of Rotational Heat Pipe," J. of Nuclear Engineering, Vol. 25, pp. 479-487, 1971.
3. Marto, P. J. and Wagenseil, L. L., "Augmenting the Condenser Heat Transfer Performance of Rotating Heat Pipes," J. of AIAA, Vol. 17, No. 6, pp. 647-652, 1979.
4. Marto, P. J. and Weigel, H., "The Development of Economical Rotating Heat Pipe," Advances in Heat Pipe Technology, Ed. D. A. Reay, pp. 709-724, Pergamon Press, New York, 1982.
5. Maezawa, S., Suzuki, Y., and Tsuchida, A., "Heat Transfer Characteristics of Disk-Shaped Heat Pipe," ibid, pp. 725-734, 1982.
6. Niekawa, J., Matsumoto, K., Koizumi, T., Hasegawa, K., Kaneko, K., and Mizoguchi, Y., "Performance of a Revolving Heat Pipes and Application to a Rotary Heat Exchanger," ibid, pp. 225-234, 1882.
7. Ohtsuka, Y., Nakatani, W., and Yoshida, T., "Performance of a Horizontal Rotating Heat Pipe," JSME Paper No. 830-13, p. 60, 1983-10 (in Japanese).
8. Marto, P. J., "Rotating Heat Pipes," Heat and Mass Transfer in Rotating Machinery, Eds. D. E. Mezer and N. H. Afgan, pp. 609-632, Hemisphere, Washington, D. C., 1984.
9. Nakayama, W., Ohtsuka, Y., Itoh, H., and Yoshida, T., "Optimum Charge of Working Fluids in Horizontal Rotating Heat Pipes," ibid, pp. 633-644, 1984.
10. Katsuta, M., Kigami, N., Nagata, K., Sotani, J., and Koizumi, T., "Performance and Characteristics of Rotating Heat Pipes," Proc. Fifth Int. Heat Pipe Conf., Tsukuba, Tokyo, Japan, 1984.
11. Vasiliev, L. L., and Kholenok, V. V., "Study of a Heat Transfer Process in the Condensation Zone of Rotating Heat Pipes," Heat Recovery Systems, Vol. 3, No. 4, pp. 281-290, 1983.
12. Marto, P. J., and Wanniarachchi, A. S., "The Influence of Internal Axial Fins on Condensation Heat Transfer in Co-Axial Rotating Heat Pipes," Heat Transfer and Fluid Flow in Rotating Machinery, Wen-Jei Yang (Ed.), Hemisphere Publishing Corporation, pp. 235-244, 1987.
13. Daniels, T. G., and Williams, R. J., "Experimental Temperature Distribution and Heat Load Characteristics of Rotating Heat Pipes," Int. J. Heat Mass Transfer, Vol. 21, pp. 193-201, 1978.
14. Nefesoglu, A., "Heat Transfer Measurements of Internally Finned Rotating Heat Pipes," M.S. Thesis, Naval Postgraduate School, Monterey, California, 1983.
15. Leppert, G., and Nimmo, B., "Laminar Film Condensation on a Finite Horizontal Surface Normal to Body or Inertial Forces," J. of Heat Transfer, Vol. 90, pp. 178-179, 1968.
16. Nimmo, B., "Laminar Film Condensation on a Finite Horizontal Surface," Ph.D. Thesis, Stanford University, California, 1968.
17. Nimmo, B., and Leppert, G., "Laminar Film Condensation on a Finite Horizontal Surface," Heat Transfer 1970, Eds. V. Grigull and E. Hahne, p. Cs. 2.2, Elsevier Publishing Co., Amsterdam, 1973.
18. Marto, P. J., "Laminar Film Condensation on the Inside of Slender, Rotating Truncated Cones," J. of Heat Transfer, Vol. 95, pp. 270-272, 1973.
19. Roetzel, W., and Newman, M., "Uniform Heat Flux in a Paper Drying Drum with a Non-Cylindrical Condensation Surface Operating Under Rimming Condition," Int. J. Heat Mass Transfer, Vol. 18, pp. 553-557, 1975.

HELICAL GUIDE-TYPE ROTATING HEAT PIPES

Akihiro Shimizu and Shinichiro Yamazaki

Department of Mechanical Engineering,
Tokyo National College of Technology, Tokyo, Japan.

ABSTRACT

The paper describes about investigation of copper-water heat pipe with rectangular section helical coil and copper-acetone heat pipe with hollow circular section helical coil. The parameters considered in the experiments are the rotating speed, the fill ratio of the working fluid, the setting angle, etc. The measured results show that the helical guide-type rotating heat pipe works well for very low rotational speeds at small setting angles. The equivalent thermal conductivity of the heat pipe decreases when the rotational speed increases.

Observation of the working fluid in the container being transported by the helical coil was also carried out using a transparent heat pipe model. Observed results show that upper limit of setting angle depends upon the pitch of coil and rotational speed and the fill ratio of the working fluid.

NOMENCLATURE

A	cross sectional area of the container (m^2)
c	specific heat of water (J/kgK)
D	inner diameter of the container (m)
G	cooling water flow rate (kg/h)
L	effective length of the heat pipe (m)
n	rotational speed (rpm)
Q_{out}	heat output from the condenser (W)
Q_{in}	heat input to the evaporator (W)
S	surface area (m^2)
T	temperature (°C)
p	pitch of the helical coil (mm)
α	heat transfer coefficient (W/m^2K)
β	geometrical maximum angle of inclination (°)
η	heat transfer efficiency (%)
θ	setting angle of the heat pipe (°)
λ	equivalent thermal conductivity (W/mK)

Subscripts

e	evaporator
c	condenser
a	adiabatic section
1	condenser inlet
2	condenser outlet

1. INTRODUCTION

Most of conventional heat pipes for rotating machinery have no wick and utilize centrifugal force in order to transport the working fluid from the condenser to the evaporator[1],[2]. They usually have tapered wall on the inner surface of the container, which is very costly to fabricate. On the other hand, rotating heat pipes with straight wall are fabricated very easily, and have been investigated much recently [3],[4],[5],[6]. Both of them, however, have difficulty to operate when the rotational speed is very low and when the evaporator is higher than the condenser. Thus, a new type of the rotating heat pipe which has a helical coil on the inner wall of the container is proposed, which works well at very low rotational speed, which is named as "the Helical Guide-type Rotating Heat Pipe".

This paper introduces the helical guide-type rotating heat pipes and describes trend of performance obtained by experiments with parameters of the rotational speed, the setting angle, the fill ratio of the working fluid, and so on. Furthermore, observation of flowing working fluid in the container with a helical coil has been also carried out in atmosphere without heating.

2. CONCEPT OF THE HELICAL GUIDE-TYPE ROTATING HEAT PIPE

A helical coil is inserted into the container with attaching onto the inner surface of it as tight as possible. Thrust force generated by rotating is used to return the condendsate back to the evaporator from the condenser, in this type of heat pipes, instead of the centrifugal force, as shown in figure 1. The thrust force is generated by the helical coil installed on the inner surface of the container during rotating. Working fluid remained in the bottom of the condenser section is transported by the thrust force along the helical coil as a "helical guide".

The case using rectangular section helical coil and the case with hollow circular section helical coil are shown in figure 2. In the case of hollow circular section helical coil, working fluid is transported also along inside the circular section coil, and it is possible to transport liquid even if there is a clearance between the coil and the inside surface of the container.

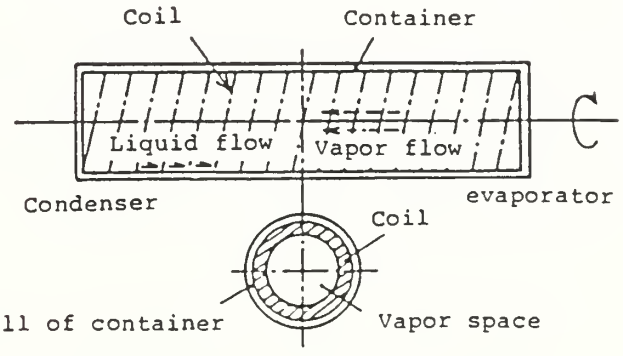

Fig.1 Helical guide-type rotating heat pipe

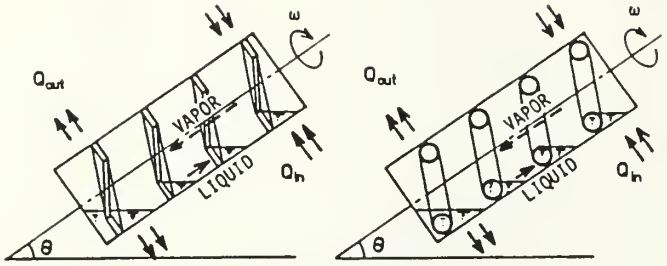

(a) the heat pipe with rectangular section helical coil

(b) the heat pipe with hollow circular section helical coil

Fig.2 Helical guide-type rotating heat pipe with rectangular section helical coil and with hollow circular section helical coil

Comparison of tapered-type rotating heat pipes and helical guide-type rotating heat pipes is shown in table 1. Rotating direction is very essential for the helical guide-type rotating heat pipes, because opposite direction of rotating makes the codensate never back to the evaporator. On the contrary, when the evaporator has to be replaced to the condenser, just opposite direction of rotating makes possible to change heat flow to opposite direction.

Table 1 Comparison of tapered-type rotating heat pipe and helical guide-type rotating heat pipe

	tapered-type	helical guide-type
to return condensate	centrifugal force	thrust force of coil
fabrication	costly	only insert a coil
rotating direction	either will do	depended on winding direction of coil
available speed	high and medium	low

As an example of applications, cooling a hot roller rotating at low rotational speed is proposed as shown in figure 3. In this figure, two helical coils of same length but different direction of winding each other are used in the container. Heat from the hot roller to shaft as a heat pipe is expected to be transferred mainly not to bearings but to radiators.

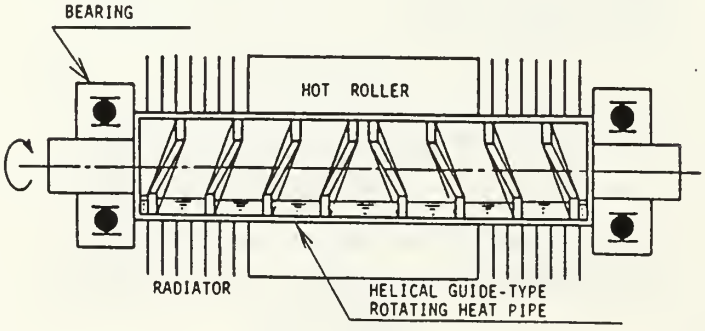

Fig.3 An application of the helical guide-type rotating heat pipe to cooling hot roller rotating at low speed

3. EXPERIMENTAL APPARATUS AND PROCEDURE

Two kinds of helical guide-type rotating heat pipes have been designed. Shape and size of two heat pipes are shown in figure 4 and figure 5. All the containers are made of copper. Figure 4 shows the heat pipe with rectangular section helical coil and the coil itself which is 9mm of pitch and is made of aluminum. Figure 5 shows the heat pipe with hollow circular section helical coil and the coil itself which is 28mm of pitch and is made of copper. Endcaps of both heat pipes are made of copper and were brazed to copper pipes as the containers. The heat pipe with hollow circular section helical coil has a vacuum valve for changing the fill ratio of the working fluid.

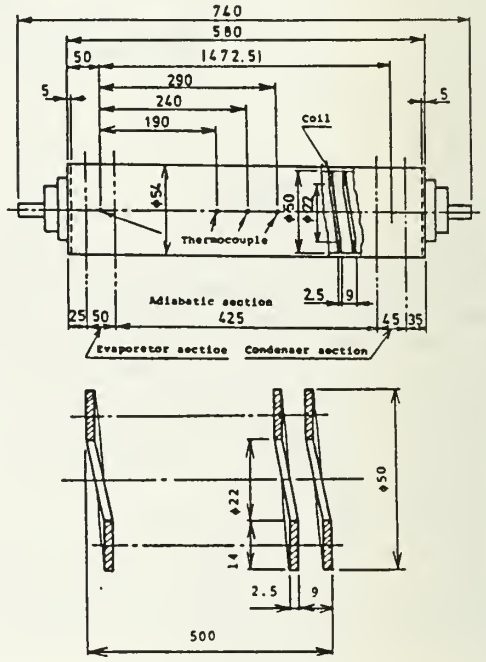

Fig.4 Heat pipe with rectangular section helical coil and the coil itself

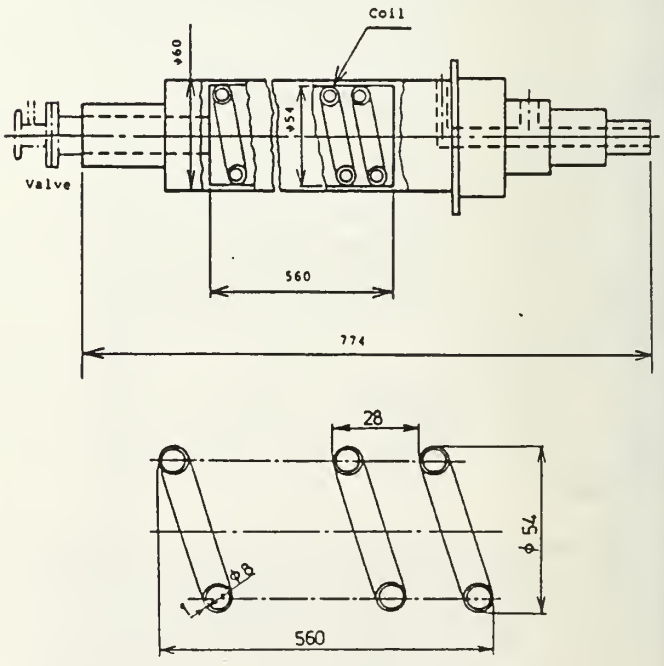

Fig.5 Heat pipe with hollow circular section helical coil and the coil itself

Materials of the heat pipes are shown in table 2. Compatibility between aluminum and water in the heat pipe with rectangular section helical coil is not good, so the experiments of it were carried out in a short period.

Table 2 Materials of the heat pipes

	with rectangular section coil	with hollow circular section coil
container	copper	copper
endcaps	copper	copper
coil	aluminum	copper
working fluid	distilled water	acetone
vacuum valve		stainless steel

Two heat pipes with rectangular section helical coil and filled with distilled water were made. One was evacuated to a pressure of 42 Torr(low vacuum) just before pouring working fluid in it and the fill ratio of it was 19.5% of the internal volume of the container with the coil, and the other was to a pressure of 5×10^{-5} Torr and the fill ratio was 19%.

The heat pipe with hollow circular section helical coil was evacuated to a pressure of 5×10^{-5} Torr and the fill ratios of the working fluid were 5, 9 and 21% by changing working fluid. Working fluid was acetone due to compatibility of materials.

A schematic diagram of overall experimental apparatus for the heat pipe with rectangular section helical coil filled with water is shown in figure 6. The heat pipe was supported by two bearings and was rotated using a variable speed motor. The regular flow of cooling water was supplied by a pump and a given quantity of electric power was supplied to the heater. In the cooler, water entered from upper inlet and was sprinkled on the surface of the condenser section of the heat pipe. In the case of the other heat pipes, the cooler was filled with water from lower inlet, and then warmed water flowed out of the cooler through upper outlet.

After reached the steady state, all the thermocouples were recorded. Temperature measurements were made with 0.32mm, copper-constantan thermocouples. The condenser heat transfer rate was determined using the measured values of the cooling water flow rate and temperature difference between outlet and inlet.

$$Q_{out} = Gc(T_2-T_1)/3600 \qquad (1)$$

In experiments with the latter cooler, to take account heat by friction between the surface of the heat pipe and seals, a correction was made to this result.

Equivalent thermal conductivity, heat transfer efficiency and heat transfer coefficient of the condenser were defined as the following.

$$\lambda = Q_{out}l_e/A(T_e-T_c) \qquad (2)$$

$$\eta = Q_{out}/Q_{in} \times 100 \qquad (3)$$

$$\alpha_c = Q_{out}/S_c(T_a-T_c) \qquad (4)$$

where it was assumed that temperatures of vapor and wall of the container in adiabatic section were same.

To visualize the state of flowing working fluid, transparent models made of acrylic tube similar to the heat pipe were used with colored water in atmosphere without heating. In the case of hollow circular section helical coil, the coil inserted was made of transparent glass because observation of flow inside the hollow coil was required. In this model, to observe mainly the state of flow inside the hollow coil, the outer diameter of the coil was shorter than the inner diameter of the container and the difference of the diameters was about 0.5mm.

4.EXPERIMENTAL RESULTS AND DISCUSSION

The heat pipe with rectangular section helical coil was operated at rotational speeds of 0, 50, 100, 120 and 200 rpm, setting at angles of 0, 10, 20, 30 and 45° from horizontal position. The heat pipe with hollow circular section helical coil was operated at rotational speeds of 100, 200, 300, 400 rpm, and its setting angles were 0, 15, 30 and 45°.

Visualization of flowing liquid using a model

In the case of rectangular section coil, the states of flowing liquid that is contained as much as 10% of the internal volume of the container at each condition, at 0 to 45°of setting angle and at 50, 100, 200, 300 and 400 rpm of rotational speed are shown in figure 7. Observed results made it clear that working fluid could be transported at up to n=400rpm for θ =0°,up to 300 rpm for 15° and up to 200 rpm for 30° or 45°.

Photographs taken in observation for a model of the heat pipe with hollow circular section helical coil are shown in figure 8(a),(b). The liquid is usually ascending through the inside of the hollow coil, as shown in figure 8(a). In the case of figure 8(b), the liquid is transported mainly through the outside of hollow circular section coil on condition of n=300rpm, θ =10°, fill ratio 21% and p=56mm. It was found that liquid was transported through not the inside but the outside of hollow circular section coil on conditions that the heat pipe was operated at angles smaller than 10° and at rotational speeds higher than 300rpm and fill ratio was 21% and p=56mm.

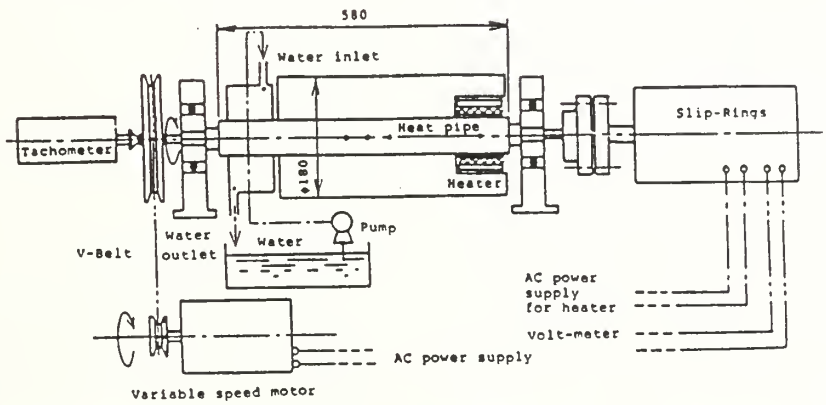

Fig.6 Schematic of overall experimental apparatus

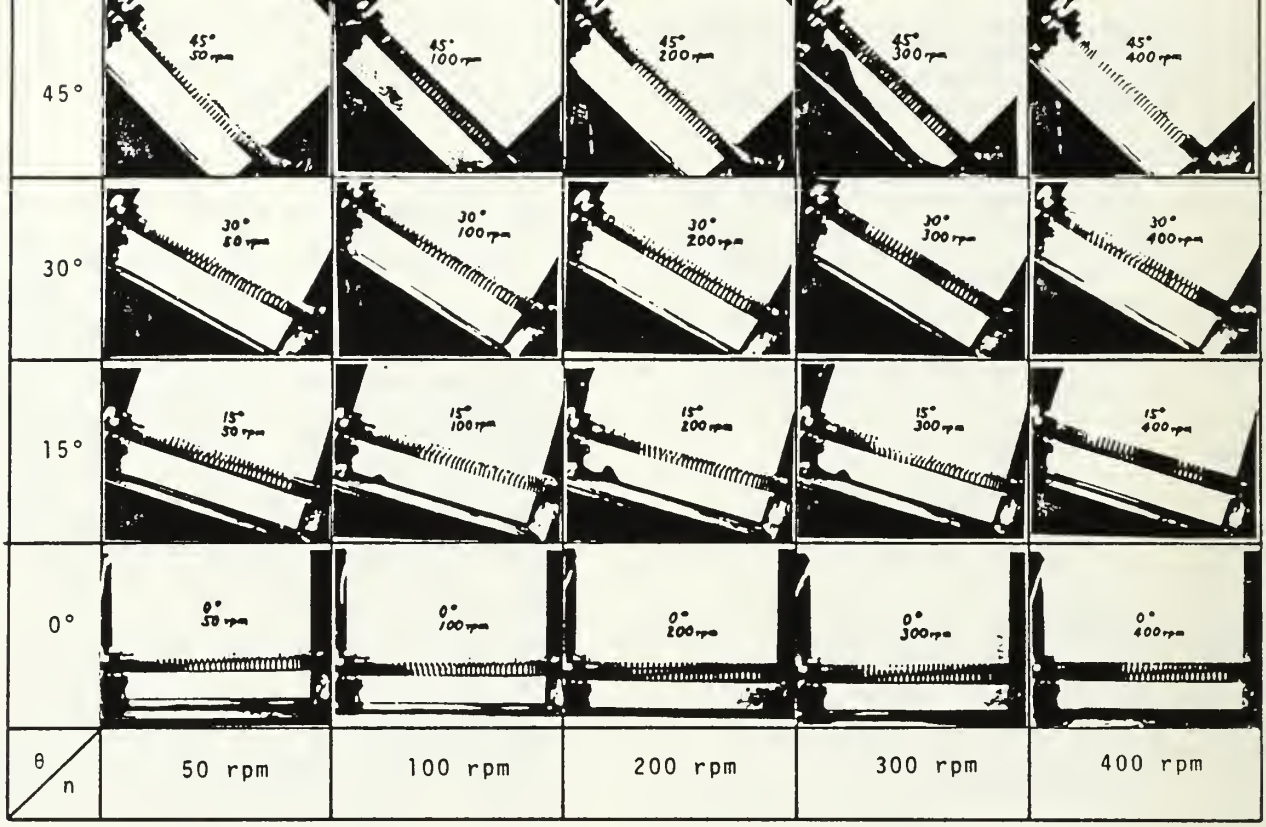

Fig.7 Liquid being transported by the rectangular section helical coil(p=9mm, fill ratio 10%)

(a) p=14mm
fill ratio 5%
n=50rpm
θ =75°

flow through the inside of the coil

(b) p=56mm
fill ratio 21%
n=300rpm
θ =10°

flow through the outside of the coil mainly

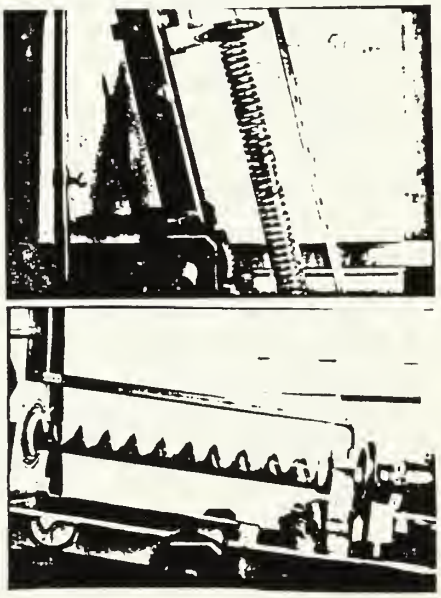

Fig.8 Liquid being transported through the inside or the outside of hollow circular section helical coil

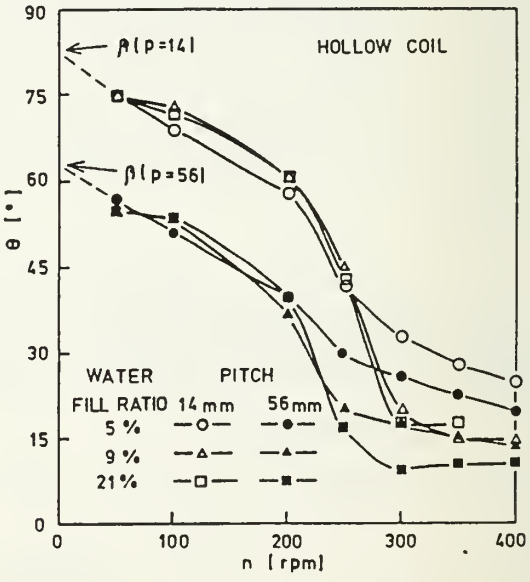

Fig.9 Upper limit of setting angle to transport liquid using hollow circular section helical coil

Upper limit of setting angle

The available angles of inclination of heat pipe were checked up at several rotational speeds with parameters of pitch of the coil and fill ratio of the liquid. Upper limit of liquid transport on each condition is shown in figure 9. The results show that upper limit of liquid transport decreases with increase of rotational speed. When the rotational speed is 300 or 400rpm and fill ratio is 9 or 21%, upper limit of inclination decreases greatly. Geometrical maximum angle of inclination determined by pitch is

expressed as

$$\beta = \tan^{-1}(2D/p) \qquad (5)$$

Maximum angle of inclination is reduced from β by rotational speed and so on. When the rotational speed nearly equals to zero, θ approaches to β. In the case that pitch is 14mm, β calculated is 83°. As for 56mm, β calculated is 63°. These values are also estimated from experimental results as shown in figure 9.

Temperature distribution and degree of vacuum

On the condition of θ=30° and Q_{in}=40W, comparison of wall temperature distribution of the heat pipes with rectangular section helical coil which were evacuated to low vacuum and high vacuum before pouring working fluid is shown in figure 10. It was certified that the heat pipe of low vacuum didn't work well, because it didn't have nearly horizontal line in temperature distribution of adiabatic section.

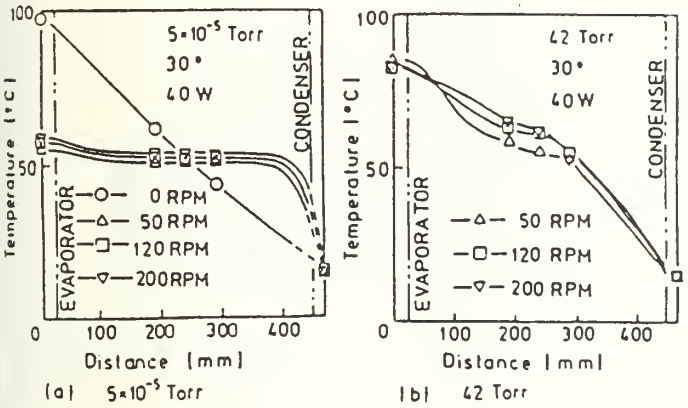

Fig.10 Comparison of temperature distributions of heat pipes with rectangular section helical coil evacuated to different pressures just before pouring working fluid

Temperature distribution of the heat pipe with hollow circular section coil on the condition of θ =30° and Q_{in}=85W are shown in figure 11. In the case of n=300 and 400rpm, it is found that the evaporator was dried out.

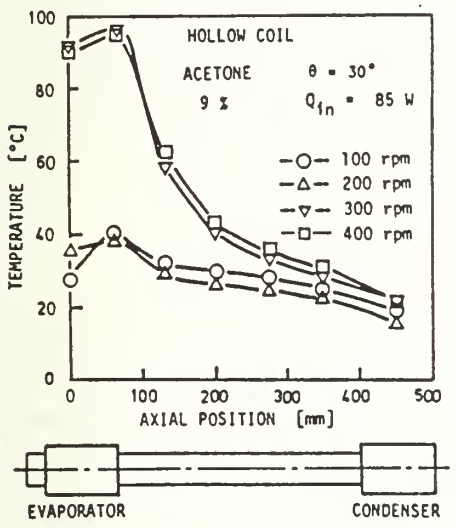

Fig.11 Temperature distribution of the heat pipe with hollow circular section helical coil

Equivalent thermal conductivity

Equivalent thermal conductivity of the heat pipe with rectangular coil on the condition that Q_{in}=40W, is shown in figure 12. The result shows that the value of equivalent thermal conductivity decreases when the setting angle or the rotational speed increases except n=0rpm. As for 0rpm, it is almost as same as thermal conductivity of copper proper. In the case of the heat pipe with hollow circular section helical coil, it is shown in figure 13. At smaller angles or lower rotational speeds, the values of equivalent thermal conductivities are high.

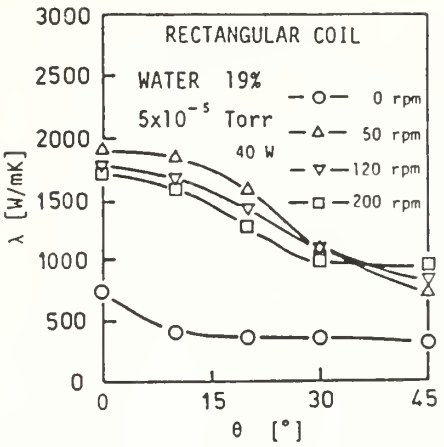

Fig.12 Equivalent thermal conductivity of the heat pipe with rectangular section helical coil

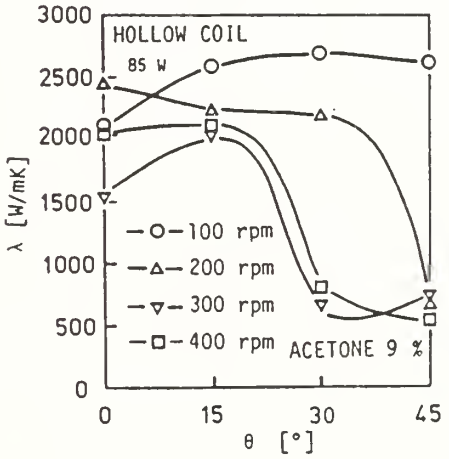

Fig.13 Equivalent thermal conductivity of the heat pipe with hollow circular section helical coil

Heat transfer efficiency

Some examples of heat transfer efficiency of each heat pipe are shown in figure 14,15 and 16. Figure 14 shows that sufficient heat flow rate is obtained at the rotational speed less than 200rpm and heat flow rate decreases with increase of the setting angle, in the case with rectangular section coil. In the case of hollow circular section coil, at the rotational speed of 100rpm, very high heat transfer efficiency is obtained at each setting angle examined, as shown in figure 15. On the other hand, at the rotational speed of 400rpm, heat transfer efficiencies are influenced greatly by the fill ratio of the working fluid, as shown in figure 16.

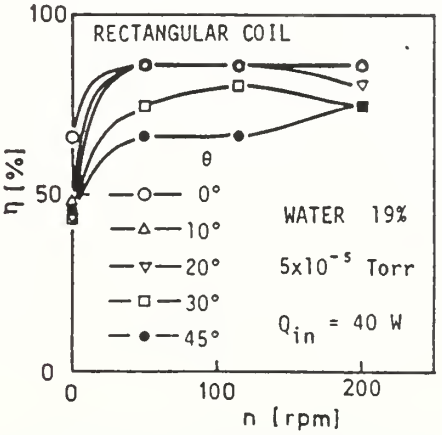

Fig.14 Heat transfer efficiency of the heat pipe with rectangular section helical coil

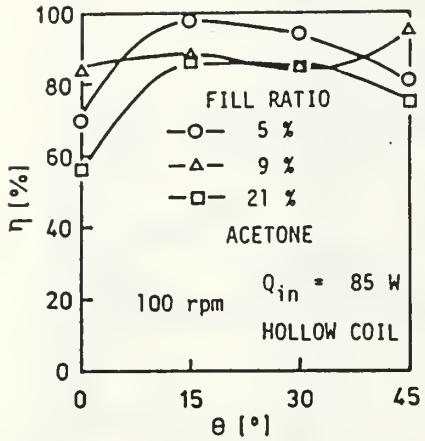

Fig.15 Heat transfer efficiency of the heat pipe with hollow circular section helical coil at n=100rpm

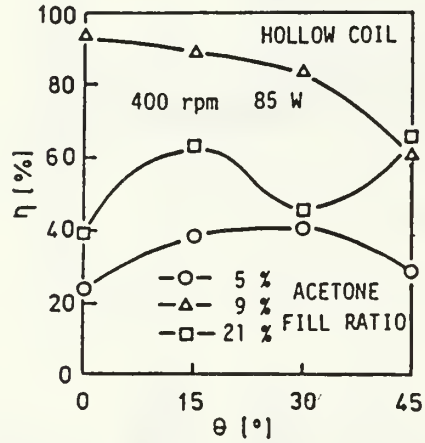

Fig.16 Heat transfer efficiency of the heat pipe with hollow circular section helical coil at n=400rpm

The quantity of working fluid

The fill ratio has influence on thermal performance of the heat pipes, as shown in figure 16. The heat transfer coefficients of the condenser at θ=30° are shown in figure 17. In the case of 21% of fill ratio, heat transfer coefficient is very low at higher rotational speeds.

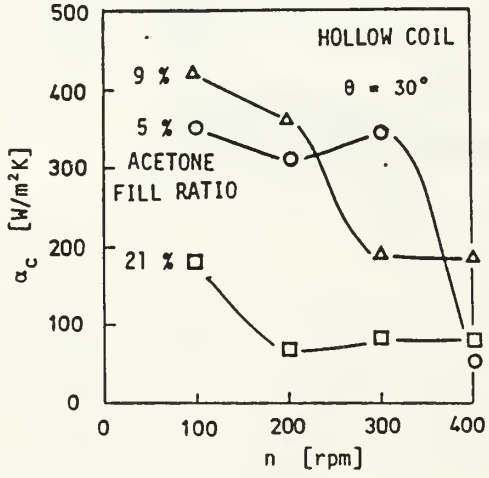

Fig.17 Heat transfer coefficient of the condenser of the heat pipe with hollow circular section helical coil (θ=30°)

When the quantity of working fluid is much and the heat pipe is inclined and the rotating speed is high, puddle of liquid is formed on the condenser surface. Most of the condenser surface is beneath the liquid puddle or thick film of liquid flowed out from the puddle during rotation, as shown in figure 18, and then it is supposed that its thermal resistance becomes high.

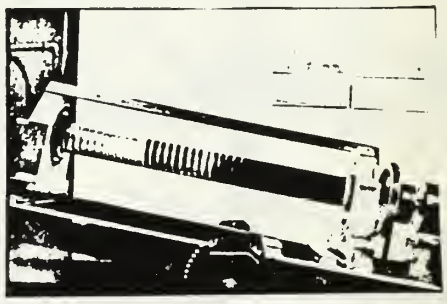

Fig.18 Long thick film and puddle covering the inner surface of the container due to high fill ratio and rotational speed(fill ratio 21%, θ=10°,n=400rpm,p=14mm)

5.CONCLUSION

From the experimental results for the helical guide-type rotating heat pipes, the following have been obtained.

(1) At very low rotational speeds.this type of rotating heat pipes work well.
(2) The smaller the rotating speed except for 0 rpm and the setting angle are, the higher the equivalent thermal conductivity becomes.
(3) Higher vacuum just before pouring working fluid gives high thermal performance.
(4) At higher rotational speeds and fill ratios of the working fluid and setting angles, heat transfer coefficients of the condenser are relatively low.
(5) As for pitch of the coil, the shorter the length of the pitch is, the higher the liquid is transported.
(6) Maximum setting angle of the heat pipe depends upon pitch of the coil.

REFERENCES

[1] Gray, V. H.,"The Rotating Heat Pipe - A Wickless, Hollow Shaft for Transferring High Heat Fluxes", ASME Paper No. 69-HT-19, 1969, pp. 1-5.
[2] Marto, P. J. and Wagenseil, L. L., "Augumenting the Condenser Heat Transfer Performance of Rotating Heat Pipes", Proceedings of the 3rd International Heat Pipe Conference, Palo Alto, 1978.
[3] Marto, P. and Weigel, H.,"The Development of Economical Rotating Heat Pipes", Proceedings of 4th International Heat Pipe Conference, London, 1981.
[4] Katsuta, M., Kigami,H., Nagata,K. Sotani,J. and Koizumi, T.,"A Study of Performance and Characteristics of the Rotating Heat Pipe", Proceedings of 5th International Heat Pipe Conference, Tsukuba,1984.
[5] Nakayama, W.,Ohtsuka, Y.,Yoshikawa, T.,"The Effectof Fine Surface Structures on the Performance of Horizontal Rotating Heat Pipes", Proceedings of the 5th International Heat Pipe Conference, Tsukuba,1984.
[6] Pokorny, B., Polasek, F., Schneller, J. and Stulc, P.,"Heat Transfer in Co-axial and Parallel Rotating Heat Pipes", Proceedings of the 5th International Heat Pipe Conference, Tsukuba,1984.

EXPERIMENTAL HEAT TRANSFER CHARACTERISTICS OF A ROTATING HEAT PIPE WITH AN AIR-COOLED CONDENSER

REDDY R.S*; VENKATESWARLU P.*; SASTRI V.M.K.**

* Heat Transfer Laboratory, Corporate Research and Development Division, Bharat Heavy Electricals Limited, Hyderabad - 500 593, India.

** Heat Transfer and Thermal Power Laboratory, Department of Mechanical Engineering, Indian Institute of Technology, Madras - 600 036, India.

ABSTRACT

Experimental performance characteristics of a rotating heat pipe as influenced by design parameters like heat input, rotational speed and inclination of heat pipe axis are presented. The range of these parameters which promote heat transfer as well as the limiting factors that critically deteriorate the rotating heat pipe performance is given. The results are in qualitative agreement with the existing correlation for the critical speed at which transition to solid body rotation of the fluid inside occurs. It is established that the speed at which heat pipe returns to normal operation during decreasing speeds is independent of heat inputs or external cooling intensity on the condenser but is a mild function of inclination. It is observed that vapour flow instabilities as recorded by fluctuating wall and vapour temperatures at low speeds are more pronounced when the heat pipe is slightly inclined to the horizontal.

INTRODUCTION

Interest in the rotating heat pipe principle, first proposed by Gray [1] and its application to practical systems has steadily grown. In particular, owing to its high heat transfer rates and fast thermal response, the rotating heat pipe has received much attention as an effective device for cooling rotors of electrical machines.

Earlier experimental studies on the rotating heat pipe are mainly due to Marto [2], Marto and Weigel [3], Ohtsuka et al. [4], Nakayama et al. [5], Katsuta et al. [6], Krivosheev et al. [7] and Curtila and Chataing [8] among others. While Ohtsuka and coworkers have developed an important correlation to predict the critical speed marking the beginning of transition of flow inside the heat pipe to solid body rotation, Katsuta et al. made visual observations of flow mechanism in addition to verification of the correlation proposed by Ohtsuka et al [4]. The investigations further suggest that there is an 'hysteresis effect' peculiar to rotating heat pipe which significantly alters its performance during variable speed operation. Purely fluid dynamical studies have also been carried out by Karweit and Corrsin[9] to understand the underlying flow pattern and instabilities in a partially filled, horizontal cylinder. We thus know from these studies that the flow behaviour inside and the overall heat transfer capability of a rotating heat pipe are intimately related.

Due to limited experimental contributions in this area and in view of the specialized nature of its application in the thermal control of rotating machinery, it is felt very desirable to investigate in detail the influence of various design variables on the heat transfer rates of a rotating heat pipe.

The purpose of this paper is to report detailed temperature measurements and determination of the inside heat transfer coefficients in the condenser and evaporator zones of a straight, smooth rotating heat pipe.

The following physical characteristics distinguish the present work from earlier studies:

1. The heat pipe has a high aspect ratio (length to diameter ratio is 33).
2. The range of rotational speeds extends from 0 to 2200 rpm.
3. The condenser consists of a large integrally finned section cooled by an external fan.

TEST HEAT PIPE

The rotating heat pipe in the present work is a 850 mm long, 35 mm O.D., 25.4 mm I.D., straight smooth copper tube, the two ends of which are closed with stainless steel end caps by means of electron beam welding to minimise end losses. Provision is made at one end for filling the tube with a measured quantity of working fluid. The air-cooled condenser section consists of an integrally finned copper body with closely spaced circular fins. It is shrunk-fit on the heat pipe, ensuring good thermal contact. The evaporator section is made of strip nichrome heater uniformly wound on the heat pipe and insulated with a semica-therm tape. Power is supplied through a pair of spring-loaded copper-brushes.

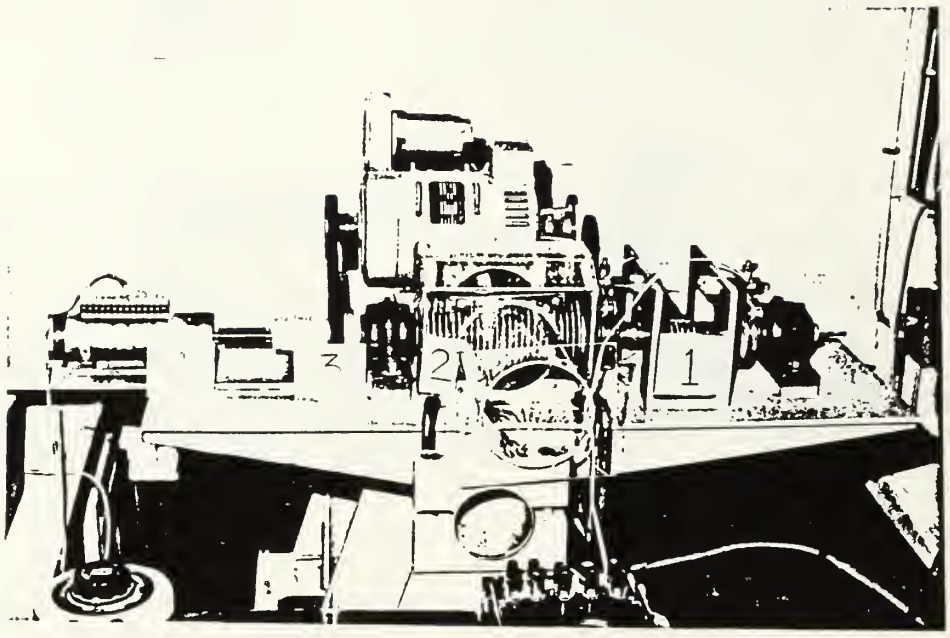

1. Evaporator 2. Condenser 3. V-belt Drive 4. Slip Ring

Fig. 1 Photograph of the Test Set-up

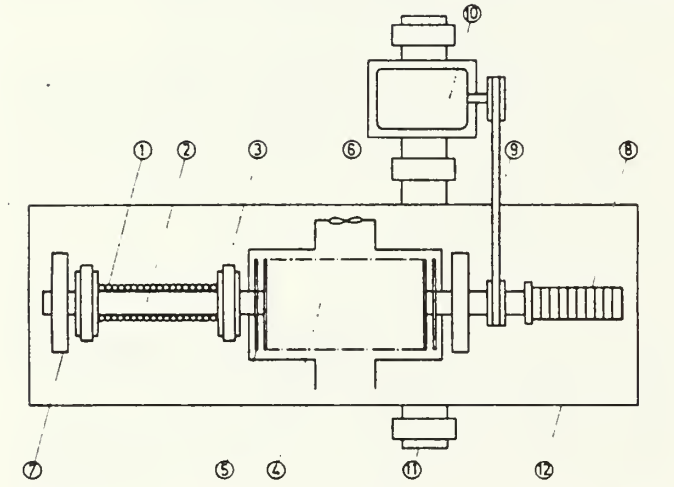

Fig. 2 Schematic Diagram of the Rotating Heat Pipe Test Set-up

Teflon insulated 32 guage copper-constantan thermocouples are used to measure the wall temperatures of evaporator and condenser as also the saturation temperature of the working fluid. For the later purpose, a grounded thermocouple in a stainless steel tube is inserted at the evaporator end along the axis of the heat pipe. The thermocouple output is picked up by a mercury wetted slipring mechanism coupled to the heat pipe at the condenser end.

Before assembling the heat pipe on the test stand, it is evacuated close to 10^{-6} torr by an evacuating - filling rig and filled with the desired quantity of highly pure distilled water. The processes of heating, cooling with liquid Nitrogen and evacuating are repeated in that sequence four times in order to expel dissolved gases and maintain a high vacuum level inside the heat pipe. The heat pipe is assembled along with the slip-ring mechanism between self-aligned ball-bearings on a test stand whose inclination can be changed easily. An adjustable, variable speed, 3000 rpm d.c. motor provides the drive through a V-belt. The test stand is mounted on cushion rubber pads to eliminate the effect of vibrations on the heat pipe performance. The experimental apparatus is shown in the accompanying photograph in Fig. 1 along with a detailed schematic diagram in Fig. 2.

EXPERIMENTAL PROCEDURE

The temperature is measured by a digital thermometer having a resolution of $0.1^{\circ}C$ and an accuracy of $\pm 0.5^{\circ}C$. The thermocouples are standardised and the readings cross-checked by Memocal microprocessor based digital thermometer. The heat losses to the surroundings from the evaporator are monitored by a remote sensing infrared thermometer. The heat losses are found to be about 7 percent of the total power input to the evaporator. The vapour temperature, the evaporator and condensor surface temperature at six locations are measured as the speed and heat input are varied. Additionally, the vapour temperature, the maximum evaporator temperature and the minimum condenser temperature are recorded on a multipen recorder to facilitate measurement of transient thermal response of the heat pipe for a step change in speed and to detect the temperature fluctuations. The speed is varied between 0-2200 rpm in steps of 200 rpm. The step change is however suitably adjusted whenever there are sharp changes in the thermal condition of the heat pipe. It takes about 15 minutes to reach steady state at each speed interval.

Initially, the experiments are conducted with an open condenser cooled by its own fanning action but heat input limited to 500 watts at a vapour temperature of 80°C. The tests are later repeated with a shrouded, forced-cooled condenser (as shown in photograph) when the heat inputs could be increased by two times for the same vapour temperature.

For the present experiments, the fill ratio is 0.3, i.e. the working fluid (pure distilled water) occupies 30 percent of the total inside volume of the heat pipe. Studies of Nakayama et al. [5] show that this fill ratio is the optimum from the point of view of achieving stable operation over a wide range of rotational speeds and avoiding local dryout of the evaporator. Too low a fill ratio causes somekind of a 'thermal runaway' at even very low speeds (less than 700 rpm) while too high fill charge makes the heat pipe operate at relatively elevated temperature due to the presence of a thick liquid layer on the interior wall.

The heat pipe is set in the horizontal position with the help of a spirit level indicator. Slight changes in the position are found to affect the heat pipe performance. Later experiments on the rotating heat pipe at different inclinations (with the evaporator always at the bottom) showed significant fluctuations in the measured temperatures.

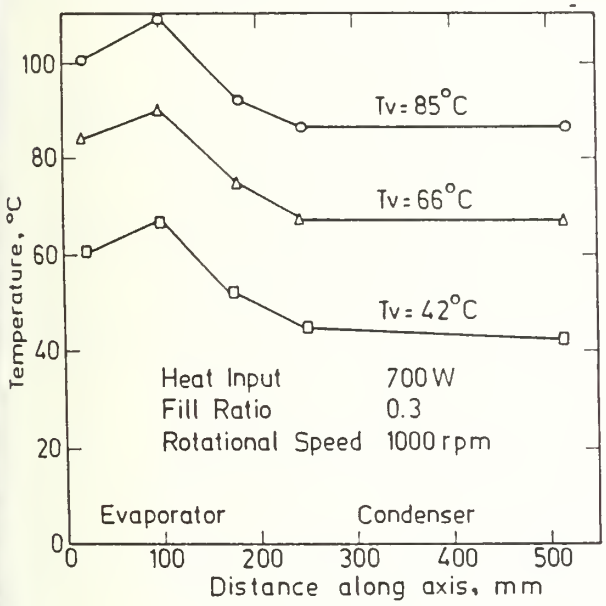

Fig. 3 Temperature Distribution along the Heat Pipe Axis

The temperature distribution along the wall of the heat pipe for a typical case is shown in Fig. 3. The temperature is fairly uniform over the condenser wall but it varies appreciably along the evaporator with the maximum occuring at the centre of the evaporator section.

RESULTS AND DISCUSSION

The results for the open condenser, cooled by its own fanning action are considered first. The maximum temperature difference, $\Delta T = T_e - T_c$, between the evaporator and condenser is plotted in Fig. 4 against the rotational speed. ΔT is uniform upto 1200 rpm but begins to increase above this speed. Steep and sudden rise in ΔT is found at 1600 rpm. The steady increase in ΔT in the intermediate speed range of 1200-1600 rpm is attributed to transition of internal flow behaviour from a stratified liquid pool scraped partially along the circumference to one of a 'disking' flow or formation of a regular axial ripples or stripes, visually observed by Karweit and Corrsin[9] and Ohtsuka et al. [4].

Beyond 1600 rpm, however, the sharp shoot up in ΔT significantly alters the heat pipe performance. At 1800 rpm, the lqiuid transforms into an annular motion so that the complete system is under solid body rotation. During this period, there is a marked worsening in the condenser behaviour due to the presence of a thick liquid layer on the wall causing increased thermal resistance on the condenser. Also, this can be attributed to inadequate return of the working fluid to the evaporator under the influence of centrifugal action. Above 2000 rpm, there is a marginal decrease in ΔT as shown in Fig. 4.

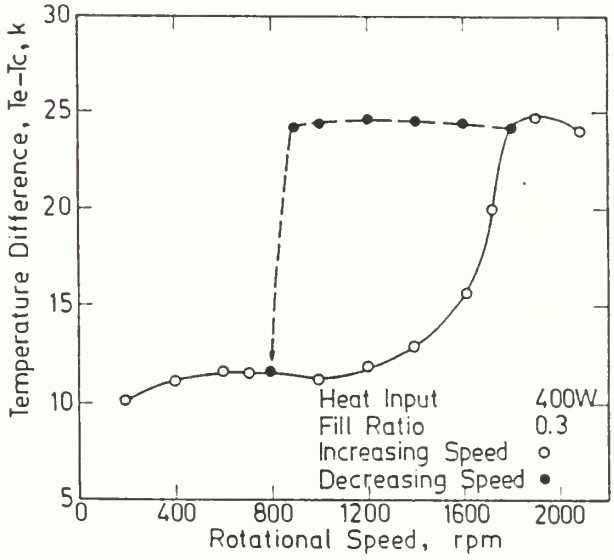

Fig. 4 Variation of Temperature Difference with Rotational Speed for Self-Cooled Condenser.

During decreasing speeds, the trend of elevated ΔT continued to a much lower speed of 850 rpm at which there is an abrupt and well marked fall and return of the heat pipe thermal conditions to the original level. This sharp change in ΔT signifies that the flow inside reverts from solid body rotation to stratified condition. There is thus a definite 'hysteresis effect' exhibited by the rotating heat pipe. It is significant that this change of events is independent of the heat input.

The heat transfer coefficient in each case is evaluated in the following manner. The net heat input to the evaporator is obtained by subtracting from the wattmeter reading, the heat losses from the evaporator. As mentioned before, the evaporator loss is measured in terms of heat flow by a direct-recording infra-red thermometer.

The inner wall temperature in the evaporator and condenser section is given by

$$T_{ei} = T_{eo} - Q \ln (r_o/r_i) / (2\pi K L_e) \quad (1)$$

and

$$T_{ci} = T_{co} - Q \ln (r_o/r_i) / (2\pi k L_c) \quad (2)$$

so that the respective heat transfer coefficients are evaluated from

$$h_{ei} = Q / [2\pi r_o L_e (T_{ei} - T_v)] \quad (3)$$

and

$$h_{ci} = Q / [2\pi r_o L_c (T_v - T_{ci})] \quad (4)$$

Where

Q = net heat input
r_o = outer radius of heat pipe
r_i = inner radius of heat pipe
K = thermal conductivity of copper
L_e = Length of evaporator section
L_c = Length of condenser section
T_v = Vapour Temperature

The evaporator heat transfer coefficient is shown in Fig. 5 for two heat inputs. It remains uniform over a wide range of speeds upto 1600 rpm beyond which, the heat transfer coefficient decreases slightly due to a corresponding increase in the temperature difference, T_e-T_v. The speed at which this change occurs depends mildly on the heat input under self-cooled condition.

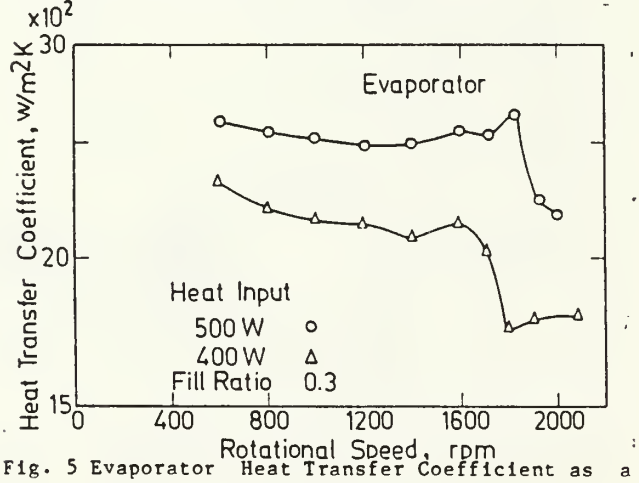

Fig. 5 Evaporator Heat Transfer Coefficient as a Function of Rotational Speed

When the heat pipe is horizontal and the condenser is cooled by an external induced - draft fan, the temperature excess, Te-Tc and Tv-Tc are plotted in Fig. 6 as a function of rotational speed. The tendency for an increased Te-Tc is observed over a speed interval of 900-1600 rpm with a corresponding reduction in Tv-Tc. Sharp rise in the temperature excess is found for 2000 rpm and more.

The extended range of speeds over which stable operation of the heat pipe is acheived should be particularly noted. Further increase in speed above 2200 rpm produced an uncontrolled thermal condition where the evaporator temperature increased sharply.

During decreasing speeds the temperature excess remained high and tended to increase down to a speed of 750 rpm at which eventually, the temperature returned to original state, rather instaneously. There is therefore a very narrow band of speeds over which the solid body rotation is disrupted and stratification occurs. This is depicted clearly in Fig. 7.

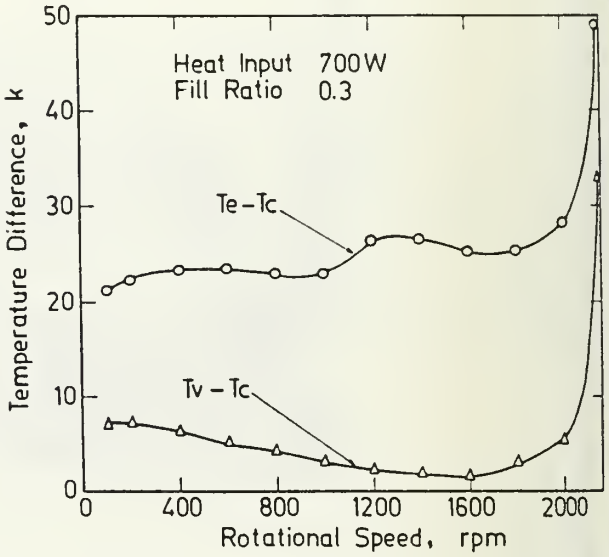

Fig. 6 Variation of Temperature Difference with Rotational Speed

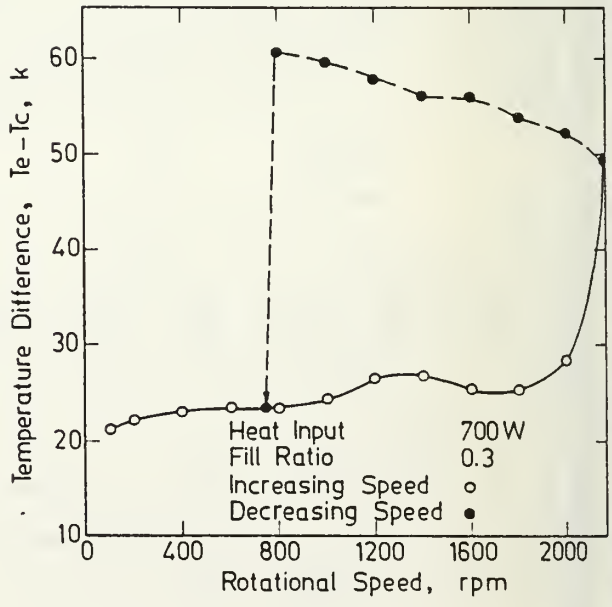

Fig. 7 Variation of Temperature Difference with Rotational Speed for Fan-cooled Condenser.

It is further noted that when the rotational speed is sought to be decreased before attaining the critical speed of 2000 rpm in this case, it is possible to retrace the original temperature curve with no hysteresis phenomena observed.

The temperature excess is minimum for speeds less than 1600 rpm. This is due to thin film evaporation over a relatively large dry evaporator surface under stratified conditions.

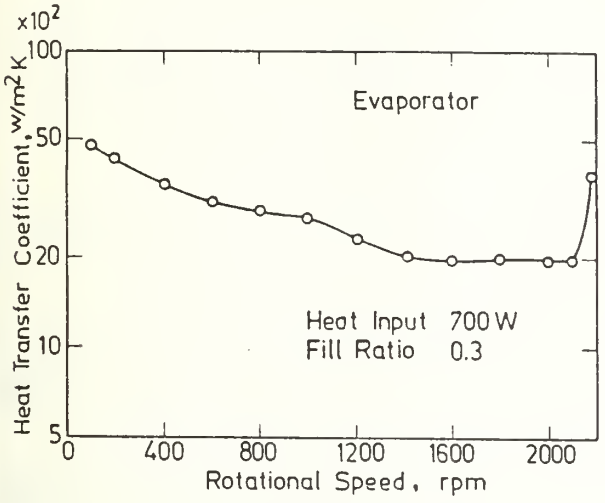

Fig. 8 Variation of Heat Transfer coefficient with Rotational Speed

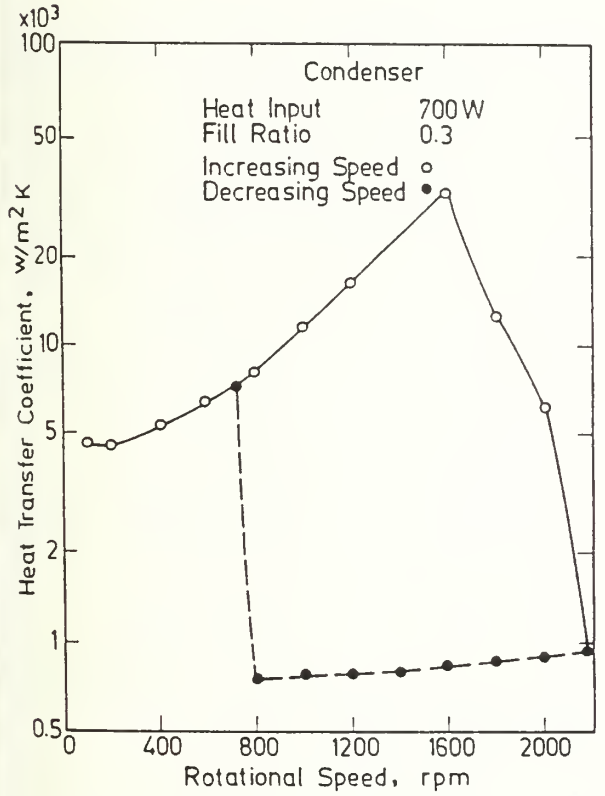

Fig. 9 Variation of Condenser Heat Transfer Coefficient with Rotational Speed

The results of present experiments fit into the correlation of Ohtsuka et al. [4] within 20 percent. The deviation in the critical speed at which transition occurs is mainly due to the fact that in the present case (a) the aspect ratio is higher, (b) the fill ratio is greater and (c) the external cooling condition on the condenser is different.

The evaporator heat transfer coefficients shown in Fig. 8 are comparitively less affected by increasing-decreasing speeds. On the otherhand, the condenser performance is profoundly affected during variable speed operation as depicted in Fig.9.

The tests are repeated when the heat pipe is slightly inclined (condenser up). The results are presented in Figs. 10 and 11 for an inclination of 2°. The evaporator heat transfer coefficients are slightly higher than in the horizontal case.

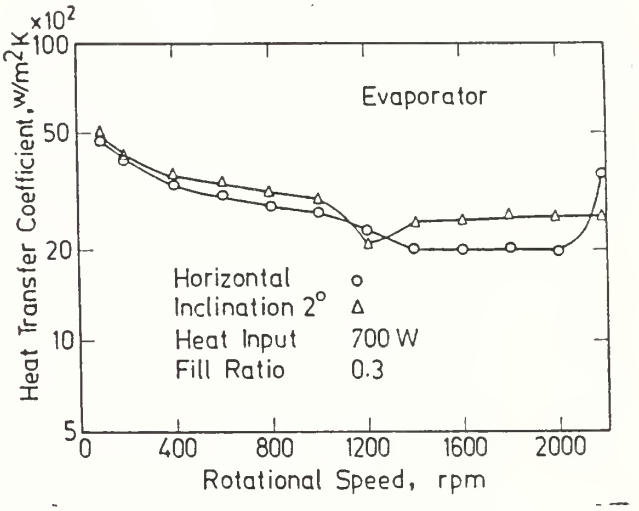

Fig. 10 Effect of Inclination on Evaporator Performance

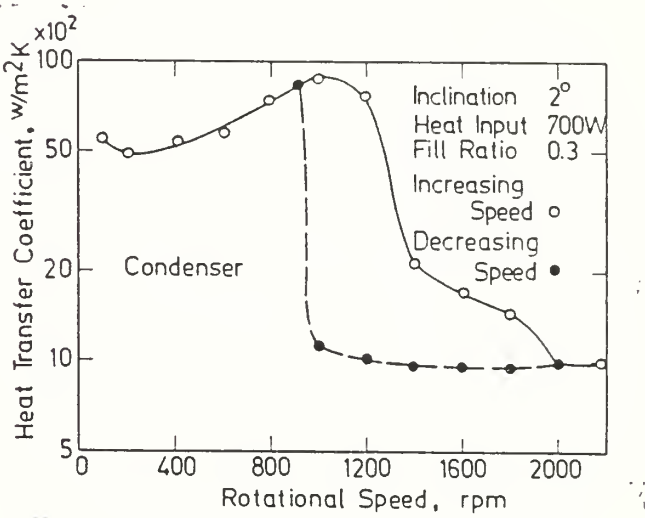

Fig. 11 Effect of Inclination on Condenser Performance.

Table 1 below gives the rotational speed at which abrupt change in the temperature difference between evaporator and condenser occurs during increasing-decreasing speeds.

Table 1 Transitional Rotational Speed

Cooling mode	Power w	Position	Increasing speed rpm	Decreasing speed rpm
Self cooling	400	Horizontal	1600	800
		2°	1800	900
		5°	1600	1000
		10°	1400	1000
Fan cooling	700	Horizontal	2000	750
		2°	1900	950
		5°	1800	1050
		10°	1200	1400

When the heat pipe is operated in the inclined position, the evaporator and vapour temperature readings have fluctuated significantly, particularly at lower speeds, the amplitude of fluctuation increasing with increased inclination. However, once the transition occured (in the range of 1400 → 2200 → 1400 rpm) the temperature oscillations have completely disappeared.

CONCLUSIONS

The following main points emerge from the present study.

1. A heat pipe rotating about its axis possesses a thermal response pattern changing critically with the rotational speed.

2. A higher fill ratio of 0.3 compared to 0.1-0.14 fill ratios recommended by Ohtsuka et al. [4], enlarges the range of speeds for which stable heat pipe operation is achieved.

3. During each test run, a well defined hysteresis phenomena is observed, particularly worsening condenser behaviour, which is detrimental to the heat pipe performance.

4. Appreciable cooling effect can be produced without any external fan by means of a slightly oversized finned condenser.

5. When the heat pipe is operated at an inclination, large temperature fluctuations and flow instabilities occur.

In the light of the above observations, it is essential to exercise greater care in the thermal design of coaxial shaft-mounted rotating heat pipes, especially with respect to variable speed operation.

To study further the heat transfer effectiveness of a rotating heat pipe on a prototype machine, a 10 KW induction motor is being manufactured with the heat pipe incorporated into the hollow shaft of the rotor.

ACKNOWLEDGEMENTS

The authors gratefully acknowledge permission granted by BHEL for publishing this work.

REFERENCES

[1] Gray, V.H.
The rotating heat pipe - a wickless, hollow shaft for transferring high heat fluxes, ASME Paper No. 69-HT-19, (1969).

[2] Marto, P.J.
Rotating Heat Pipes, Heat and Mass Transfer in Rotating Machinery edited by Metzger, D. and N. Afgan, Hemisphere, pp. 609-632, (1984).

[3] Marto, P.J. and H. Weigel
The development of economical rotating heat pipes, Proc. IV Int. Heat Pipe Conf., London, pp. 709-724, (1981).

[4] Ohtsuka, Y., Nakayama, W. and T. Yoshikawa
The performance of horizontal rotating heat pipes (Part I) Trans. JSME, 50, pp. 2862-2170, (1984).

[5] Nakayama, W., Ohtsuka, Y. and T. Yoshikawa
The effect of fine surface structure on the performance of horizontal rotating heat pipes, Proc. V Int. Heat Pipe Conf., Tsukuba, Vol. 2, pp. 121-125, (1984).

[6] Katsuta, M., Kigami, H., Nagata, K., Sotani, J. and T. Koizumi
Performance and characteristics of a rotating heat pipe, Proc. V Int. Heat Pipe Conf., Tsukuba, vol. 2, pp. 126-132, (1984).

[7] Krivosheev, B.N., Kukharskii, M.P. and V.D. Portnov
Heat Transfer in the evaporator section of a rotating heat pipe at low rotational speeds, J. of Engg. Phys. Vol. 37, pp. 773-778, (1980).

[8] Curtila, R. and T. Chataing.
Experimental study of a revolving heat pipe, Proc. V Int. Heat Pipe Conf., Vol. 1, pp. 268-273, (1984).

[9] Karweit, M.J. and S. Corrsin
Observation of cellular patterns in a partly filled, horizontal, rotating cylinder, Phys. Fluids. Vol. 18, pp. 111-112, (1975).

HEAT PIPE COOLING OF ELECTRICAL MACHINES

F. Giessler *, Ph.K. Sattler *, F. Thoren **

* Institute for Electrical Machines
Aachen University of Technology, Schinkelstrasse 4, D-5100 Aachen, Germany
** During the researches member of the institute

ABSTRACT

The desired low mass of motors for special purposes demands new cooling devices. Different types of heat pipes for motor cooling are described and their principle of operation is explained. The test results of four heat pipe cooled induction motors of 75kW and 150kW respectively are presented.

I. INTRODUCTION

Motors for special purposes, e.g. traction drives are supposed to have weights and volumes as low as possible. A decrease of motor size at the same power output, however, means an increase of motor losses per volume unit. Consequently motor cooling has to be improved to avoid inadmissible temperature rises of the winding insulation. For that purpose heat pipes favourably can be used. Because of their high thermal conductivity they allow the efficient transport of power loss to regions from where the heat easily can be removed with the help of a cooling medium, e.g. air or water. They need no external pumps to be kept in continuous operation and no maintenance. Up to the present, however, they where only seldom used for motor cooling.

2. POSSIBILITIES TO INSTALL HEAT PIPES IN STATOR AND ROTOR OF AN ELECTRIC MOTOR

In the stator of an electric motor stationary heat pipes with capillary structure and in the rotor concentrically or eccentrically rotating heat pipes can be used. Most important for all types of heat pipes is the thermal coupling with the heat source and the cooling medium. As mentioned in reference /9/ there are the following possibilities for the installation of heat pipes in electric motors:

1. The conductors in the stator slots are capillary heat pipes
2. Capillary heat pipes in the end turns
3. " " " in the stator slots
4. " " " in the stator yoke
5. The rotor bars (of the squirrel cage induction) motor are eccentrically rotating heat pipes
6. Eccentrically rotating heat pipes in the rotor yoke
7. Capillary heat pipes to cool the internal air penetrate housing or end shield
8. The shaft is a concentrically rotating heat pipe

The two open motors which are presented in the following are equipped with heat pipes of type No.3, 4 and 5. For totally enclosed motors, however, the use of heat pipes of type No.3 and 4 is rather problematic, since they would have to penetrate the end shield. So the totally enclosed motor presented first has only a concentrically rotating heat pipe in the shaft (type No.8) whereas the other has a cooling system similar to type No.3 in addition.

3. DIFFERENT HEAT PIPE TYPES

3.1 Capillary Heat Pipes With Longitudinal Grooves

Various structures can be used for heat pipe wicks: wrapped screens, sintered metals, longitudinal grooves, annular grooves, arteries etc. Especially suitable for the use in the stator of an electric motor are heat pipes with longitudinal grooves. Their main advantages are simplicity and reliability whereas their only possible disadvantage is the sensivity to operation against gravity at a corresponding inclination to the horizontal.

A typical cross section of a longitudinal grooved copper-water heat pipe is shown in fig.1. The fill charge should be sufficient to just fill the grooves, but a slight overfill usually can be tolerated.

Fig.1: Cross section of a longitudinally grooved heat pipe of 14mm outer diameter

The transport capacity depends as well on the fluid properties as on the geometry of container and wick. It is essentially determined by the maximum possible capillary pressure.

A copper-water heat pipe of 500mm length with the cross section shown in fig.1 was examined in horizontal and several inclined positions. In the evaporator section it was heated electrically over a length of 160mm and in the condensor section it was cooled by a 100mm long water jacket.

At horizontal operation and 120°C the heat transfer capability amounts to 700W. At inclined operation with gravity assistance it still increases a bit whereas it decreases rapidly even for only small inclinations against gravity and is down to zero at an inclination angle of only 4° to 5°.

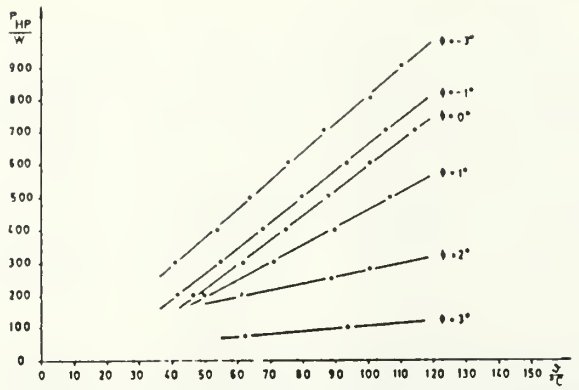

Fig.2: Capability of examined heat pipe for several angle of inclination

3.2 Concentrically Rotating Heat Pipes

The axis of a concentrically rotating heat pipe is identical to the axis of rotation, that means the shaft itself is used as a heat pipe. With respect to mechanical strength usually only steel can be used as shaft material. Because of the low thermal conductivity of steel which increases the thermal resistance of the heat pipe the steel wall should be only as thick as mechanically necessary whereas inner heat transfer surface should be large. It is of highest importance that the evaporator contains sufficient amount of equally distributed liquid at all working points.

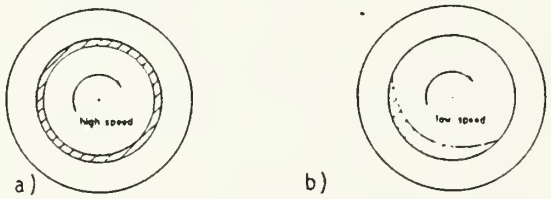

Fig.3: Liquid distribution in concentrically rotating heat pipe at a) high and b) low speed

At high rotational speed the liquid is distributed in form of an annular layer (fig.3a). Because of the low thermal conductivity of possible working fluids, e.g. water, the layer thickness should be as small as possible. To avoid a second passing of the heat through the liquid layer the cooling zone can be designed with a smaller inner diameter than the evaporator zone. This is possible by using a step in diameter or a cone. Centrifugal force than cause an almost dry cooling zone and a corresponding decrease of the effectiv thermal resistance.

At low rotational speed , however, the working fluid accumulates in the lower portion of the heat pipe (fig.3b). Tests with several concentrically rotating heat pipes at low speed showed that smooth inner surfaces in the evaporator zone result in a dry out of the upper portion and a subsequent increase of the thermal resistance even for rather low added heat power. A sufficient liquid distribution on the inner surface proved to be possible only by using appropriate inner surface structures. Successful was the use of irregular, rough surfaces and of longitudinal grooves which act like paddle-wheels and take the liquid along on their way up.

For low speed operation the inner diameter in the heating zone likewise should be greater than in transport and cooling zone. By this means and with the help of gravity the liquid is accumulated within the heating zone where it is badly needed. The chosen amount of liquid has to be relatively high in order to avoid dry out at the far end of the heating zone. A high amount of liquid chosen with respect to the lower rotational speeds, however, at high speeds effects undesirebly thick liquid layers. A concentrically rotating heat pipe for variable speed operation therefor should be designed with a big annular slot in the inside wall. At high rotational speed this annular slot acts as a liquid store whereas at lower speed it releases the additionally required liquid.

In the following some experimental results are presented concerning the concentrically rotating heat pipe which had be designed for a variable speed 75kW induction motor (see 5.3).

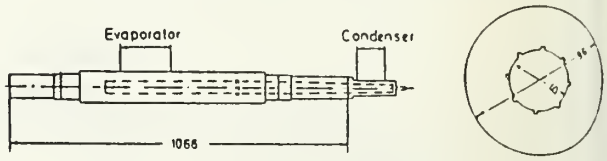

Fig.4: Longitudinal and cross section of concentrically rotating heat pipe with longitudinal grooves in evaporator section

Fig.4 shows its longitudinal and cross section within the heatimg zone. The generally smooth, cylindrical heating zone contains eight longitudinal grooves. Transport zone as well as cooling zone are conically shaped and smooth. To reduce the heat pipe's thermal resistance the cooling zone was manufactured of copper. The heating was done electrically over the length of 160mm at the far end and the cooling by means of a jacket.

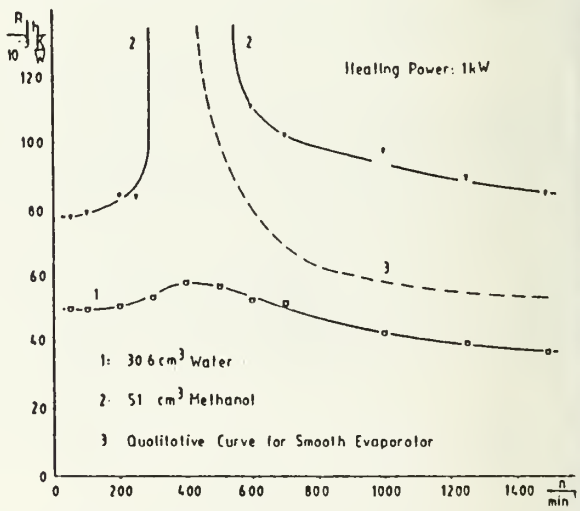

Fig.5: Thermal resistance of concentrically rotating heat pipe

In fig.5 the measured thermal resistances versus rotational speed are compared for water and methanol fill. Additionally the qualitative characteristic for a completely smooth inner surface is given. In this case the thermal resistance rapidly increases with decreasing speed.

At high rotational speed the general thermal behaviour is not problematic and hardly dependend on heating zone surface structure or liquid fill. Due to the longitudinal grooves at low speed also favourable results are achieved. Between lies the speed range in which the thermal behaviour is partly critical. In spite of the greater fill volume the methanol fill leads to a partly dry out of the evaporator. This is due to the worse properties of methanol compared with water and results in a rapid increase of thermal resistance. On the other hand the smaller water fill leads in the same speed range and at the same heating power only to insignificant increases. Altogether the thermal resistance of this concentrically rotating heat pipe with longitudinal grooves and water fill is almost independend on rotational speed.

4. INDUCTION MOTORS WITH HEAT PIPE COOLING

4.1 150kW Motor With Heat Pipes In The Stator Yoke

The first heat pipe cooled motor (fig.6) that was designed and examined in our institite is an open type 150kW induction motor /5,6,9,11/. The used heat pipes were manufactured by IKE, Stuttgart University, whereas all other heat pipes mentioned in this paper were build in our own institute.

The stator contains 36 longitudinally grooved copper-water heat pipes which are placed in axial holes at the outer diameter of the stator yoke

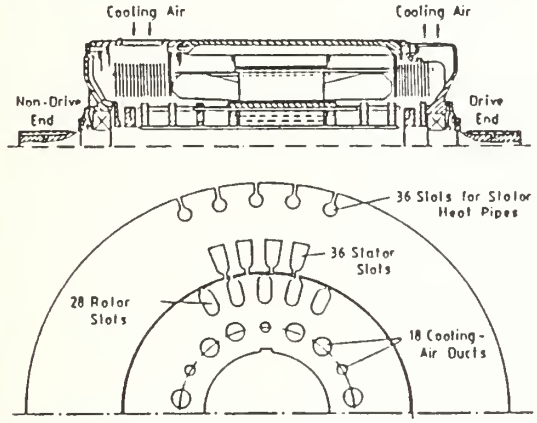

Fig.6: Longitudinal and cross section of 150kW motor with heat pipes in the yoke

To avoid the simultaneous failure of all heat pipes at inclined operation the finned cooling zones are alternately led to both sides. They are placed beyond the end turns. In the rotor the 28 copper bars of the squirrel cage are constructed as heat pipes with internal thread (M8x0.3) (fig.7b). For better cooling they are lengthened beyond both end rings but remain unfinned. Consequently they have one heating zone in the middle and two cooling zones. With regard to the asymetrical design of the given housing the centrifugal forces in the condensor sections are taken up by two supporting rings at the drive end and three at the non-drive end. Because of the same reason the condensor sections of the stator heat pipes are also asymetrical, they have ten and fifteen fins respectively. The volume of the rotor heat pipe's water filling equals about one third of the total volume.

The stator heat pipes (fig.7a) are similar to the above mentioned type (fig.1). Because of the wider groove openings, however, they are even more sensible to inclined operation. Measurement of a single heat pipe showed a total failure at a three degree inclination against gravity.

Fig.7: Cross sections of a) stator and b) rotor heat pipe

During the first time the motor was operated without integrated stator heat pipes. Fig.8 shows the considerable reduction of the stator winding's temperature rise after their installation /6/.

In the following the behaviour of both heat pipe systems in extreme working conditions is examined. For that purpose the motor was tested on a ramp with an inclination of 3^{o} to the horizontal. Such working conditions are possible for traction drives when going uphill, downhill or in curves. motor was operated with drive end up, non-drive down and vice versa. Due to the overdimensioning the rotor heat pipes the maximum rotor temperat for horizontal as well as for inclined operat remains rather low.

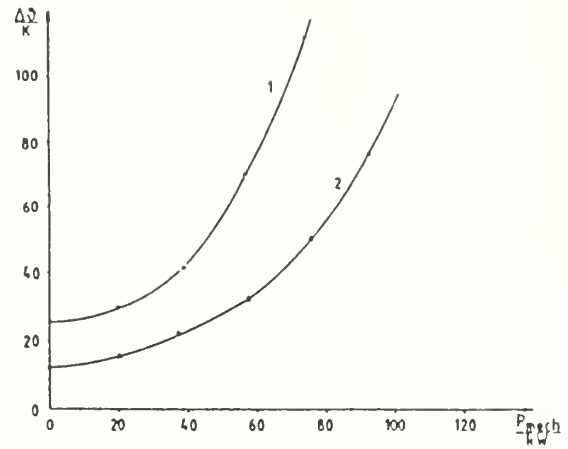

Fig.8: Temperature rise of hottest spot of stator winding when network supplied. No.1 witho and No.2 with installed stator heat pipes

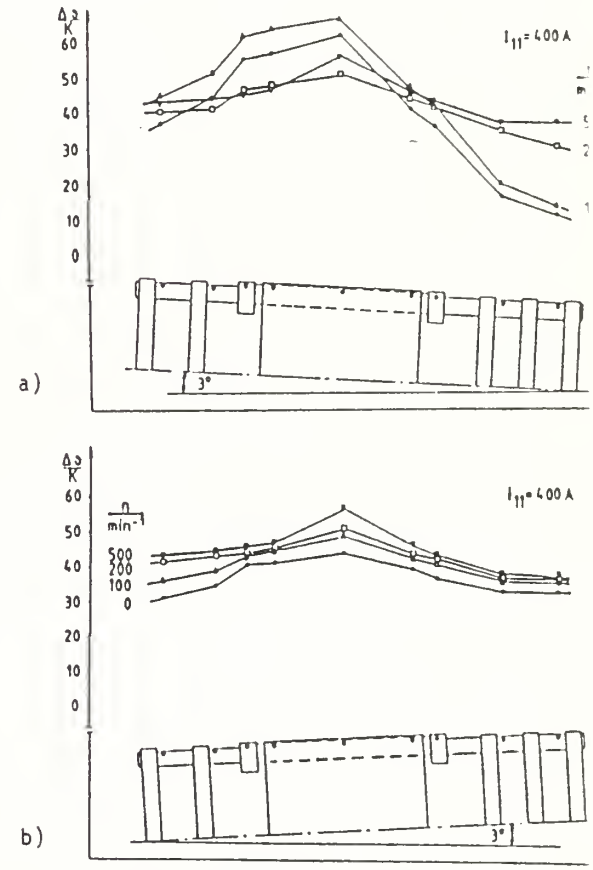

Fig.9: Effect of speed on temperature rise distri bution of rotor bar at inclined position with drive end a) up and b) down

The motor was fed by a current-source inverter operated at several speeds including standstill. temperature rise distributions of the rotor bar inclined position with drive end up are compared fig.9a. At standstill and 100min^{-1} heat pipe pe formance is very poor. Obviously the heating zone almost dry since the whole water filling is absor by the low long cooling zone which consequently blocked. With increasing speed the liquid distri tion becomes more and more uniform and thermal

behaviour improves gradually. The results with non-drive end up are somewhat different (fig.9b). The volume of the now lower short cooling zone is insufficient to take up the whole water filling. Therefor always at least part of the heating zone is wetted and a total dry out cannot occur. The heat pipe is always serviceable with at least one cooling zone and that is the higher one. Consequently now the temperature rise in the middle of the rotor bar is much lower.

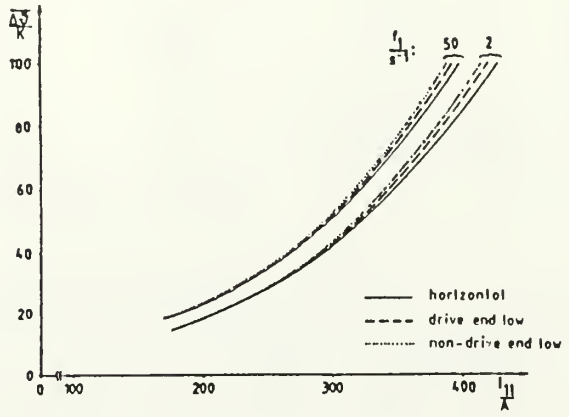

Fig.10: Mean temperature rise of stator winding for all three examined motor positions at two different stator frequencies

The effect of a three degree inclination on the mean temperature rise of the stator winding is only small. This is shown in fig.10 for two different stator frequencies.
Although for both inclinations half of all stator heat pipes are inactive only a slight increase of stator winding temperature can be noticed. The other half of the heat pipes perform well enough to cool the stator alone. During the inclination tests no critical hot spot could be observed. So motor operation at small inclination to the horizontal is possible almost without any reduction of working capacity. The alternate position of the stator heat pipe cooling zones at both sides proved good.

4.2 150kW Motor With Heat Pipes In The Stator Slots

The second heat pipe cooled motor (fig.11) with heat pipes in the startorslots is also an open type 150kW induction motor /11/. With the exception of punching and packing of the laminated core and of the inserting and impregnation of the stator winding the whole construction was executed in our institute's own workshop. A comparison shows that the data of this motor are almost identical to those of the first motor.

Obviously the heat pipe system of the first motor needed unnecessarily much volume. So the dimensions of the second motor's heat pipe systems were designed much smaller. On both sides they are flush with the end turns and no longer cause an extention of the motor. The cooling zones of the stator heat pipes are placed above and below the end turns and the rotor heat pipes can do with only one support ring on each side. The stator heat pipes are on the bottom of each stator slot, that means in close contact with the winding which is a main source of power loss. They have to be insulated as well against the winding as against the laminated iron core. The vicinity between heat pipe an winding makes possible a very effective stator cooling. The finned condensor sections again are alternately at the motor's drive and non-drive end. The end turns and the corresponding stator heat pipe cooling zones before impregnating are shown in fig.12.

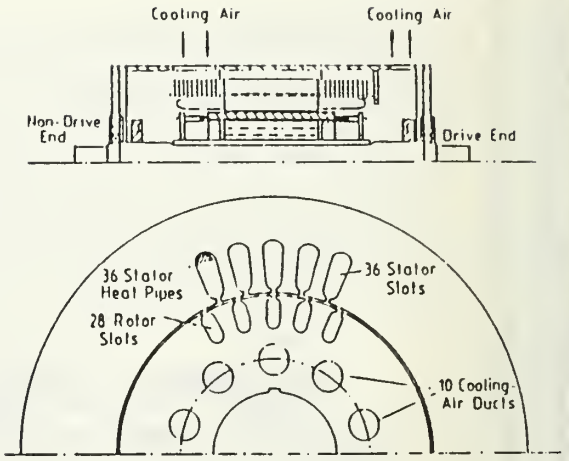

Data:

U_{1N} = 320 V I_{1N} = 340 A $\cos\varphi_{1N}$ = 0,85

P_N = 150 kW f_{1N} = 83,3 s^{-1} n_N = 2470 min^{-1}

Insulation class F IP 23 p = 2

Fig.11 Longitudinal and cross section of 150kW motor with heat pipes in the stator slots

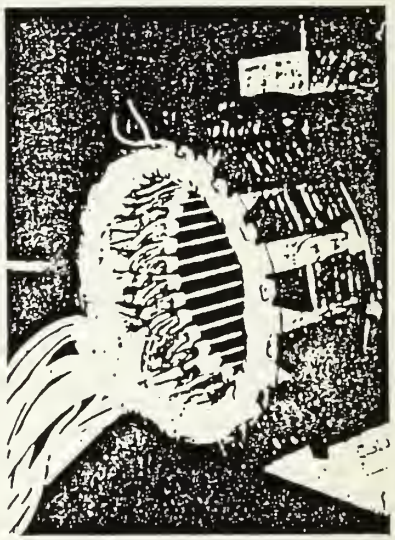

Fig.12: View of end turns and stator heat pipe cooling zones before impregnating

To achive a flat contact area between heat pipe and winding and to reduce necessary area for the heat pipe itself a semicircular heat pipe cross section was chosen. For this purpose the already known longitudinal grooved copper pipe material (fig.1) was pressed into the new shape (fig.13a). Because of the considerable reduction of vapour area and number of existing grooves the performance of the corresponding semicircular heat pipe is considerably worse compared with the original cicular one. Experiments for horizontal position showed, however, that it can

a) b)

Fig.13: Cross sections of a) stator and b) rotor heat pipe

transport at least 200W in the interesting temperature range and this is sufficient for all working points. Since the groove opening width of several grooves is reduced the semicircular heat pipes are much less sensitive to small inclinations than the original circular ones.

The copper bars of the squirrel cage (fig.13b) again are constructed as heat pipes with internal thread (M8x0.5). In both cooling zones the cross section is reduced to a part named "a" which contains the heat pipe. The total cooling surface was increased by soldering a finned copper tube on it. The volume of the rotor heat pipe's water filling again equals about one third of the total volume. Because of the relatively short cooling zone by this even at inclined operation a total dry out of the heating zone becomes impossible.

Weigth reduction shall be demonstrated with some numerical results. The active stator material weight (laminated iron core and copper winding including heat pipes) amounts to 117.3kg whereas the corresponding weight of a 90kW, $50s^{-1}$, IP23 machine is about 140 to 150 kg. This corresponds to a reduction of 16.2% to 21.8% respectively.

Another interesting comparison provides the product of current density and current loading. It is approximately $6300A^2/mm^2cm$ for the inverter-fed heat pipe cooled machine but only about $2500A^2/mm^2cm$ for an open type mains-operated 90kW machine. The ratio of the cross section area which is claimed by the insulated copper wires to the total cross section area of the slot is 36% for the heat pipe cooled machine and about 50% for a conventional machine. The suitability of the used stator and rotor heat pipe systems could be proved for horizontal as well as inclined positions of the motor. Because of the shorter cooling zones the rotor temperatures are somewhat higher than those of the first machine.

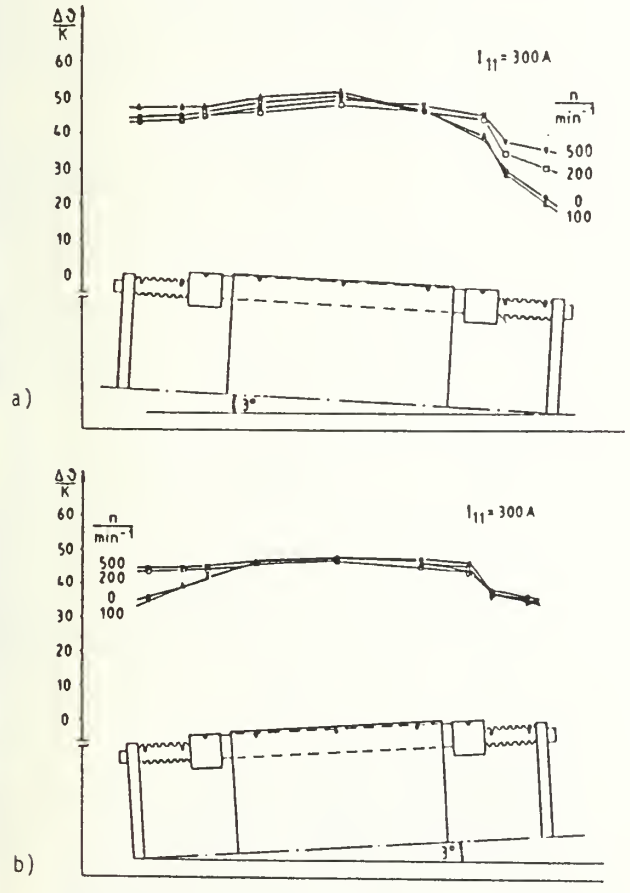

Fig.14: Effect of speed on temperature rise distribution of rotor bar at inclined position with drive end a) up and b) down

Altogether they are yet rather low. As already mentioned such a rotor heat pipe system is more appropriate to a motor of higher output and higher rotor loss.

As expected at inclined operation the temperature peaks in the middle of the rotor bars have vanished even for standstill and very low speed (fig.14). The temperature profiles for drive end up and drive end down are almost identical. Apart from that the thermal behaviour corresponds to that of the first motor.

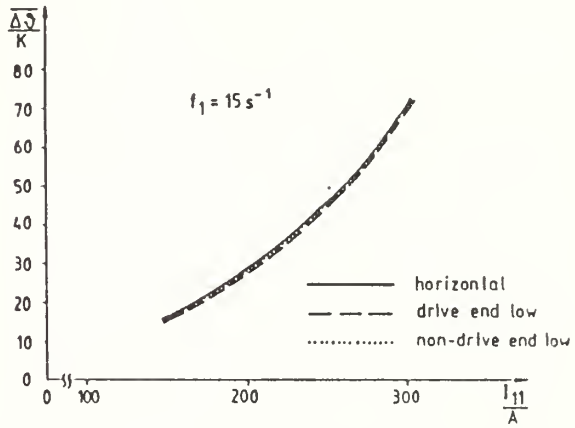

Fig.15: Mean temperature of stator winding for all three examined motor positions at $f_1=15s^{-1}$

At inclined operation the thermal behaviour of the stator winding differs from that of the first motor (fig.15,10). The results for horizontal and inclined operation are almost identical. At first it is amazing that the highest temperatures always occur in horizontal position. At inclined machine the performance of the gravity assisted heat pipes is improved whereas the performance of those which have to work against gravity deteriorates only insignificantly. Altogether at inclined position from this results a tiny but measurable improvement compared with horizontal position.

4.3 75kW Motor With Heat Pipe In The Shaft

The third examined heat pipe cooled machine is a totally enclosed motor with heat pipe in the shaft /10,11/ which was examined at variable speed.

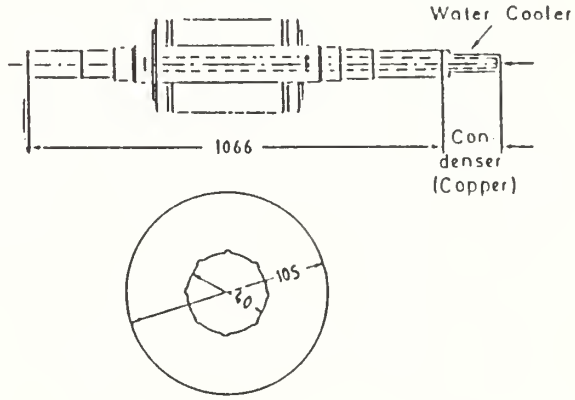

Data of original machine:

U_{1N} = 380V I_{1N} = 139A $\cos\varphi_{1N}$ = 0,87

P_N = 75kW f_{1N} = $50 s^{-1}$ n_N = 1475 min^{-1}

Insulation class F IP54 p = 2

Fig.16: Longitudinal section of rotor, cross section of shaft and data of original motor

For this purpose in our institute a new rotor with heat pipe in the shaft was built for a conventionally totally enclosed fan-cooled 75kW induction motor (fig.16). The inner dimensions of the heat pipe are identical with those of the above described heat pipe with grooves in the evaporator section (see fig.4). Some minor changes were carried out.

The outer shaft diameter was increased from 96mm to 105mm and the copper cooler was friction welded with the steel shaft whereas it was only screwed in the case of the individual heat pipe mentioned above. Additionally the inner surface of the heat pipe now was coppered galvanically to avoid compatibility problems between liquid and wall material. It has to be considered, too, that now the heating zone is more than double as long as before.

The original rotor was exchanged for the newly built rotor with still unfilled heat pipe in the shaft. The fan was removed and the motor seperately ventilated. The air flow rate was permanently adjusted at a value which brought about an unchanged mean temperature rise in the stator winding at the rated speed of 1475 min^{-1}.

The motor's thermal behaviour with still unfilled shaft was examined when fed by a sinusoidal $50s^{-1}$ system and by a current-source inverter at lower frequencies. After filling the heat pipe in the shaft with $30.6cm^3$ of destilled water the measurements were repeated. The heat pipe's cooling zone was cooled by a water jacket. The used cooling water flow was three liters per minute.

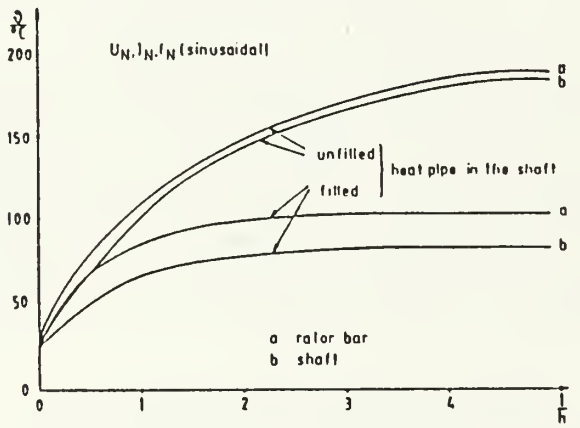

Fig.17: Rotor temperatures with unfilled and filled heat pipe in the shaft

In fig.17 the temperatures of rotor bar and shaft (in the middle of the rotor stack) as a function of time are compared for unfilled and filled heat pipe in the shaft. Both times the motor was mains-operated with its rated voltage, rated current and rated frequency. Heat pipe action reduces the rotor

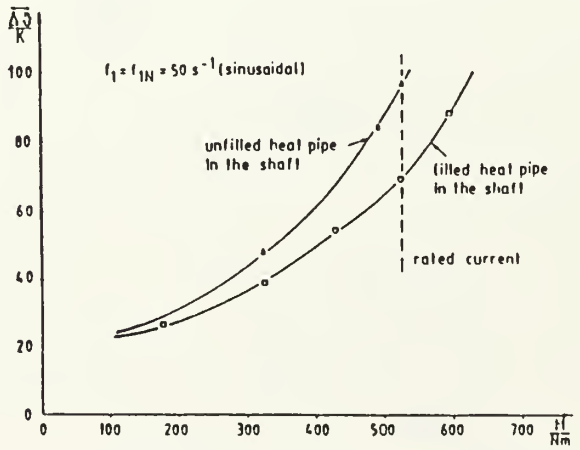

Fig.18: Mean temperature rise of stator winding with unfilled and filled heat pipe in the shaft

bar temperature from 185°C to 102°C and the shaft temperature from 180°C to 82°C. With unfilled heat pipe there is only a very low temperature difference between rotor bar and shaft. The thermal contact seems to be as good as desired. The temperature difference increases with filled heat pipe because of the high heat flow of 1350W from cage to shaft.

The mean temperature rise of the stator winding is also significantly decreased by the heat pipe action although not as much (fig.18). At rated current the temperature rise is decreased by 27K. The use of the heat pipe in the shaft allows a power increase of about 17% without exceeding the permissible temperature rise of insulation class F.

At lower speeds the thermal behaviour of the now inverter-fed motor is very similar. The results of all test runs are summarized in fig.19.

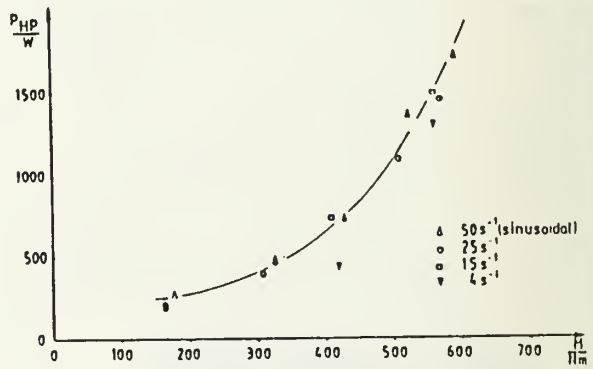

Fig.19: Power transferred by the heat pipe in the shaft at different frequencies

The chosen frequencies correspond to speeds of approximately 1500, 700, 400 and 100min^{-1}.A significant speed dependence cannot be found out. Firstly the rotor loss does not differ too much for the considered frequencies and secondly the thermal resistance of the heat pipe in the shaft is more or less independent of speed (see fig.5).

If a greater inner shaft diameter is used /8/ or a longer evaporator section the transferable amount of heat still can be increased significantly. But even for the given heat pipe the highest achieved power of about 1700W is not yet the performance limit. The limit is the temperature rise of the stator winding.

The results show that for steady-state operation the use of a heat pipe in the shaft can be interesting not only for small motors but also for motors of a magnitude which are applicable for example on subway systems.

4.4 Totally Enclosed 150kW Induction Machine With Heat Pipe Cooling In Stator And Rotor

As mentioned above it is advantageous to apply heat pipes in the bottom of the stator slots for heat transfer. In a changed form this solution is applicable for a totally enclosed machine. If there is the demand of variable speed operation of the drive a cooling water circuit must exist for heat transfer from the concentrically rotating heat pipe. So it is possible to integrate the stator cooling apparatus in this water circuit.

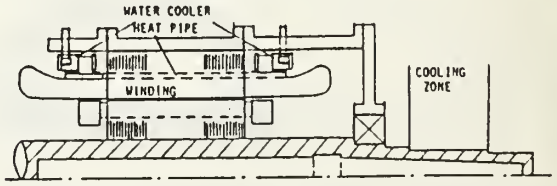

Fig.20: Longitudinal section of 150kW enclosed motor with heat pipes in stator slots and shaft

The stator of the second enclosed induction machine (fig.20) whose investigation is not finished yet was built up in the same way as the open machine described above but pieces of copper are soldered at the cooling sections of the stator heat pipes which are clamped in a ring-like water cooler placed above the end turns of the stator winding. The water supply connections go through the housing not through the end shields. The heat pipes have the same inner structure as those in the open machine but the condensor section has been shortened from 80mm to 50mm because of the more effective cooling.

Preliminary investigations proved this cooling method to be as efficient as that of the open machine. In horizontal operation each heat pipe can transfer 190W at a temperature level of 111°C in the evaporator section. With an inclination of 3° each gravity assisted heat pipe will transfer 290W and those operating against gravity 96W at a slightly increased temperature level in the heating section (125°C).

Two rotors each with a concentrically rotating heat pipe were built for this machine. Their construction data were the same however one had 16 longitudinal grooves in the evaporator section. The manufacture of these grooves is rather difficult. Therefor investigations were carried out with the second concentrically rotating heat pipe which should prove that the roughness of the copper layer inside the heat pipe is sufficient to wet the inner surface of the evaporator even at low speed operation. The cone angle of the condensor and transport section is 2.8°. Because the maximum speed of the machine should be 5000min^{-1} the cooling section had to be manufactured from steel.

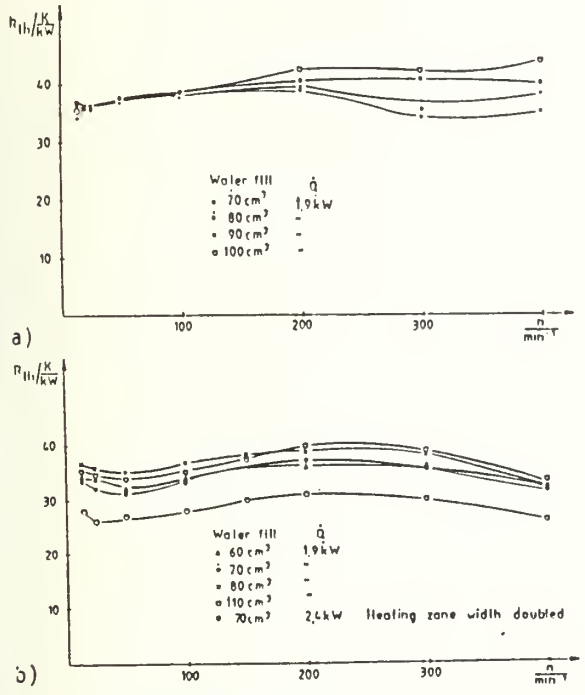

Fig.21: Thermal resistance of heat pipe shaft a) without and b) with longitudinal grooves

The thermal resistances of both heat pipes are rather independent on speed. The heat pipe with grooves in the evaporator seems to be slightly better. The heat transfer is 1.9kW (fig.21a). The measurements were carried out with an electric heater element half as long as the active part of the rotor. Measurements with two heaters proved the capability of the heat pipe to transfer 2.4kW minimum. As a result of the enlarged surface of the heating section the thermal resistance was reduced by about 20% (fig.21b).

This totally enclosed induction machine will perform the same electrical data and approximately the same volume as the open type 150kW machine with heat pipes in the stator slots whereas conventional enclosed induction motors are much heavier than open machines.

6. CONCLUSIONS

The desired low mass of motors for special purposes, for example traction drives, demands new cooling devices. Such systems with heat pipes are shown for both open type and totally enclosed induction motors. The different heat pipe types are described and their principle of operation is explained. For open type motors obviously the use of heat pipes both in stator yoke or slots and in the rotor bars can be favourable. For totally enclosed motors the use of a heat pipe in the shaft seems to be very promising. It could be advantageous especially for modern urban railway motors.

ACKNOWLEDGEMENTS

The authors wish to thank the Deutsche Forschungsgemeinschaft for its financial support and the Schorch GmbH for the provision of the totally enclosed motor.

REFERENCES

/1/ Fries P., "Experimentelle Ergebnisse mit einem dochtfreien Zentrifugal-Waermerohr", Int. J. Heat Mass Transfer, 13 (1970), pp. 1503-1504.

/2/ Kucharskij M.P., Noskov V.A., "Investigation of closed evaporative cooling of electric machines" (original in Russian), Asinchronnye dvigateli, Trudy Niptiem, Vladimir (1974), No.3, pp. 204-214.

/3/ Bubenicek M., Oslejsek O., Polasek F., "The cooling of the rotor of an electric motor by means of a cylindrical rotating heat tube" (original in Czech)", Elektrotechn. Obz., 83 (1974), pp. 40-46

/4/ Corman J.C., Edgar R.F., McLaughlin M.H., Merchant B.W., Tompkins R.E., "Heat pipe cooled induction motor", IEEE PES Winter Meeting, New York, Jan.27-Febr.1, 1974, Paper T74001-4, pp.1069-1075.

/5/ Groll M., Krähling H., Münzel W.D., Sattler Ph.K., Weidemann B., "Waermerohre zur Kühlung eines Elektromotors", Elektrizitätsverwertung, 1/2/79, pp. 10-15

/6/ Weidemann B., "Wärmerohrgekühlter Asynchronmotor mit Stromrichterspeisung als Bahnantrieb", Ph. D. Thesis, TH Aachen, 1979

/7/ Furuya S., Wake A., Matsumoto K., Koizumi T., "Developement of heat pipe shaft for motor cooling" (original in Japanese), Furukawa Denko Jiho, N71, march 1981

/8/ Brost O., Unk J., Canders W.R., "Heat pipes for electric motors", Proc. 5th Int. Heat Pipe Conf., Tsukuba (Japan), 1984, pp. 359-364

/9/ Thoren F., "Heat pipe cooled induction motors", Proc. 5th Int. Heat Pipe Conf., Tsukuba (Japan), 1984, pp. 365-371

/10/ Sattler Ph.K., Thoren F., "Totally enclosed heat pipe cooled induction motor (theoretical and experimental results)", Int. Conf. on Electrical Machines (ICEM), Lausanne (Switzerland), 1984, pp. 683-686

/11/ Thoren F., "Verschiedenartige Wärmerohr-Systeme zur Kühlung von Asynchronmaschinen", Ph. D. Thesis, TH Aachen, 1985

APPENDIX B

Bibliography on Rotating Heat Pipe Technology (From Ph.D. Thesis of Dr. F. Thoren)

Kapillarstruktur bzw. Docht (wick)
Wechselrichter; Wand
Zentrifugal
Wärmeübergang
Stator
Rotor
1 Grundschwingung

H. Literaturverzeichnis

[1] Asselman, G.A.A.; Green, D.B.:
Das Wärmerohr
Philips techn.Rdsch. 33, S.108-117, 1973/74, Nr.4

[2] Basiulis, A.; Prager, R.C.:
Compatibility and Reliability of Heat Pipe Materials
AIAA Paper No.75-660, AIAA 10th Thermophysics Conference,
Denver, Colorado, May 1975

[3] Bergmann, D.:
Betriebseigenschaften von wärmerohrgekühlten Asynchronmaschinen mit gerilltem Massivrotor und Kurzschlußkäfig unter besonderer Berücksichtigung der Stromrichterspeisung
Diss. RWTH Aachen, 1982

[4] Bienert, W.B.; Skrabek, E.A.:
Heat Pipe Design Handbook, Part I
Report Aug.1972, Dynatherm Corp., Cockeysville, Maryland,
Contract No.NAS 9-11927

* [5] Brinkman, W.G.:
Dynamoelectric Machine Cooled by a Rotating Heat Pipe
US Patent 3715610, patented Feb.6, 1973

* [6] Brost, O.; Unk, J.; Canders, W.R.:
Heat Pipes for Electric Motors
Proc.5th Int.Heat Pipe Conf.,Tsukuba (Japan),1984,pp.359-364

* [7] Bubeníček, M.; Ošlejšek, O.; Polášek, F.:
Kühlung des Rotors eines Elektromotors mittels eines zylindrischen rotierenden Wärmerohrs (Original in Tschechisch)
Elektrotechn.Obz.83(1974), pp.40-46

[8] Busse, C.A.:
Pressure Drop in the Vapor Phase of Long Heat Pipes
Thermionic Conversion Specialist Conf., Oct.30-Nov.1,1967,
Palo Alto, Calif.

[9] Cady, E.C.; Robertson, A.S.:
Development and Operational Testing of a Heat Pipe Dry Cooling Tower
Joint Power Generation Conf., Phoenix, Arizona, Sept.28-Oct.2,1980

[10] Chalmers, B.J.; Herman, J.:
Induction-motor fan drive with unlaminated rotor and heat pipe cooling
Proc.IEE, Vol.124, No.5, May 1977

[11] Chi, S.W.:
Heat Pipe Theory and Practice, A Sourcebook
Hemisphere Publishing Corporation, 1976

[12] Corman, J.C.; McLaughlin, M.H.:
Thermal Design of Heat Pipe Cooled AC Motor
ASME Preprint 71 WA/HT-14, 1971

[13] Corman, J.C.; Edgar, R.F.; McLaughlin, M.H.; Merchant, B.W.; Tompkins, R.E.:
Heat Pipe Cooled Induction Motor
IEEE PES Winter Meeting, New York, Jan.27-Feb.1,1974

[14] Cotter, T.P.:
Theory of Heat Pipes
Los Alamos Scientific Laboratory, LA-3246-MS

[15] Dunn, P.D.; Reay, D.A.:
Heat Pipes
2nd Edition, Pergamon Press, 1978

[16] Eastman, G.Y.:
The Heat Pipe
Scientific American, May 1968, pp.38-46

[17] Edelstein, F.; Haslett, R.:
Heat Pipe Manufacturing Study
Final Report, Aug.1974, Grumman Aerospace Corp. Bethpage, New York, Contract No. NAS 5-23156

[18] Ernst, D.M.:
Evaluation of Theoretical Heat Pipe Performance
Thermionic Conversion Specialist Conf., Oct.30-Nov.1,1967, Palo Alto, Calif.

[19] Feldman, K.T.Jr.; Kenney, D.D.:
The Compatibility of Mild Carbon Steel and Water in a Heat Pipe Application
Proc. 4th Int.Heat Pipe Conf., London, 1981, pp.439-450

[20] Fries, P.:
Experimentelle Ergebnisse mit einem dochtfreien Zentrifugal-Wärmerohr
Int.Journal of Heat & Mass Transfer, 13, 1970, S.1503-1504

[21] Fries, P.; Schulze, P.:
Anordnung zur Kühlung von Rotationskörpern
Deutsche Patentschrift 1928358, Ausgabetag: 13.12.1973

[22] Furuya, S.; Wake, A.; Matsumoto, K.; Koizumi, T.:
Development of Heat Pipe Shaft for Motor Cooling (Original in Japanisch)
Furukawa Denko Jiho, N71, March 1981, pp.29-34

[23] Gaugler, R.S.:
Heat Transfer Device
US Patent 2350348, patented June 6, 1944

[24] Gay, F.W.:
Heat Transfer Means for Closed Rotating Electrical Machinery
US Patent 1700840, patented Feb.5, 1929

[25] Gray, V.H.:
The Rotating Heat Pipe - A Wickless, Hollow Shaft for Transferring High Heat Fluxes
ASME paper 69-HT-19, 1969, pp.1-5

[26] Groll, M.; Krähling, H.; Münzel, W.D., Sattler, Ph.K.; Weidemann, B.:
Wärmerohre zur Kühlung eines Elektromotors
Elektrizitätsverwertung, 54(1979), S.10-15

[27] Grover, G.M.; Cotter, T.P.; Erickson, G.F.:
Structures of very high Thermal Conductance
J.Appl.Phys., 35, pp.1990-1991, 1964

[28] Hermann, E.; Koch, H.; Kreeb, H.; Perdu, M.:
Handbuch der Rillenwärmerohre
BMFT, Forschungsbericht W 76-17, Dezember 1976

[29] Hufschmidt, W.; Burck, E.; Di Cola, G.; Hoffmann, H.:
Der Einfluß der Scherwirkung des Dampfstromes auf den laminaren Flüssigkeitsstrom in Kapillaren von Wärmerohren
Wärme- und Stoffübertragung 8d.2(1969), S.222-239

[30] Ivanovskii, M.N.; Sorokin, V.P.; Yagodkin, I.V.:
The Physical Principles of Heat Pipes
Clarendon Press, Oxford, 1982

[31] Koch, H.; Kreeb, H.:
Offenlegungsschrift 2756141

[32] Köhler, P.:
Heizkörper für Back- und Dörröfen nach Art der Perkinsrohre
Kaiserliches Patentamt, Patentschrift 194047, 10.11.1905

[33] Kreeb, H.:
Zur Wahl von Werkstoff und Wärmeträger bei Niedertemperatur-Wärmerohren
Diss. Universität Stuttgart, 1972

[34] Kukharskii, M.P.; Noskov, V.A.:
Die Untersuchung der geschlossenen Verdampfungskühlung an Elektromaschinen (Original in Russisch)
Asinchronnye dvigateli, Trudy NIPTIEM, Vladimir, (1974), Nr.3, S.204-213

[35] Kukharskii, M.P.:
Closed Evaporative Cooling of Rotating Electrical Machines (Original in Russisch)
Inzhenerno-Fizicheskii Zhurnal, Vol.27, No.3, pp.446-456, Sep.1974

[36] Kukharskii, M.P.; Noskov, V.A.; Efimov, G.M.; Marynov, S.V.:
Results of Tests of an Induction Motor using a Heat Pipe in the Shaft
Elektrotekhnika, Vol.46, No.12, pp.48-49, 1975

[37] Kukharskii, M.P.; Ivannikov, V.A.:
Effectiveness and Applications of Centrifugal Heat Pipes in Electric Machines
Elektrotekhnika, Vol.53, No.9, pp.47-59, 1982

[38] Limoges, R.F.:
The Rotating Heat Pipe - Implementation as a Uniform-Temperature Heat Source
ASME, Winter Annual Meeting, Nov.15-20, 1981, Washington, D.C.

[39] Löser, F.:
Flußanpassung und On-Line-Identifikation der Rotortemperatur bei stromrichtergespeisten Asynchronmaschinen zur Erhöhung von Wirkungsgrad und Leistungsfaktor unter Anwendung neuer Verfahren zur Verlustberechnung
Diss. RWTH Aachen, 1984

[40] Marcus, B.D.:
Theory and Design of Variable Conductance Heat Pipes
Report Apr.1972, TRW Systems Group, Redondo Beach, Calif.
Contract No. NAS 2-5503

[41] Markert, W.:
Einsatz von Wärmerohren zur Kühlung elektrischer Maschinen
Elektrie 36(1982)H.1, S.30-32

[42] Marto, P.; Weigel, H.:
The Development of Economical Rotating Heat Pipes
Proc. 4th Int.Heat Pipe Conf., London, 1981, pp.709-724

[43] Midwest Research Institute:
Heat Pipes
Report Jan.1975, Contract No. NASW-2454

[44] Münzel, W.D.; Krähling, H.:
Lifetest Investigations with Stainless Steel/Water Heat Pipes
Proc.4th Int.Heat Pipe Conf., London, 1981, pp.459-476

[45] Nakayama, W.; Ohtsuka, Y.; Yoshikawa, T.:
The Effects of Fine Surface Structures on the Performance of Horizontal Rotating Heat Pipe
5th Int.Heat Pipe Conf., Tsukuba (Japan), 1984,
Pre-Prints IV, pp.99-103

[46] Ošlejšek, O.; Polášek, F.:
Cooling of Electrical Machines by Heat Pipes
2nd Int.Heat Pipe Conf., Bologna (Italy), 1976

[47] Pittinato, G.F.:
Hydrogen Gas Generation in Water Heat Pipes
Journal of Engineering Materials and Technology, July 1978,
Vol.100, pp.313-318

[48] Sattler, Ph.K.; Thoren, F.:
Inverter-fed Induction Motors, Design and Construction with Respect to Inverter Type and Cooling Method
Symposium on "Electrical Drives for Ground Transportation"
Positano (Italy), May 1983, pp.245-253

[49] Sattler, Ph.K.; Thoren, F.:
Totally Enclosed Heat Pipe Cooled Induction Motor (Theoretical and Experimental Results)
Int.Conf.on Electrical Machines (ICEM), Lausanne (Switzerland),
Sept.1984, pp.683-686

[50] Schroeter, J.F.:
Hochdruckheizrohr für Backöfen, Darren und dgl.
Kaiserliches Patentamt, Patentschrift 136131, 26.04.1900

[51] Thoren, F.:
Heat Pipe Cooled Induction Motors
Proc.5th Int.Heat Pipe Conf., Tsukuba (Japan), 1984, pp.365-371

[52] Tubis, Ja.B.; Fanar, M.S.; Alekseev, K.V.: Ersujeva, S.A.:
Ein neues Verfahren zur Kühlung elektrischer Maschinen
(Original in Russisch)
Asinchronnye dvigateli, Trudy NIPTIEM, Vladimir,(1974),
Nr.3, S.194-203

[53] Turner, E.P.:
Evaporative Cooling Systems for Electric Motors
US Patent 2743384, patented Apr.24, 1956

[54] Weidemann, B.:
Wärmerohrgekühlter Asynchronmotor mit Stromrichterspeisung als Bahnantrieb
Diss. RWTH Aachen, 1979

Diplomarbeiten am Institut für Elektrische Maschinen:

Diegeler, J.:
Untersuchung der Wärmerohrkühlung bei offenen und geschlossenen Maschinen

Hillmann, D.:
Experimentelle Untersuchungen verschiedener Möglichkeiten der Kühlung elektrischer Maschinen mit Wärmerohren

Wagner, U.:
Experimentelle Untersuchungen zur Kühlung von Statoren und Rotoren elektrischer Maschinen mit Wärmerohren

APPENDIX C

FANUC AC Spindle Motor
Brochure

FANUC AC SPINDLE MOTOR series

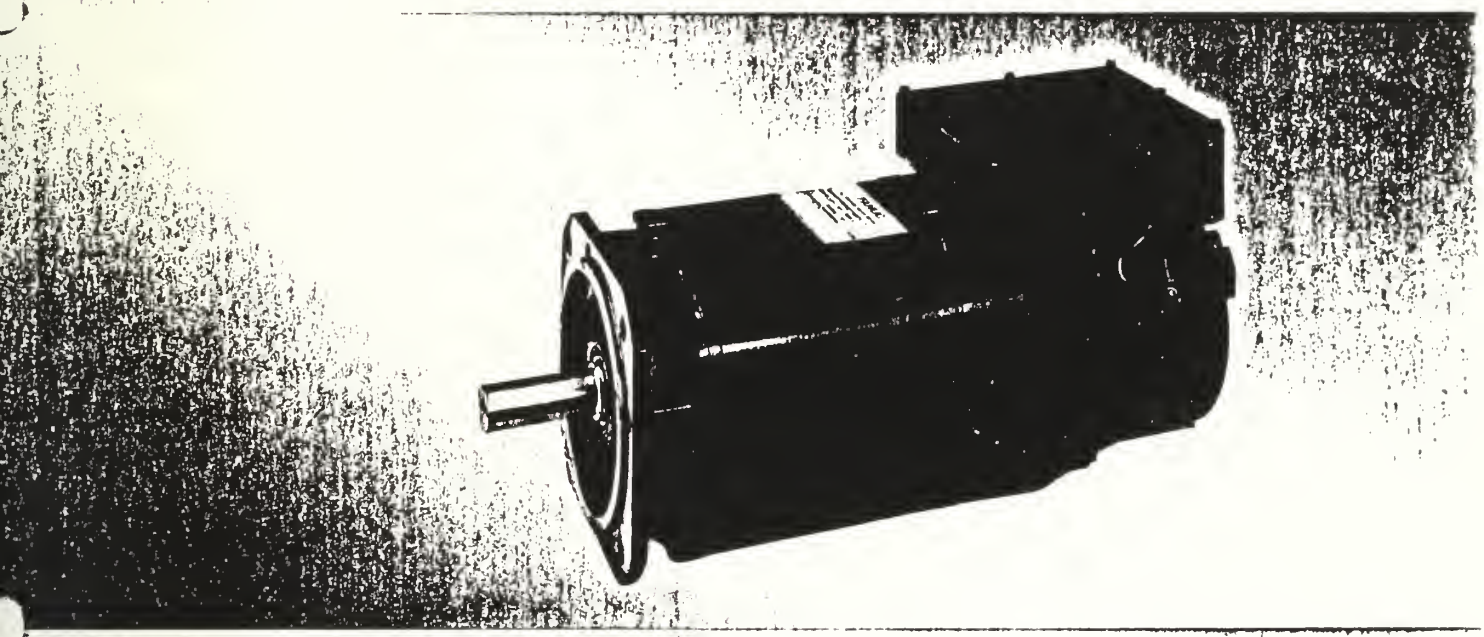

FANUC

FANUC AC SPINDLE

概　要

FANUC AC SPINDLE MOTOR シリーズはNC工作機械用として特に開発され，塵埃や切削油の浮遊する機械工場内での過酷な運転にても，十分な信頼性があり，ブラシがないので定期的点検・保守は不要な可変速ACスピンドルモータです。

FANUC AC SPINDLE MOTOR は従来の概念を打ち破り，電磁鋼板を直接冷却する斬新な固定子冷却方式（特許出願中）の採用により，コンパクトな外形にもかかわらず，高出力な特性を余裕を以て発揮できます。
NC工作機械の性能をより高めることができます。

FANUC AC SPINDLE SERVO UNIT は最新のパワーエレクトロニクス技術を駆使しています。低速から高速まで振動，騒音が少なく，安定で滑らかな駆動を行い，回生制動（特許出願中），純電気式主軸オリエンテーション制御（特許出願中）などの機能は，最新のNC工作機械の要求に十分応えることができます。

OUTLINE

The FANUC AC Spindle Motor series developed for the NC machine tool has high reliability even in severe operating conditions in machine shops full of dust and cutting oil. The variable speed AC Spindle Motor greatly reduces periodic inspection and maintenance.
The FANUC AC Spindle Motor with a unique stator cooling system (patent pending) enables excellent characteristics of high output, and therefore improves the performance of the NC machine tool.
The FANUC AC Spindle Servo Unit uses the latest techniques of power electronics. It can be smoothly operated at all speeds with every little vibration and low noise. The function of regenerative braking control (patent pending), electric spindle orientation control (patent pending), etc. can fully satisfy the requirement of the latest NC machine tools.

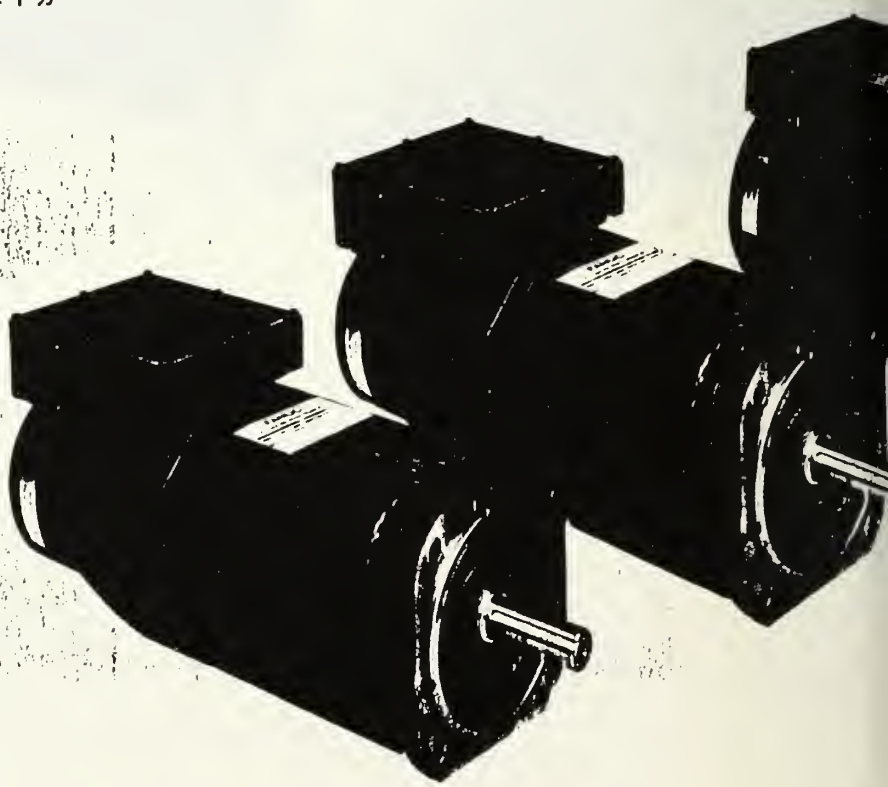

特　長

HIGHLIGHTS

1. NC工作機械へ豊富なシリーズ

5.5KWから26KW（30分定格）までシリーズ化され，フランジ形，足取付け形が用意されています。
足取付け形については，冷却風は2方向のタイプを用意しています。(モデル3～15) 旋盤，マシニングセンタなどあらゆるNC工作機械にご使用いただけます。

1. Wide variety of models for NC machine tools

There is a wide variety of models (foot mount type & flange type) with output power ranging from 5.5kW to 26kW (rated output for 30 min). Two types of cooling air direction are prepared for foot mount type. (Model 3 ~ 15)
These can be used for lathes, machining centers, and any other NC machine tools.

2. 機械工場環境に耐えられるモータ

塵埃や切削油の飛散する機械工場内で安心してご使用できる全閉構造です。
ブラシなどの摩耗部品がなく，定期的な点検・保守は不要です。

2. Reliability in severe environments

Because all models of the FANUC AC Spindle Motor series are completely enclosed, they can be used with safety even in machine shops full of dust and cutting oil. Since there are no brushes nor other wearing parts, periodic inspection and maintenance are rarely necessary.

3. コンパクトな外形で高速・高出力なモータ

従来の概念を打ち破り，モータから鋳物ケースを取り去りました。この斬新なモータ構造（特許出願中）により，固定子を直接空冷する高効率の冷却方式を採用しています。
また，従来にない小型・軽量なモータです。NC工作機械の切削能力向上に役立ちます。

3. Compact high-speed/high-output motors

The motor stator is directly air-cooled (pat. pend.) efficiently without motor case.
This unique construction results in extremely small and light weight of motors. The motors can greatly assist you in improving the cutting performance of NC machine tools.

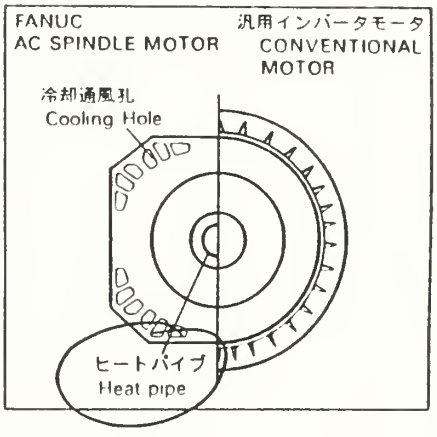

4. 高性能で高信頼性のサーボユニット

ACスピンドルサーボユニットは高度の電子的機能が必要ですが，マイクロプロセッサ技術を駆使して部品点数を少なくし，高信頼性設計となっています。また制御方式はパワートランジスタによるパルス幅変調方式を採用し，独得なベクトル制御により，高性能な特性が得られます。

4. High-performance/high-reliability servo unit

The FANUC AC Spindle Servo Unit employs the latest technology of microprocessor control to provide sophisticated, highly reliable electronic functions with a minimum number of parts. The pulse width modulation method using power transistors is adopted for control. A unique vector control system guarantees high performance characteristics.

5. 広い定出力範囲

主軸回転速度はますます高速化していますが，低速領域でも強力切削できることが必要です。
モデル3，モデル6では従来にない広い定出力範囲をもっていますので，この要求に応えることができます。
モータと主軸をベルトにて直結した小型マニシングセンタ，小型旋盤には最適です。

5. Wide constant output range

Increasingly higher speeds are being required of the spindle, and yet motors must also be capable of powerful cutting even in the low speed region.
Models 3 and 6 have the wide range of constant output power, and can meet these widely various needs. They are suitable for small machining centers and small lathes in which a motor is directly coupled with the spindle through belts.

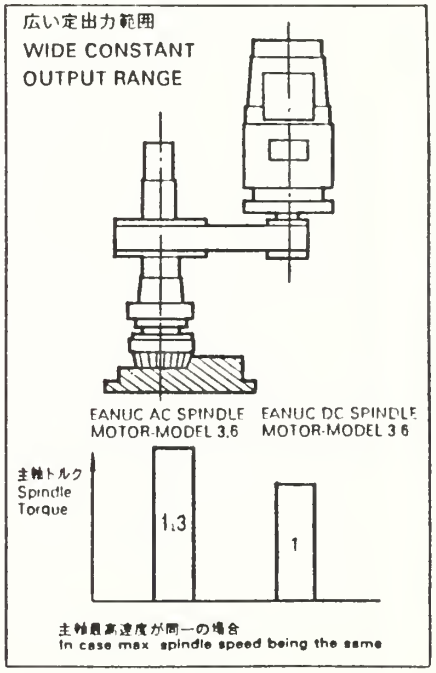

6. 優れた加速・減速応答

モータのロータイナーシャは小さく，ACインバータでは技術的に困難とされている電源への回生制動（特許出願中）の採用により高応答，高頻度の加速・減速が可能です。
マシニングセンタにて軽合金のタッピングを高速回転で行うことも可能となりました。

6. Excellent acceleration/deceleration response

Small rotor inertia of FANUC AC Spindle Motor series and the regenerative braking control (pat. pending) which has been difficult with the conventional technology have realized high response, high frequency acceleration and deceleration.
The FANUC AC Spindle Motors also enable machining centers to tap a light alloy at high speed.

7. 滑らかな回転

サーボユニットでは極限にまで滑らかに回転する方式（特許出願中）を採用していますので，低速から高速まで滑らかな回転が得られます。
独特な速度検出器（特許出願中）を用い，水晶発振器のクロックパルスをもとにしてディジタルコントロールされていますので，一定回転時の速度ムラも極めて小さくなっています。

7. Smooth rotation

The FANUC AC Spindle Servo Unit employs a system designed to rotate the motor smoothly up to an extremity (pat. pending). This provides with smooth rotation for min. to max. speed. A unique speed detector (pat. pending) is employed, and speeds are digitally-controlled based on clock pulses from a quartz oscillator. Thus, speed fluctuation during constant rotation is extremely small.

8. 低騒音モータ

一般にACスピンドルモータではチョッパ電流にて磁気力が変動し，不快な音が発生します。
FANUC ACスピンドルサーボユニットでは新駆動方式（特許出願中）を採用し，モータは低騒音となる最適設計をしており，不快な騒音の発生はありません。

8. Low-Noise motor

In conventional AC spindle motors, the electromagnetic force fluctuation as a result of chopper current generates uncomfortable noise. The FANUC AC Spindle Servo Unit adopts a new drive system (pat. pending) to eliminate such a motor noise.

9. 省エネルギー

ACスピンドルモータは，DCスピンドルモータに比較して省エネルギーです。
基底速度以下では特にDCスピンドルモータより電気料金が安くなります。
FANUC ACスピンドルサーボユニットは減速時に回転エネルギーを工場電源に戻す独特な回生制御方式を採用していますので，さらに省エネルギーです。

9. Energy saving

AC spindle motors require less energy than DC spindle motors especially in the range below the base speed. Moreover by adopting the regenerative braking control, FANUC AC Spindle Motor series is more beneficial for the purpose of energy saving.

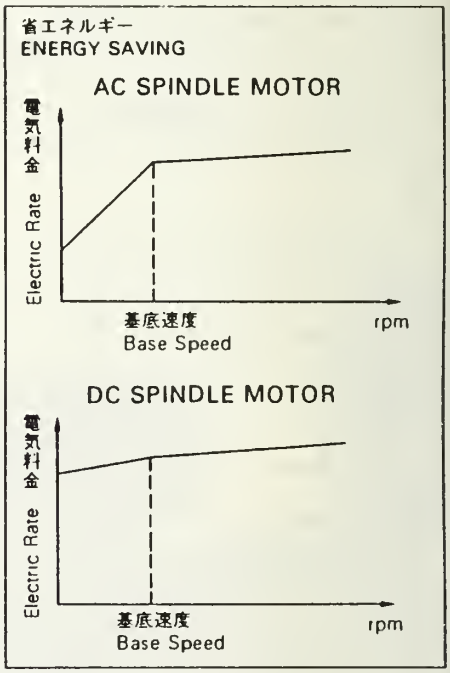

10. 主軸オリエンテーション(オプション)

電気的な高精度の主軸定位置停止が可能です。
従来使用された機械部品が不用となり機械構造がシンプルになります。

10. Spindle orientation (option)

Electric spindle orientation control enables a spindle to oriented stop.
You can design the machine simpler by eliminating mechanical parts which otherwise are required.

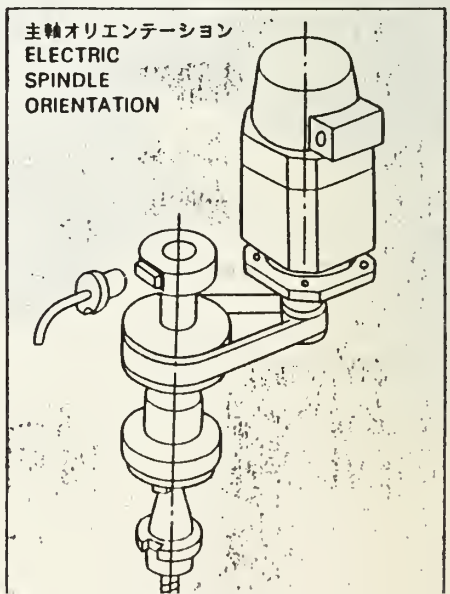

11. NCとの結合を容易にする主軸制御機能

NCと結合するときに必要なDAコンバータ，オーバライド入力，速度メータ用出力，ロードメータ用出力，トルク制限指令入力などの機能が用意されています。(一部の機能はオプションです。)

11. Spindle control functions for easy connection to NC

The functions for combining NC are provided, such as DA converter, override input, speed meter and load meter output, torque limit command signal input, etc. (some of these are optional).

INITIAL DISTRIBUTION LIST

1.	Mr. G. Green, Code 2712 David Taylor Research Center Annapolis, MD 21402	2
2.	Library, Code 0142 Naval Postgraduate School Monterey, CA 93943	2
3.	Professor P.J. Marto Code 69Mx Department of Mechanical Engineering Naval Postgraduate School Monterey, CA 93943	2
4.	Dr. A.S. Wanniarachchi ERC-CRSS University of California Santa Barbara, CA 93106	2